

RD-A167 186

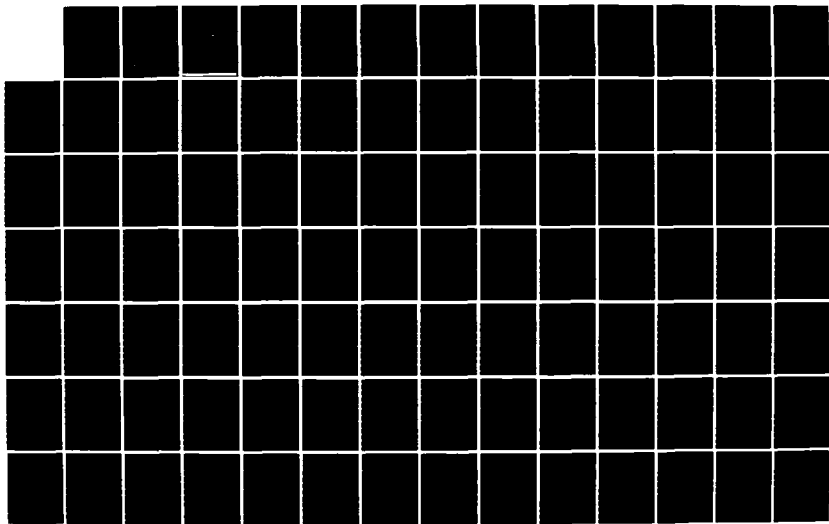
FRACTURE IN STABILIZED SOILS VOLUME 2(U) TEXAS
TRANSPORTATION INST COLLEGE STATION D M LITTLE ET AL.
31 DEC 85 AFOSR-TR-86-0242-VOL-2 F49620-82-K-0027

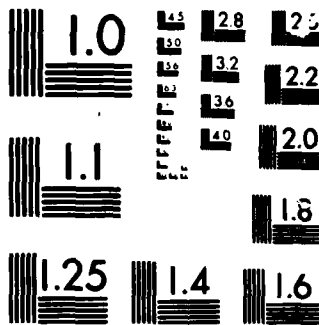
1/2

UNCLASSIFIED

F/G 8/13

NL





MICROCOPI

CHART

AFOSR-TR- 86-0242

(2)

AD-A167 106

FRACTURE IN STABILIZED SOILS

VOLUME 2

FINAL TECHNICAL REPORT

DECEMBER 31, 1985

Prepared for
Texas A&M University
and the Air Force Office of Scientific Research

Prepared by
The Texas Transportation Institute



Approved for public release;
distribution unlimited.

The Texas A&M University System
College Station, Texas

DTIC ELECTED
APR 28 1986
S D

B

86 4 28 175

b-1a-classified

SECURITY CLASSIFICATION OF THIS PAGE

AD-A167106

REPORT DOCUMENTATION PAGE

1. REPORT SECURITY CLASSIFICATION Unclassified		1b. RESTRICTIVE MARKINGS	
2. SECURITY CLASSIFICATION AUTHORITY		3. DISTRIBUTION/AVAILABILITY OF REPORT Approved for public release; distribution unlimited.	
4. DECLASSIFICATION/DOWNGRADING SCHEDULE			
5. PERFORMING ORGANIZATION REPORT NUMBER(S)		6. MONITORING ORGANIZATION REPORT NUMBER(S) AFOSR-TR- 86-0242	
7a. NAME OF PERFORMING ORGANIZATION Texas A&M University Texas Transportation Institute 7b. ADDRESS (City, State and ZIP Code) College Station, Texas 77843		7c. NAME OF MONITORING ORGANIZATION Air Force Office of Scientific Research 7d. ADDRESS (City, State and ZIP Code) <i>Bolling AFB, DC 20332</i>	
8. NAME OF FUNDING/Sponsoring Organization Office of Scientific Research ADDRESS (City, State and ZIP Code) <i>BOLLING AFB DC 20332-6448</i>		9. PROCUREMENT INSTRUMENT IDENTIFICATION NUMBER F49620-82-K-0027	
10. SOURCE OF FUNDING NOS. PERSONAL AUTHORIS) D. N. Little, W. W. Crockford, and Y. Kim		PROGRAM ELEMENT NO. <i>61102F</i>	PROJECT NO. <i>2302</i>
11. TYPE OF REPORT Final Technical		TASK NO. <i>C2</i>	WORK UNIT NO.
12. SUPPLEMENTARY NOTATION		13. DATE OF REPORT (Yr., Mo., Day) 851231	
14. PAGE COUNT 300			

15. COSATI CODES			16. SUBJECT TERMS (Continue on reverse if necessary and identify by block number)	
FIELD	GROUP	SUB. GR.	Fracture Mechanics	

17. ABSTRACT (Continue on reverse if necessary and identify by block number)
 Conventionally the thickness design of stabilized soil layers has been based upon the tensile strength of the stabilized soil layer and/or the appearance of the first crack. The design literature does not allow one to consider the true development of cracking in the stabilized soil layer. Knowledge of the mode of such cracking could drastically alter the philosophy behind thickness design of layers.

In this research the principles of theoretical fracture mechanics are used to explain the mode and mechanism of fracture in fine grained media stabilized with portland cement. Experimental fracture mechanics is used to validate or verify and in some cases to investigate more fully the hypothesized mechanisms of fracture. The influence of osmotic and matrix soil section, temperature, binder content, thermal and kinetic energy, from sources outside the crack, are considered in the study.

Linear elastic fracture mechanics is proven to be a highly acceptable analytical tool for these materials.

18. DISTRIBUTION/AVAILABILITY OF ABSTRACT <input checked="" type="checkbox"/> UNCLASSIFIED/UNLIMITED <input type="checkbox"/> SAME AS RPT. <input type="checkbox"/> DTIC USERS <input type="checkbox"/>		19. ABSTRACT SECURITY CLASSIFICATION Unclassified	
20. NAME OF RESPONSIBLE INDIVIDUAL <i>LAWRENCE D. HOKANSON</i>		21. ABSTRACT TELEPHONE NUMBER (Include Area Code) <i>(202) 767-4935</i>	22c. OFFICE SYMBOL <i>NA</i>

TABLE OF CONTENTS	ii
LIST OF TABLES	iv
LIST OF FIGURES	v

TABLE OF CONTENTS

	Page
CHAPTER I: INTRODUCTION	1
Purpose.	1
Pavement System.	1
Loading.	3
Solution Philosophy.	3
Solution Sequence.	10
CHAPTER II: THE FINITE ELEMENT PROGRAM	12
The Singularity Problem.	12
The Crack Element.	16
Operational Parameters	24
CHAPTER III: SOLUTION PROCEDURE	33
Development of Stress Distributions.	33
Linearize Stress Distributions	37
Mesh Considerations for Finite Element Runs.	40
Applying Reverse Stresses to Crack Lengths	42
Uncorrected K_I Values	42
Stress Intensity Correction Factors.	45

AIR FORCE OFFICE OF SCIENTIFIC RESEARCH (AFSC)
 NOTICE OF APPROVAL
 This document has been reviewed and approved.
 Distribution is limited to AFSC personnel.
 MATTHEW J. ROBERTS
 Chief, Technical Information Division

TABLE OF CONTENTS continued

CHAPTER V: CALCULATING FRACTURE LIFE	54
Regression Equations for Stress Intensity Factors	54
Computation of Crack Propagation Histories	61
Calculations With Actual Laboratory Fracture Properties	74
CHAPTER V: CONCLUSIONS AND RECOMMENDATIONS	76
REFERENCES	78
APPENDIX A: LIST OF SYMBOLS	79
APPENDIX B: DESCRIPTION OF PROGRAM UNITS	80
Finite Element Fracture program	80
Input Guide	83
Sample Input Guide for Finite Element Fracture Program . .	98
Sample Output From Finite Element Fracture Program	104
Crack Propagation Calculation Program	118
Input Guide	120
Sample Input Guide for Crack Propagation Program	126
Sample Output for Crack Propagation Program	128

Accepted by:	✓
NTB:	
Ref:	
Unit:	
Date:	
By:	
Division:	
Avg:	
Dist:	
APPROVAL STAMP	
Dist:	
A-1	



LIST OF TABLES

Table	Page
1. Pavement Data Used in Developing Structural Data	2
2. c/b Values Used in Analysis	30
3. Pavement Parameters Used in the Factorial Analysis	35
4. Stress Distributions for Superposition Phase one, psi.	36
5. Linearized Stress Distributions, psi	39
6. An Example of a Reverse Stress Profile for Figure 3, MC = 1 . . .	43
7. Uncorrected Stress Intensity Factors, psi/ in.	44
8. Stress Intensity Correction Factors, psi/ in	46
9. Corrected Stress Intensity Factors	48
10. Regression Coefficients for Cubic Polynomial Fit to Stress Intensity Distribution.	55
11. Endpoints for Crack Propagation Histories.	68

LIST OF FIGURES

Figure	Page
1. Loading Condition Modelled with Finite Element Fracture Program.	4
2. Schematic of Superposition Principle to Solve for Stress Intensity on Crack.	5
3. Schematics of Possible Stress Intensity Factor Distributions . . .	9
4. Two Major Modes of Fracture Analyzed in Finite Element Fracture Program	15
5. Crack Tip Elements	17
6. Crack Tip Element Used in Analysis	26
7. Illustration of Errors Produced by Variation in Crack Tip Length Within the Element (4)	27
8. Illustration of Accuracy Related to Crack Length (4).	28
9. Example of a "Humped" Crack Tip Element.	32
10. Finite Element Mesh used for Pavement Structural Analysis. . . .	34
11. Illustration of Mesh Around Crack.	38
12. Stress Distributions for Modulus Condition 1, Parenthesis Contain Base Thickness and Surface Thickness Respectively. . . .	41
13. Distribution of Stress Intensity Factor.	49
14. Distribution of Stress Intensity Factor.	50
15. Stress Intensity Factor Distribution	51
16. Stress Intensity Factor Distribution	52
17. Stress Intensity Factor Distribution	53
18. Comparison of Computed and Regression Stress Intensity Factors .	56
19. Comparison of Computed and Regression Stress Intensity Factors .	57
20. Stress Intensity Factor Distribution	58

LIST OF FIGURES (cont.)

Figure	Page
21. Distribution of Stress Intensity Factor	59
22. Distribution of Stress Intensity Factors.	60
23. Distribution of Stress Intensity Factors Calculated by Regression Equations for Various Modulus Conditions	62
24. Distribution of Stress Intensity Factors Calculated by Regression Equations for Various Modulus Conditions	63
25. Distribution of Stress Intensity Factors Calculated by Regression Equations for Various Modulus Conditions	64
26. Distribution of Stress Intensity Factors Calculated by Regression Equations for Various Modulus Conditions	65
27. Distribution of Stress Intensity Factors Calculated by Regression Equations for Various Modulus Conditions	66
28. Progression of Crack (c) Through Base (b) as a Function of Load Cycles, N.	69
29. Progression of Crack (c) Through Base (b) as a Function of Load Cycles, N.	70
30. Progression of Crack (c) Through Base (b) as a Function of Load Cycles, N.	71
31. Progression of Crack (c) Through Base (b) as a Function of Load Cycles, N.	72
32. Progression of Crack (c) Through Base (b) as a Function of Load Cycles, N.	73
B-1. Flow Diagram of Program for Finite Element Fracture Calculations	81
B-2. Flow Diagram of Program for Solution of Paris Equation.	120

CHAPTER I: INTRODUCTION

Purpose

The purpose of this research is to establish a preliminary model to investigate the crack propagation history in a given pavement system. This is accomplished through a multi-step process. First, a suitable program is used to calculate the stress distribution in the pavement layers under the load, in this study an elastic layer program. Second, through successive application of a finite element program, the stress intensity factor as a function of crack length is determined. Third, using the stress intensity factor distribution, the number of load cycles required to advance the crack a given increment is calculated. These increments carry the crack from its initial to its final value, which defines failure. The load cycles are calculated using the Paris equation. The remainder of the report is taken up by a detailed description of the problem and an in-depth account of the solution process and results.

Pavement System

The pavement system used in this study consists of a combination of three layers: a subgrade, a base, and a surface. Each layer has variable values for the modulus of elasticity and the thickness. This information is summarized in Table 1.

The subgrade thickness is listed as 50 inches. This is an arbitrary value selected so that the subgrade thickness does not affect the solution.

Table 1. Pavement Data Used in Developing Structural Data.

LAYER	MODULUS VALUES,PSI	THICKNESSES,IN.	POISSON'S RATIO
overlay	350000.0	0	0.35
		3	
		6	
base	400000.0 800000.0 1200000.0	8	0.35
		12	
		16	
subgrade	4000.0 9000.0	50	0.35
MODULUS CONDITIONS			
MODULUS CONDITION	BASE MODULUS,PSI	SUBGRADE MODULUS,PSI	
1	1200000.0	4000.0	
2	1200000.0	9000.0	
3	800000.0	4000.0	
4	800000.0	9000.0	
5	400000.0	4000.0	
6	400000.0	9000.0	

In the analysis of the pavement system, all possible combinations of the values in Table 1 are used to develop the influence of pavement properties on fracture.

Loading

The loading shown in Figure 1 approximates that of an F-4 aircraft. It consists of a total load of 27,000 pounds. This load is distributed over a circle with a radius of 5.7 inches to provide a pressure of 265 psi.

Solution Philosophy

Strictly speaking, this problem is a three dimensional axi-symmetric one. However, because crack propagation itself is generally a plane strain phenomenon, it is considered preferable to rely on a simpler solution scheme. The approach here is to use a two-dimensional plane strain finite element program to obtain approximate stress intensity factors developing under the stresses calculated from an elastic layer analysis. For a single load, as assumed here, the results are satisfactory.

The cornerstone of the solution procedure is the computation of the stress intensity factor as a function of crack length. This is done with the finite element program described in a later chapter and with the aid of superposition techniques. When dealing with boundary values over an infinite region such as a pavement structure, the problem can be analyzed as the superposition of two problems (1) as illustrated in Figure 2. In the first phase, one applies the total loading to the pavement with no crack. For the second phase, the crack is included in the pavement. The stresses where the

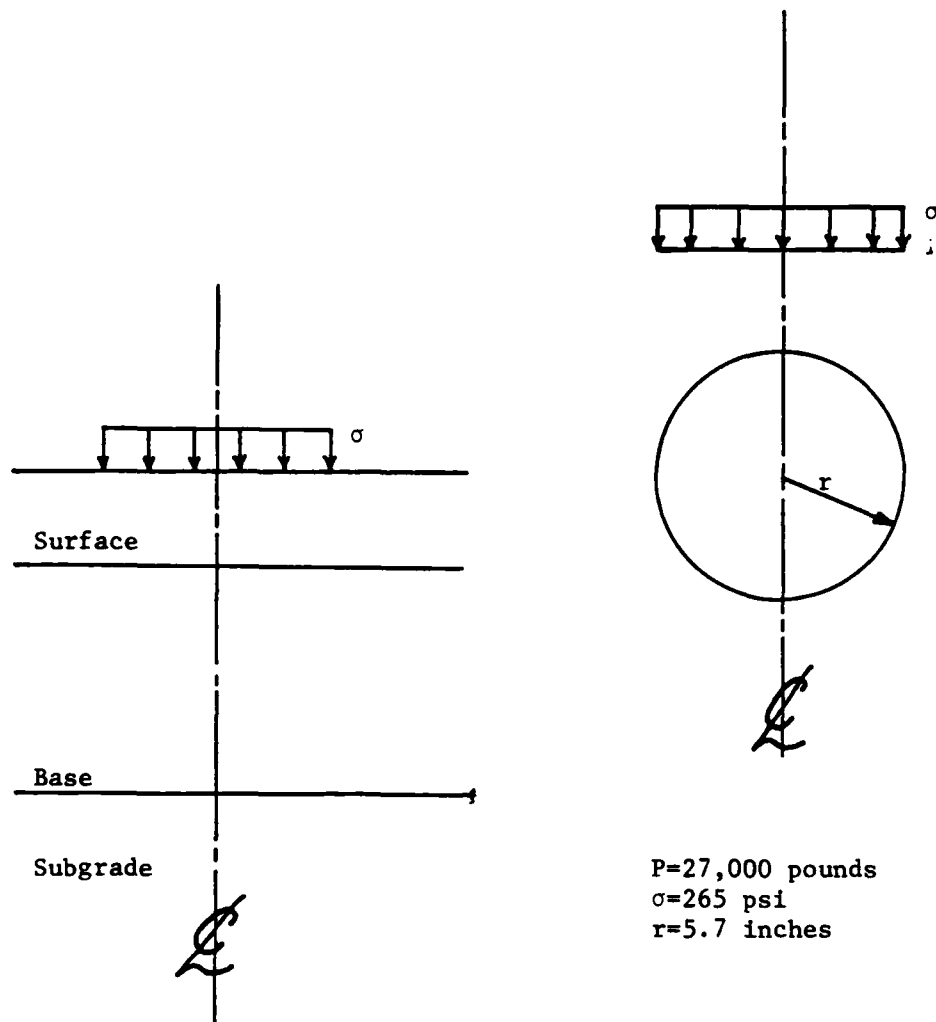


Figure 1. Loading Condition Modelled With Finite Element Fracture Program.

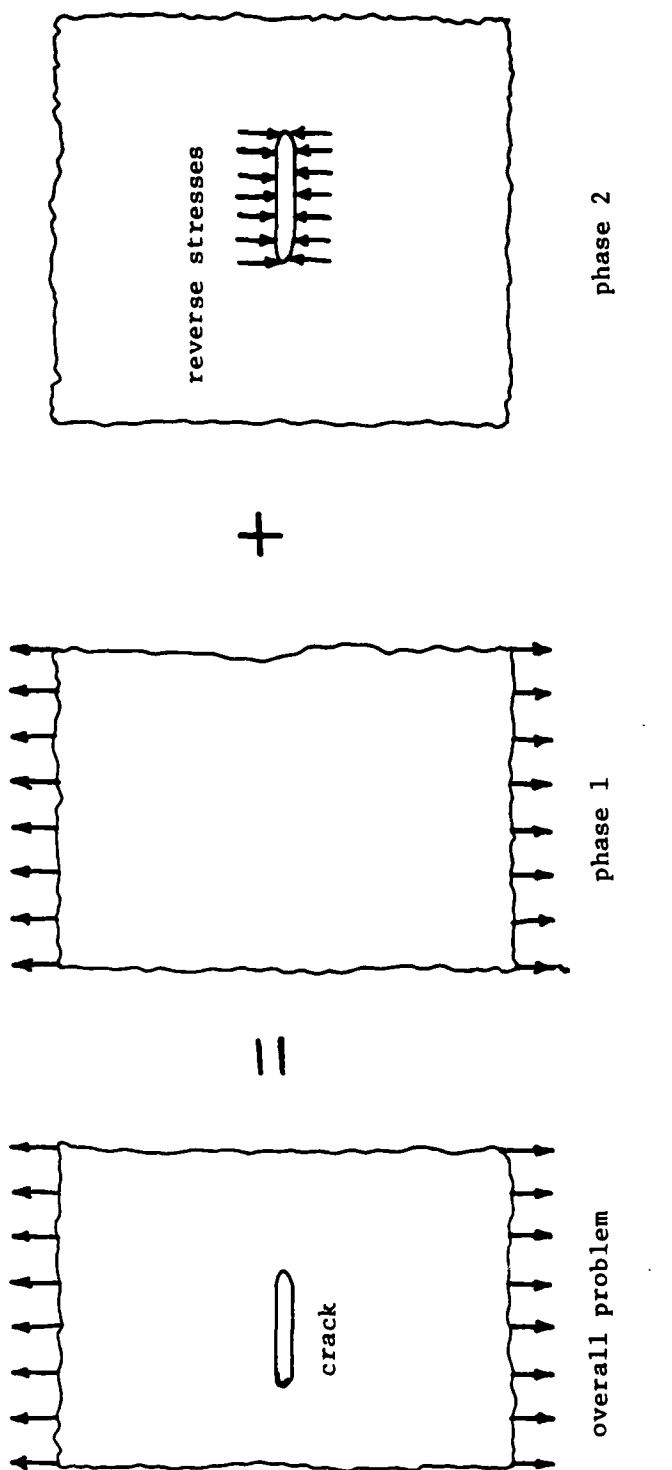


Figure 2. Schematic of Superposition Principle
to Solve for Stress Intensity on Crack

crack would be in the first phase are applied in the reverse direction to the crack in the second phase. The stress intensity factor found from the second phase, although of opposite sign, is equal in magnitude to that of the overall problem. Thus the task of finding K_I becomes one of discovering the correct stress distribution due to loading at the crack, applying the reverse stresses to the crack, and analyzing the pavement.

A further difficulty arises when using the above superposition. As will be noted, stresses cannot be applied to the portion of the crack which lies within the crack tip finite element. Thus, a correction factor is required to account for this. The correction factor is given by (1) as:

$$C_k = \frac{\sqrt{2}}{\pi} \int_0^z \frac{\sigma_e(\xi) d\xi}{\sqrt{\xi}} \quad (1)$$

where ξ is the distance away from the crack tip and $\sigma_e(\xi)$ is the stress to be applied to the portion of the crack that lies within the crack element. If z is sufficiently small, $\sigma_e(\xi)$ can be assumed to be a constant, and equation (1) reduces to (1):

$$C_k = \left(\frac{8}{\pi}\right)^{1/2} \sigma_e \sqrt{2} \quad (2)$$

The final, correct stress intensity factor is found from C_k and K_I computed in superposition phase two by

$$K_I \text{ final} = K_I \text{ computed} + C_k \quad (3)$$

Crack propagation is calculated using this stress intensity factor in

numerical integration of the Paris equation. The Paris equation consists of the following:

$$dc/dN = AK_I^n \quad (4)$$

where

dc = differential crack extension

dN = differential increase in the number of load cycles

K_I = stress intensity factor

A, n = dimensionless material constants determined experimentally

Manipulation of the Paris equation gives:

$$dN = dc/AK_I^n \quad (5)$$

from which ΔN_f , the number of load cycles required to advance the crack an increment can be calculated as:

$$\Delta N_f = \int_{c_0}^{c_f} \frac{dc}{AK_I^n} \quad (6)$$

Writing the integral in terms of c/b leaves:

$$\Delta N_f = b \int_{(c/b)_0}^{(c/b)_f} \frac{d(c/b)}{AK_I^n} \quad (7)$$

When the current crack length equals the crack length at failure, the final value of N_f is reached.

The total number of load cycles required to advance the crack from the initial crack length to the current crack length, N_{fn} , is found by summing the ΔN_f values for the n crack increments which total the current crack length. Thus,

$$N_{fn} = \sum_1^n \Delta N_{fn} = N_{f(n-1)} + \Delta N_{fn} \quad (8)$$

Note that K_I is considered a function of (c/b) now, not crack length. This allows regression equations to be developed for the range of materials and loading conditions which lessens the reliance on the finite element computer code.

In this analysis the crack is assumed to form directly beneath the center line of the load, on the line of symmetry. It is assumed to originate at the interface of the base and the subgrade and to propagate upward through the base. The greatest crack length at which the pavement is assumed to have failed is the full thickness of the base. If c = crack length in the base and b = thickness of the base, then $c/b = 1.0$ is the maximum value at which failure can occur. This would lead one to believe that the life of the pavement ranges between c/b values of 0.0 and 1.0. However, this is true only if two conditions exist. First, K_I , the stress intensity factor, must be positive for all c/b . Second, the critical value of the stress intensity factor, K_{IC} , must not be exceeded. In the first case, if K_I is negative, then the crack cannot propagate in that region and that region cannot figure in the fracture life of the pavement. The areas defining the fracture life of the pavement when K is negative are illustrated in Figure 3, where typical K_I distributions for this problem are depicted. Case I and II are self-explanatory. In case III, it is assumed that some perturbation advances

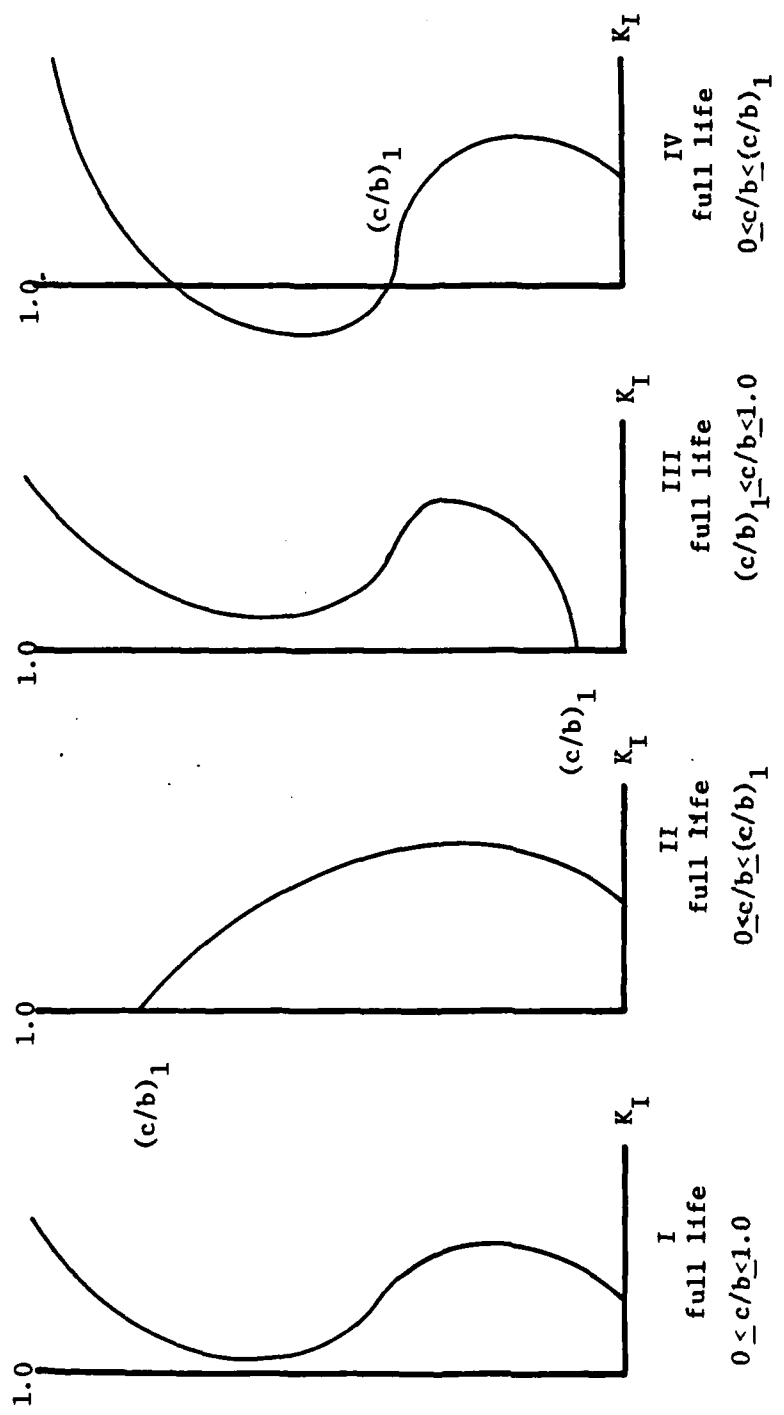


Figure 3. Schematics of Possible Stress Intensity Factor Distributions

the crack to $(c/b)_1$, so that the crack can propagate. Here $(c/b)_1$ is considered small so that this is readily possible and handled with the concept of starter flaws. If $(c/b)_1$ is not small, then the crack may never propagate. In case IV, the crack propagates to $(c/b)_1$ in the normal fashion and once there encounters negative K_I values and stops. It is unlikely that the crack will somehow be advanced suddenly through the relatively extensive negative K_I region, and if it is, the pavement will be nearly destroyed and can be said to have failed. Thus $(c/b)_1$ is the upper limit of the fatigue life in this case. One should note that if $(c/b)_1$ is significantly less than 1.0, then exhausting the fatigue life may not constitute failure of the pavement. The pavement may still maintain its structural integrity.

If K_{IC} is exceeded, then the crack instantly propagates to a point where $K_I = K_{IC}$. The fatigue life would then range between c/b values where K_I is less than or equal to K_{IC} . If K_I never falls below K_{IC} again, then the crack instantly propagates to failure. Unfortunately, K_{IC} values for the pavements in this problem are unknown, so there is no way to incorporate them into the solution algorithm. Therefore, for purposes of analysis, it is assumed that K_{IC} is greater than K_I for all c/b .

Solution Sequence

The solution sequence briefly described here will be described in detail in the following chapters. The stress distribution calculations will not be described, as this program can be replaced with any program which calculates stresses and strains under a loading. Other elastic theory programs can be used which will allow multiple wheel loadings to be used to produce the

stress distribution which is then used in the finite element fracture program. The Hybrid crack tip element of Pian and Tong used in a plane strain finite element program is used to determine the stress intensity factors resulting when a cracked base course is subjected to the calculated stress distribution. Regression equations have been developed in this study to reduce the use of the finite element program for simple pavement structures. Finally, the Paris equation is used in a program to calculate the number of loads to failure under the given stress intensity distribution.

CHAPTER II: THE FINITE ELEMENT PROGRAM

The Singularity Problem

For linearly elastic plane strain and plane stress problems, in the vicinity of a crack tip the stress varies as $1/\sqrt{r}$, where r is the radial coordinate of any point in the plane measured from the crack tip. Thus, at the crack tip where $r = 0$ the stress is singular. In the equations for stress, the coefficient of the singular $1/\sqrt{r}$ term is called the stress intensity factor and is representative of the "strength" of the singularity. It has units of (force/area)* $\sqrt{\text{length}}$. There are two main types of crack which govern the behavior of linearly elastic plane stress/stain problems.

These are:

- 1) mode I or opening mode
- 2) mode II or in-plane shearing

These modes are illustrated in Figure 4.

For isotropic materials, the singular terms of the stress distribution in the vicinity of a crack tip are (3):

mode I:

$$\{\sigma\} = \begin{Bmatrix} \sigma_x \\ \sigma_y \\ \sigma_{xy} \end{Bmatrix} = \left(K_I \sqrt{2\pi r} \right) \begin{Bmatrix} \cos(\theta/2)[1 - \sin(\theta/2)\sin(3\theta/2)] \\ \cos(\theta/2)[1 + \sin(\theta/2)\sin(3\theta/2)] \\ \sin(\theta/2)\cos(\theta/2)\cos(3\theta/2) \end{Bmatrix} \quad (8)$$

mode II:

$$\{\sigma\} = \begin{Bmatrix} \sigma_x \\ \sigma_y \\ \sigma_{xy} \end{Bmatrix} = \left(K_{II} \sqrt{2\pi r} \right) \begin{Bmatrix} -\sin(\theta/2)[2 + \cos(\theta/2)\cos(3\theta/2)] \\ \sin(\theta/2)\cos(\theta/2)\cos(3\theta/2) \\ \cos(\theta/2)[1 - \sin(\theta/2)\sin(3\theta/2)] \end{Bmatrix} \quad (9)$$

In many formulations, the coefficient involving K in front of the vectors containing trigonometric terms in equations (8) and (9) is given as $(K/\sqrt{2r})$. The finite element program used in this research uses equations (8) and (9) as is. With the use of these equations it is necessary to multiply the results of the finite element program by $\sqrt{\pi}$ in order to match any results obtained from stress distributions based on the alternative coefficient. It is a minor point but mix-up in definitions can lead to confusion and incomprehensible results.

The stress intensity factors K_I and K_{II} are directly proportional to the magnitude of applied loading and are dependent on the geometry of the structure, the size and shape of the crack, and the nature of the applied loading.

Displacement fields in the vicinity of a crack tip are also functions of the stress intensity factors and can be written as :

mode I:

$$\begin{bmatrix} u \\ v \end{bmatrix} = \left(K_I \sqrt{\frac{2r}{\pi}} \right) / 8G \quad \begin{bmatrix} (2K - 1)\cos\theta/2 - \cos(3\theta/2) \\ (2K + 1)\sin(\theta/2) - \sin(3\theta/2) \end{bmatrix} \quad (10)$$

mode II:

$$\begin{bmatrix} u \\ v \end{bmatrix} = \left(K_{II} \sqrt{\frac{2r}{\pi}} \right) / 8G \quad \begin{bmatrix} (2K + 3)\sin(\theta/2) + \sin(3\theta/2) \\ -(2k - 3)\cos(\theta/2) - \cos(3\theta/2) \end{bmatrix} \quad (11)$$

In equations (10) and (11), u and v are the displacements along the x and y axes in Figure I-1, G is the shear modulus, $k = (3 - 4\nu)$ for plane strain and $(3 + \nu)/(1 + \nu)$ for plane stress, and ν is Poisson's ratio.

The stress intensity factor is also related to the strain energy release rate, that is the change in strain energy in the structure per unit distance of crack extension. For linearly elastic plane strain/stress problems the strain energy release rate is given by (3):

mode I:

$$\mathcal{E}_I = K_I^2(k + 1)/8G \quad (12)$$

mode II:

$$\mathcal{E}_{II} = K_{II}^2(k + 1)/8G \quad (13)$$

where k and G are as defined previously.

The computer program provides for the calculation of the stress intensity factor in two ways. The first and far more emphasized way is to utilize eqs. (8)-(11) and solve for the stress intensity factor directly. The second method is to run the program twice, the second time with a slightly longer crack, note the difference in strain energy, and apply equation (12) and (13). This option is there if the analyst wants to take advantage of it, but it is not the main thrust of the program and is limited in that if both mode I and mode II are present equations (12) and (13) are not applicable.

The justification for using elements with assumed stress and displacement distributions that have the $1/\sqrt{r}$ singularity built in is based on the convergence rate of problems with singularities. The convergence of such problems has been shown to be of order h , where h is the maximum size of the elements used in the solution. The convergence rate is independent of p , the order of the complete polynomial used in the interpolation functions for stress and displacement. The quantities for which the convergence rate was established are the strain energy U and the stress intensity factors K_I and K_{II} . Given the above, in order to achieve good results for U or K using elements without singularities built in, the number of elements needed

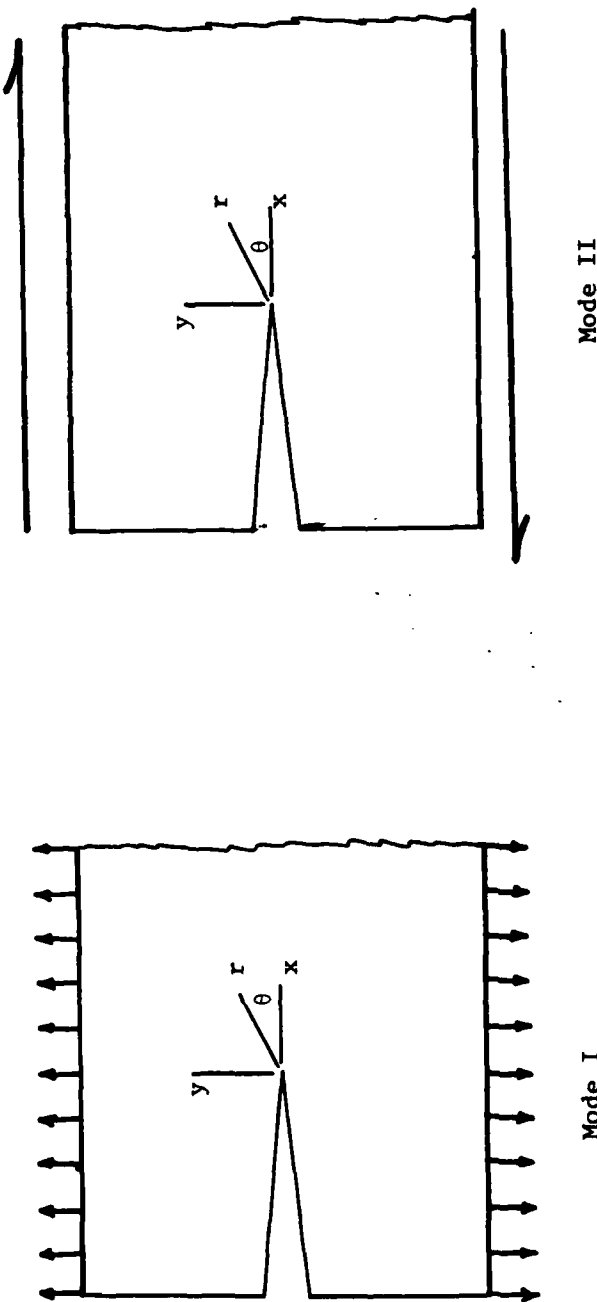
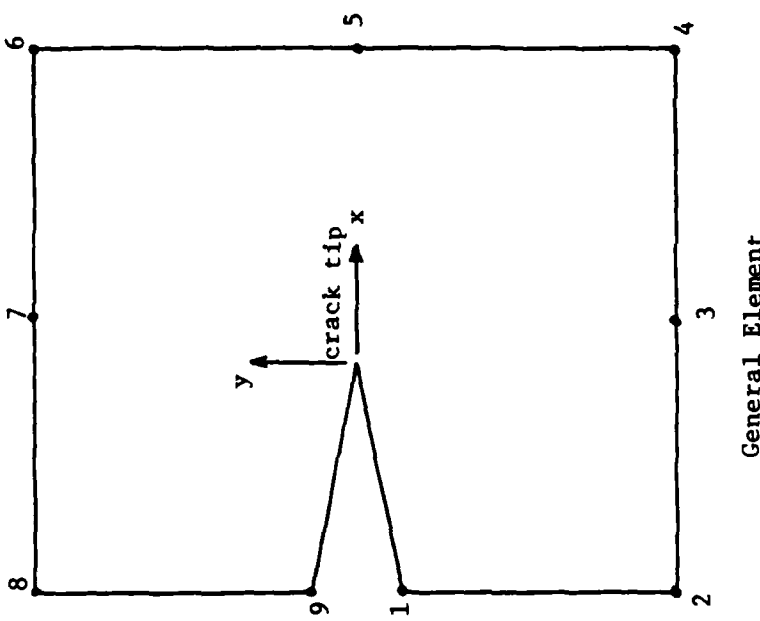


Figure 4. Two Major Modes of Fracture Analyzed
in Finite Element Fracture Program.

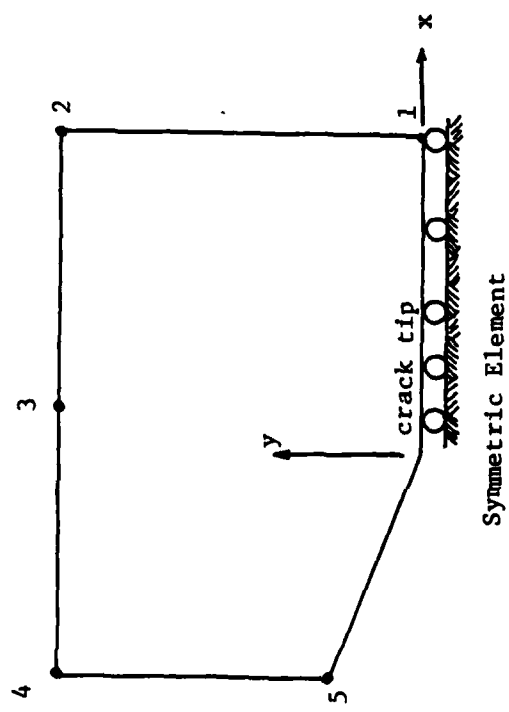
becomes impractical because results for relatively large h are highly inaccurate. This is the value of solutions using elements with singularities in the region around the crack tip. Although they converge no faster, for relatively large element sizes they give acceptable results. Indeed, making the elements that include singularities too small can have an adverse effect on the results. This peculiarity occurs for this reason. If the elements containing singularities are small enough, the region in the structure significantly affected by the crack will extend beyond the scope of the singular elements and cause errors in adjacent non-singular elements. In the limit of mesh refinement, as all element sizes go to zero, the beneficial effects of elements with singularities disappear, leaving only a solution based on conventional elements.

The Crack Element

The crack element first developed by Pian and Tong (3), and which is shown in Figure 5 is the element used in the finite element program. It must be of sufficient size to insure good results, as mentioned above. The crack element is developed using a functional and methods which are a combination of both assumed stress and displacement models. As such, in this development, internal stresses and displacements as well as boundary displacements and tractions can be assumed independently. The necessary equilibrium and compatibility requirements are incorporated into the Euler equations, which result from the stationary condition of the functional. The Euler equations can be satisfied either exactly or in a average sense, the latter condition being the source of approximation in the finite element method.



General Element



Symmetric Element

Figure 5. Crack Tip Elements

In the previous section a \sqrt{r} term is included in the equations for displacements. It is not desirable to introduce this term into the assumed boundary displacements, for two reasons. First, it can be incorporated into the assumed internal displacements. Second, one of the virtues of this crack element is that it can be used in conjunction with conventional finite elements, and if a \sqrt{r} term were included in its boundary displacement, boundary compatibility between it and a conventional element could not be insured. Of course, insuring this compatibility causes internal and boundary displacements for the crack element to be incompatible, a source of error.

The functional used in this development is, for plane problems,

$$\pi_m = \int_{\partial A_m} (\tilde{u}_i - u_i) T_i ds - \int_{S_{\sigma_m}} u_i T_i ds + \frac{1}{2} \int_{A_m} [\sigma_{ij} (u_{i,j} + u_{j,i}) - C_{ijkl} \sigma_{ij} \sigma_{kl}] dA \quad (14)$$

where

A_m = area of the m^{th} element

∂A_m = the boundary of A_m

S_m = the portion of ∂A_m over which tractions are prescribed

S_u = the portion of ∂A_m over which displacements are prescribed

C_{ijkl} = the elastic compliance tensor

u_i = a smooth internal displacement field

\tilde{u}_i = assumed boundary displacements

\bar{u}_i = prescribed boundary displacements

T_i = assumed boundary tractions

\bar{T}_i = prescribed boundary tractions

\tilde{u}_i is assumed such that \tilde{u}_i equals \bar{u}_i on S_u . Note that the thickness t is absent from equation (14) as unity is assumed, but can be multiplied in if the thickness is variable variable.

The Euler equations for the functional in equation (7) are

$$\frac{1}{2} (U_{i,j} + U_{j,i}) = C_{ijKl} \sigma_{Kl} \quad \text{in } A_m \quad (15a)$$

$$\sigma_{ij,j} = 0 \quad \text{in } A_m \quad (15b)$$

$$J_i = \sigma_{ij} v_j \quad \text{on } A_m \quad (15c)$$

$$U_i = \bar{U}_i \quad \text{on } A_m \quad (15d)$$

$$T_i = \bar{T}_i \quad \text{on } m \quad (15e)$$

Note that the body force is excluded for simplicity, and that v_j is a direction cosine.

Equation (15a) represents compliance with stress-strain laws by assumed stresses and displacements, equation (15b) represents the satisfaction of internal equilibrium, equation (15c) represents compatibility of assumed stresses and boundary tractions, equation (15d) represents compatibility of internal and boundary displacements, and equation (15e) represents satisfaction of boundary conditions by boundary tractions. The crack element provides for internal equilibrium and compatibility, interelement compatibility, and boundary conditions on displacements identically. The exact solution satisfies all the Euler equations. Also, if the solution is exact, then the stationary condition on equation (14) will provide for interelement equilibrium and compatibility. Otherwise, interelement equilibrium is satisfied only in a work equivalent sense, while interelement compatibility will be satisfied by assuming the same boundary displacement functions for all elements, crack or conventional.

The element stiffness matrix, whose development is discussed in the following pages, is derived using complex variable techniques.

To begin with, let $z=x+iy$, where x and y are as depicted in Figure 4. As shown previously, $(\sigma)^{-1}/\sqrt{r}$ & $(\frac{u}{v}) \sim \sqrt{r}$, so that stresses and displacements can be expressed as (3):

$$\left. \begin{aligned} \sigma_y + \sigma_x &= 2[\phi'(z) + \bar{\phi}'(\bar{z})] \\ \sigma_y - \sigma_x + \frac{1}{i} \sigma_{xy} &= 2[Z\phi''(z) + \chi'(z)] \end{aligned} \right\} \quad (16)$$

$$Z_u (U+iV) = \eta\phi(z) - Z\bar{\phi}'(\bar{z}) - \bar{\psi}(z) \quad (17)$$

where $\eta = E/2(1+\nu)$, $\eta = 3-4\nu$ for plane strain and $(3-\nu)/(1+\nu)$ for plane stress. E and ν are Young's modulus and Poisson's ratio, respectively. It can be seen that $\mu = G$ and $\eta = k$ in Section I. $(\cdot)'$ denotes differentiation and (\cdot) denotes the complex conjugate. ϕ and ψ are analytic functions. The above definitions of stress and displacement satisfy Euler equations (15a) and (15b). In addition, boundary tractions are chosen in this development so that they satisfy equation (15c).

In order to choose proper stresses and displacements for the crack element that account for singularities of all order, the following mapping function is introduced (4).

$$Z = W(\mathcal{L}) = \zeta^2 \quad (18)$$

or

$$\mathcal{L} = Z^{1/2} \quad (19)$$

with $-\pi/2 \leq \arg \zeta \leq \pi/2$ and $-\pi \leq \arg z \leq \pi$. On the \mathcal{L} plane, the element lies on the region where the real part of \mathcal{L} is positive and the crack lies on the imaginary axis. ϕ and ψ are analytic functions of \mathcal{L} , enabling simple polynomials in terms of \mathcal{L} to be used in the finite element solution.

Using the mapping given above, equations (16) and (17) become

$$\begin{aligned}\sigma_x + \sigma_y &= 4R_e [\phi'(L)/w'(L)] \\ \sigma_x + \sigma_y - 2\sigma_{xy} &= 2 \overline{\{w(L)[\phi'(L)/w'(L)]' + \psi'(L)\}/w'(L)} \\ 2\mu(+iv) &= \eta\phi(L) - w(L)\phi'(L)/w'(L) - \psi(L)\end{aligned}\quad (20)$$

In order to satisfy the stress free condition on the crack tip given by (3).

$$\sigma(L) + w(L)\overline{\phi'(L)/w'(L)} + \overline{\psi(L)} = 0 \quad (21)$$

the following form of ψ is chosen

$$\psi(L) - \overline{\phi(-L)} - w(-L)\phi'(L)/w'(L) \quad (22)$$

By using equations (15c), (19), (20), and (22) all of the Euler equations except for equation (15d) are satisfied by this crack element model. Substituting equations (21) into (14) gives in matrix form (4):

$$\pi_m = \int_{\partial A_m} (T)^T (\tilde{U}) ds - \int_{\partial A_M} (T)^T (U) ds \quad (23)$$

in which

$$(T) = \begin{bmatrix} T_1 \\ T_2 \end{bmatrix} = \begin{bmatrix} \sigma_x v_x + \sigma_{xy} v_y \\ \sigma_{xy} v_x + \sigma_y v_y \end{bmatrix} = \text{boundary tractions}$$

$$(u) = \begin{bmatrix} u \\ v \end{bmatrix} = \text{internal displacements} \quad (24)$$

$$(\tilde{u}) = \begin{bmatrix} \tilde{u} \\ \tilde{v} \end{bmatrix} = \text{boundary displacements}$$

For the derivation of the element stiffness matrix, the following forms of $\phi(L)$ and $\psi(L)$ may be assumed: (4)

$$\begin{aligned}\phi(\xi) &= \sum_{j=1}^N b_j \xi_j \\ \psi(\xi) &= -\sum_{j=1}^N [\bar{b}; (-i)^{j+1} \frac{b_i}{2}] \xi_j\end{aligned}\quad (25)$$

where N is a finite integer and $b_j = \beta_j + i\beta_{N+j}$ with the β 's being real constants and $\beta_{N+2} = 0$. This is because $\phi = i^2$ and $\psi = 0$ give no contribution to the stresses in equations (20).

Using equations (20), (24), and (25) one can express the following: (3)

$$(T) = [R](\beta) \quad (26)$$

$$(u) = [U](\beta)$$

where (β) includes components $\beta_1, \beta_2, \dots, \beta_{2N}$ excluding β_{N+2} . The boundary displacements (\tilde{u}) are expressed as

$$(\tilde{u}) = [L](q) \quad (27)$$

(q) is the vector of nodal displacements and $[L]$ is an interpolation matrix defined on ∂A_m . $[L]$ is such that boundary displacements for the crack element and adjacent conventional elements are the same. For instance, if, as in the finite element program, linear boundary displacements are employed, then between any two nodes on the crack element $[L]$ will be such that (\tilde{u}) has a linear variation.

The number of nodes in the crack element used in the finite element program varies from 5 to 9 depending on symmetry, as shown in Figure 5. Boundary displacements are not assumed along the crack edge of the element because tractions are zero and there is no adjacent element. Because of this, in the program, there is no way to load the portion of the crack within the element and there is no way to control the crack's displacement within the element.

Substitution of equations (26) and (27) into equation (23) gives

$$\pi_m = (\beta)T[G](q) - 1/2 (\beta)T[H](\beta) \quad (28)$$

in which

$$[G] = \int_{\partial A_m} [R]^T [L] ds \quad (29)$$

$$[H] = 1/2 \int_{\partial A_m} ([R]^T [U] + [U]^T [R]) ds \quad (30)$$

As the β 's can be assumed independently from surrounding elements, the stationary condition of equation (28) with respect to (β) gives

$$[H](\beta) = [G](q) \quad (31)$$

or

$$(\beta) = [H]^{-1}[G](q) \quad (32)$$

With equation (31), one can substitute back into equation (28) and eliminate (β). One does not have to. Instead, one could solve for (β)'s simultaneously with the (q)'s. However, in the finite element program the (β)'s are eliminated.

Substituting equation (32) into equation (28) gives (3)

$$\pi_m = 1/2(q)^T [k](q) \quad (33)$$

where the element stiffness matrix for the crack element is

$$[k] = [G]^T [H]^{-1} [G] \quad (34)$$

After global assembly and solution for the global displacement vector, the stress intensity factors can be found from the now known (q). The stress intensity factors can be shown to be related to (β) in the following manner: (4)

$$K_I = (\beta_1)\sqrt{2} \quad (35)$$

$$K_{II} = (\beta_{N+1})\sqrt{2}$$

Because (β) is related to (q) by equation (32), one can write

$$K_I = (B_I)^T(q) \quad (36)$$

$$K_{II} = (B_{II})^T(q)$$

It appears that $(B_I)^T$ is the first row of $[H]^{-1}[G]$ multiplied by $\sqrt{2}$ and that $(B_{II})^T$ is the $(N+1)^{th}$ row of $[H]^{-1}[G]$ multiplied by $\sqrt{2}$ as is shown in the program.

The reference followed in the development of this chapter gives details as to how the integrations implied by equations (29) and (30) are to be accomplished in terms of complex variables, and it gives certain properties of $[H]$ (namely that its upper right and lower left quadrants are blocks of zeros) that make it more efficient to invert (4).

The finite element program uses the crack element of the previous section in conjunction with CST triangular elements and 4-CST quadrilateral elements obtained by condensing the middle node. In fact, the program is essentially the program in Desai and Able's finite element text (2) modified to incorporate the crack element.

A complete discussion of the entire program and its input requirements is given in Appendix B.

Operational Parameters

It is convenient to define certain parameters which are used to describe and discuss the crack element. The first parameter is ϵ .

$$\epsilon = (\text{Length of crack within crack element}) / (\text{Total Crack Length}) = a/c$$

The second parameter is the ratio a/l .

$$a/l = (\text{Length of crack within crack element}) / (\text{Length of Crack Element})$$

The last parameter is the ratio c/b .

$$c/b = (\text{Total crack length}) / (\text{Depth of Base})$$

The element shown in Figure 6 is used for all the finite element meshes in the solution procedure yet to be described. Because of the symmetry of the problem, the five node element is used here. It is desirable to use one element for all the meshes so that one can create and build meshes quickly and easily. This particular element is chosen for various reasons. First, it gives a reasonable value of a/l for all c/b ratios. A plot of a/l versus percent error in K_I is shown in Figure 7 for the crack element applied to the Bowie crack problem (5). The above element has a constant a/l ratio of 0.5. It is seen that this a/l ratio yields about a 3 percent error, which is relatively small.

A second reason that the element of Figure 6 is used is that as the crack propagates, ϵ remains within reasonable limits for accuracy. This can be seen from Figure 8, which is a plot of ϵ versus K_I for the Bowie crack problem (5). The element used in this research is the 2 element. From this plot, a value of $\epsilon > 0.2$ is needed to insure reasonable accuracy in K_I . In the solution process for the problem of this report, a maximum value of c/b of $1/2$ is used, and a minimum c/b value of $1/12$ is used. Also, the greatest b value is 16 inches, and the least is 8 inches. Thus, c_{\max} is 8 inches, and c_{\min} is $2/3$ inches. ϵ is therefore such that $0.03125 < \epsilon < 0.375$, and within the range of acceptable accuracy shown in Figure 8.

The above two reasons for using the element shown in Figure 6 are important, but many elements which satisfy the a/l and criteria could be created. The main reason to use the Figure 6 element is that it is small enough so that reverse stresses can be applied to enough of the crack length to make the solution process viable. For instance, c_{\min} is $2/3$ inches.

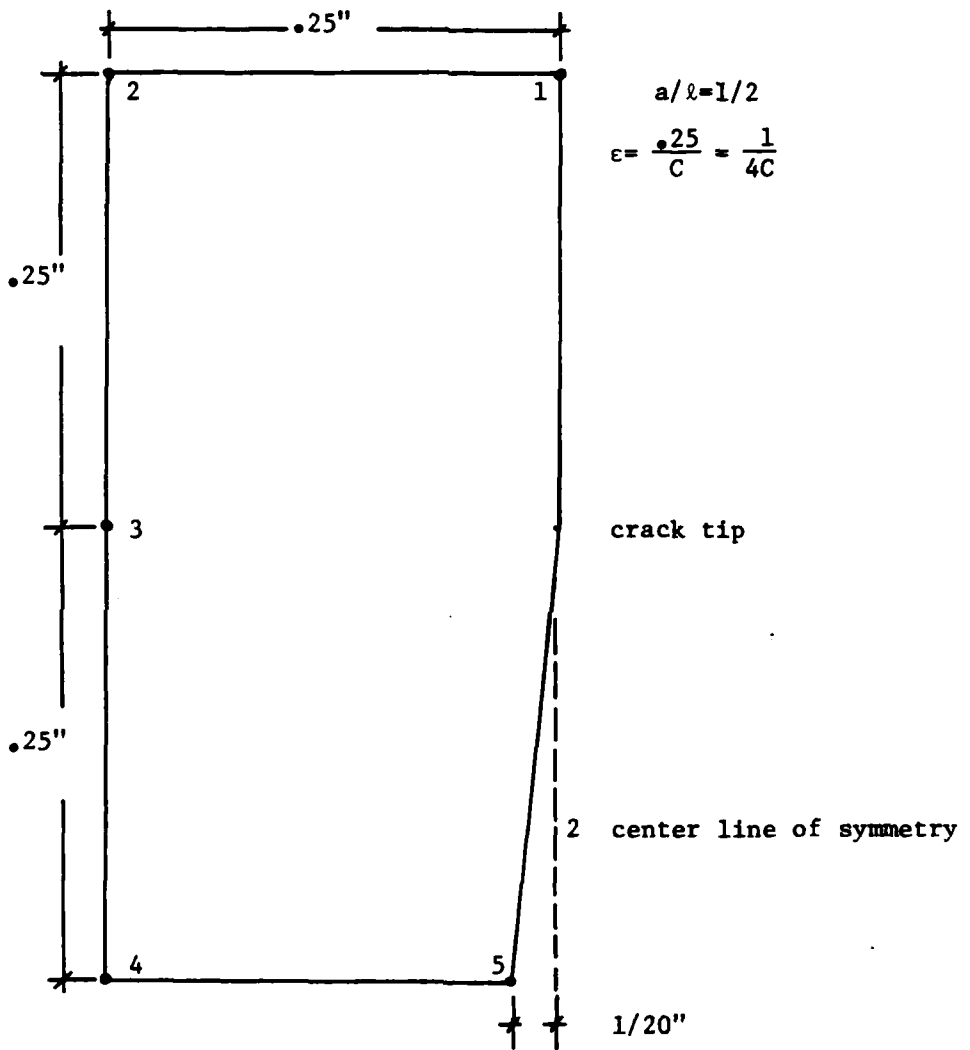


Figure 6. Crack Tip Element Used in Analyses

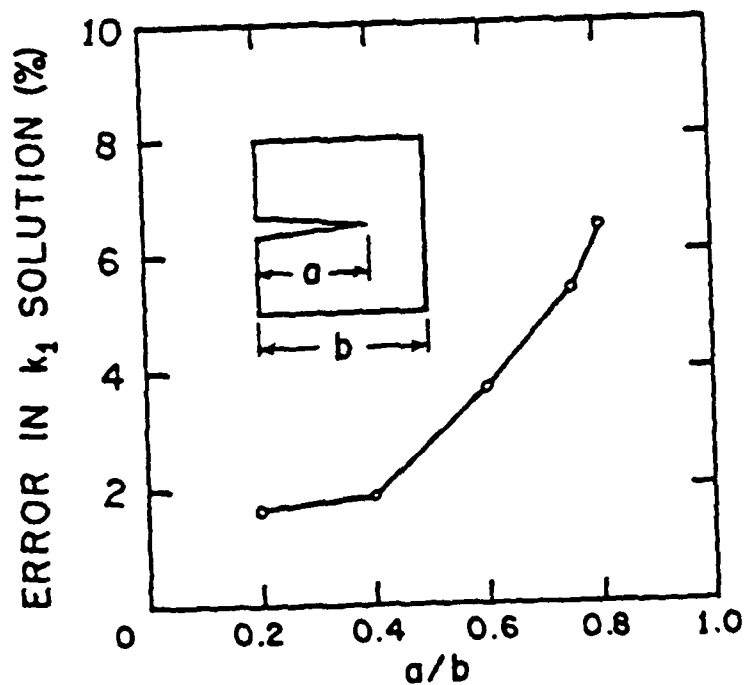


Figure 7. Illustration of Errors Produced By Variation in Crack Tip Length Within The Element (4)

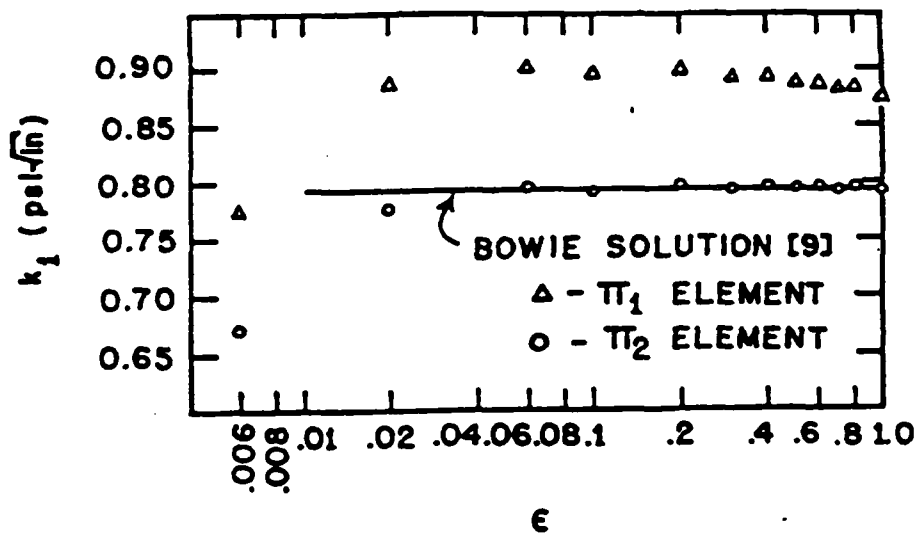


Figure 8. Illustration of Accuracy Related to Crack Tip Length (4)

With $a = 1/4$ inches, as in Figure 6, one can apply tractions to $5/12$ inches, or 62.5%, of the crack length. Remember, one cannot apply tractions to the portion of the crack within the crack element. The 62.5% value can be considered to be a significant amount and meaningful results can be obtained from it. However, as a increases, this percent value decreases and quickly becomes insignificant. If $a = c$, or $\epsilon = 1$, then there is no crack length available to apply reverse stresses to, and the solution philosophy outlined earlier 1 is impossible.

There will be five values of c/b used in the finite element analysis of each combination of base, overlay, and modulus. These are shown in Table 2. These values were chosen for accuracy, uniformity, and from an initial study that $c/b < 1/2$ was the most critical range. Concerning accuracy, it was seen above that $c/b = 1/2$ produced a maximum c for the 16 inch base of 8 inches and a minimum ϵ of 0.03125, which is very near the limit for accuracy of 0.02. Actually, the absolute greatest value of c possible is 16 inches in the 16 inch base, and for the element of Figure 6 this corresponds to an ϵ of 0.015625, which is quite close to 0.02. Therefore, accuracy is not a compelling reason to keep c/b less than $1/2$, although for c/b greater than $1/2$ one approaches the ragged edge of accuracy.

The uniformity criteria is mainly for convenience. For purposes of comparing trends in K_I distributions from one base-overlay combination to another, it is very helpful to have results computed for the same or similar c/b values. The differences seen in Table 2 for the 12 inch base are because of ease in mesh creation.

The main reason why $c/b < 1/2$ values are used is that it was thought that they were the most critical values, especially those $< 1/6$. This thought

Table 2. C/B Values Used in Analysis

BASE, IN	C/B VALUES
8, 16	1/12, 1/8, 1/6, 7/16, 1/2
12	1/12, 5/36, 1/6, 5/12, 1/2

arose from intuition and previous experience, and is not necessarily borne out by the results in Chapter III.

Other details concerning the element in Figure 6 should be addressed. In Figure 6, the side opposite the crack is straight. For other problems, like the Bowie crack problem, better results are obtained if the side is humped, as in Figure 9. For this problem, however, results using the humped element were poor. Thus the straight side is strongly recommended for this problem. Also, note that in Figure 6 an offset appears at the bottom of the element. This is to simulate the physical opening of the crack. For convenience, this offset is present all the way through the subgrade.

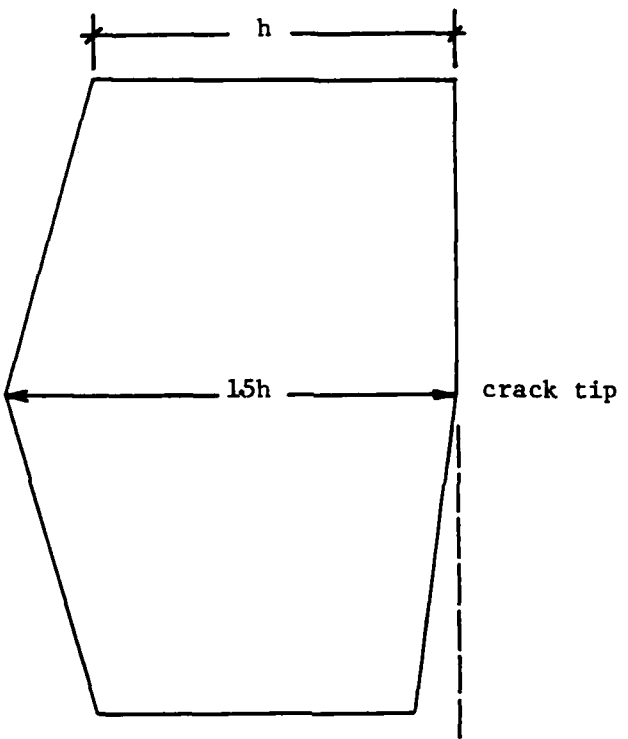


Figure 9. Example of a "Humped" Crack Tip Element

CHAPTER III: SOLUTION PROCEDURE

Development of Stress Distributions

The first step in the solution process is the calculation of the stress distributions to be used in superposition phases discussed in Chapter I. In this problem there is no crack, and thus the finite element program with no crack element can be used to calculate the stress distribution. A distribution must be found for each combination of base thickness, overlay thickness, and modulus to be analyzed. The following combinations are analyzed in this study: all modulus conditions for all base thicknesses with no surface, and all modulus conditions for a base thickness of 8 inches and surfacing of 3 and 6 inches. This information is summarized in Table 3. These specific combinations are analyzed so that all base thicknesses for a given surface (0 inches) can be compared, and all surfaces for a given base thickness (8 inches) can be compared. A sample mesh is shown in Figure 10 for reference. In this mesh, the base thickness is equal to 8 inches and the overlay thickness is 3 inches. The input corresponding to this mesh is listed in Appendix B, along with the corresponding output file. Note that the different modulus conditions can be achieved by simply changing the input values. Also note that the thickness of the meshes in this section is one inch, allowing the 270 psi load to be applied as a traction of the same magnitude.

The results are shown in Table 4. The numbers in the headings are element numbers, and correspond to the elements in the base, along the line of symmetry, where the cracks would run. Lower element numbers refer to elements at the bottom of the base, while higher numbers refer to elements at

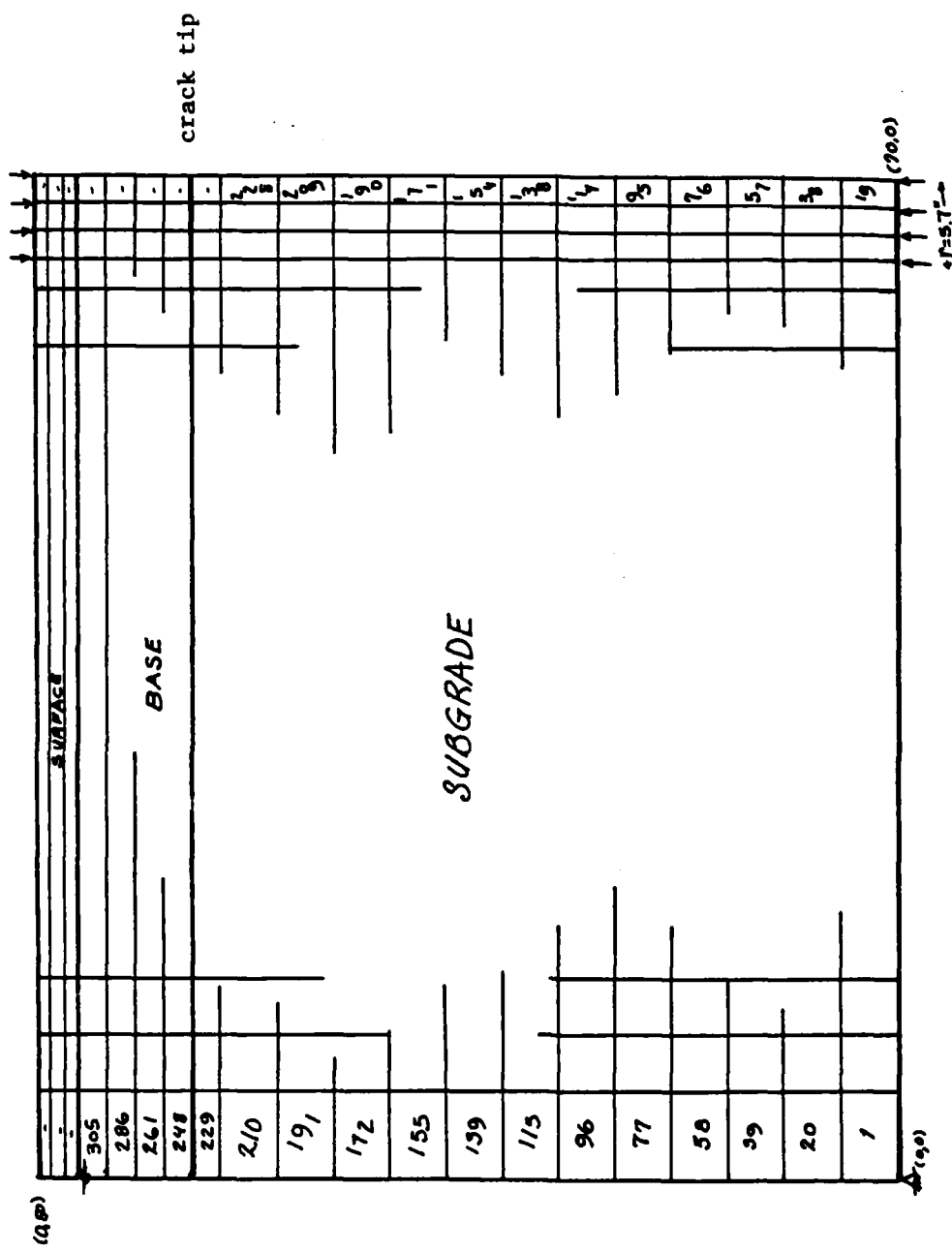


Figure 10. Finite Element Mesh Used for Pavement Structural Analysis

Table 3. Pavement Parameters Used in the Factorial Analysis

BASE, IN	SURFACE	MODULUS CONDITIONS
8	0	1-6
	3	
	6	
<hr/>		
12	0	1-6
<hr/>		
16	0	1-6
<hr/>		

Table 4. Stress Distributions for Superposition Phase one, psi

MC	8 inch base, no overlay				
	266	285	304	323	
1	1705.1	546.4	-584.5	-1772.1	
2	1229.7	383.75	-438.09	-1314.2	
3	1455.1	461.01	-507.06	-1530.6	
4	1032.3	315.74	-378.84	-1126.6	
5	1086.8	334.56	-395.06	-1178.2	
6	751.6	218.24	-297.81	-864.87	

MC	12 inch base, no overlay						
	266	285	304	323	342	361	
1	1205.5	704.01	234.94	-230.70	-725.58	-1279.1	
2	942.39	545.64	178.77	-185.68	-578.79	-1028.9	
3	1078.3	627.40	207.79	-208.84	-654.43	-1157.7	
4	807.06	464.26	149.79	-162.89	-503.95	-900.41	
5	845.81	487.56	158.10	-169.37	-525.31	-936.99	
6	597.49	338.45	104.64	-128.65	-389.89	-704.47	

MC	16 inch base, no overlay							
	266	285	304	323	342	361	380	
1	825.67	572.11	340.62	120.46	-98.98	-331.43	-597.65	-915.71
2	699.45	482.34	285.93	99.95	-85.69	-284.17	-515.73	-798.05
3	786.64	531.53	315.90	111.20	-92.96	-310.04	-560.58	-862.48
4	620.79	426.45	251.89	87.61	-77.50	-254.89	-464.93	-725.03
5	644.37	443.19	262.09	91.00	-79.94	-263.64	-480.13	-746.89
6	478.20	325.34	190.36	63.95	-62.95	-202.42	-373.73	-593.71

TABLE I-2(D): 8 inch base, 3 inch overlay					
MC	8 inch base, 3 inch overlay				
	266	285	304	323	
1	1466.0	629.89	-172.65	-998.51	
2	1075.8	457.60	-130.19	-741.01	
3	1232.9	566.90	-66.59	-717.41	
4	887.08	402.36	-53.30	-526.53	
5	903.29	469.46	69.95	-345.38	
6	632.18	321.91	37.94	-255.06	

MC	8 inch base, 6 inch overlay				
	266	285	304	323	
1	1190.6	615.34	69.38	-382.55	
2	911.27	467.40	50.40	-308.17	
3	1003.4	561.06	146.45	-376.58	
4	751.0	415.71	105.63	-296.51	
5	745.18	468.70	216.88	-312.75	
6	535.85	332.48	150.93	-236.52	

the top of the base. The numbers below the heading MC refer to the modulus condition, all of which are depicted previously in Table 1. The numbers below the element headings are the stresses at the element centroids, in psi. A positive value denotes tension. The stresses for modulus condition one in each table are graphed in Figure 11.

Linearize Stress Distributions

As can be seen from Figure 11, the stress distributions are very nearly linear, especially in the range of Y coordinate values which encompass the crack lengths to be investigated, up to 1/2 the base thicknesses. As a result, for the purpose of applying the reverse stresses to the crack lengths, it is expedient to linearize the stress distributions by assuming a linear distribution between each element centroid. Note that element centroids are two inches apart in Figures 10 and 11. This is because each horizontal line of elements in the base is two inches thick, for all meshes. Figure 10 shows an 8 inch base. Additional elements for 12 and 16 inch bases shown in Table 4 reflect these supplemental lines of elements.

The linearized distributions are given in Table 5. Listed are the slopes, m , and the initial stress value for each interval between element centroids. Values are listed for each modulus condition. The intervals are delineated by the Y coordinate values of the appropriate element centroids. Only intervals up to 1/2 the base thickness are listed. Note that the interval between the lowest element centroids, that is between 51 and 53 inches, is extended to the bottom of the base, which is located at a Y value of 50 inches. The stress at the bottom of the base is unknown, and the same slope that acts between 51 and 53 inches is assumed to hold between 50 and 51. The stress at the bottom of the base, or the value for the initial

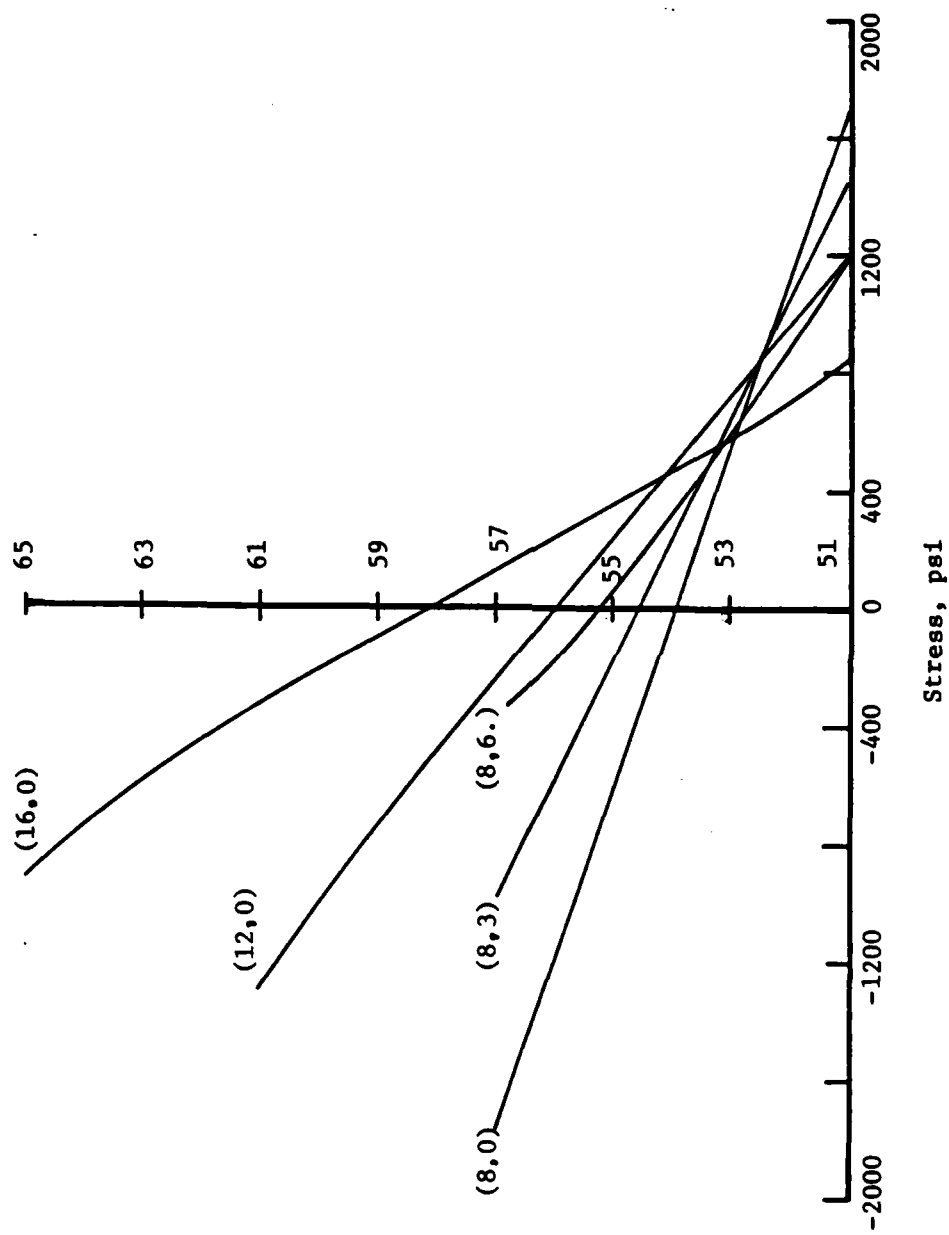


Figure 11. Stress Distributions for Modulus Condition 1, Parenthesis Contain Base Thickness and Surface Thickness Respectively

Table 5. Linearized Stress Distributions, psi

8 inch base, no overlay

MC	<u>50-53 inches</u>		<u>53-55 inches</u>	
	m	n	m	n
1	579.35	2284.5	565.45	546.40
2	422.98	1672.7	410.92	383.75
3	497.05	1952.1	484.04	461.01
4	358.28	1390.6	347.29	315.74
5	376.12	1462.9	364.81	334.56
6	266.68	1018.3	258.03	218.24

12 inch base, no overlay

MC	<u>50-53 inches</u>		<u>53-55 inches</u>		<u>55-57 inches</u>	
	m	n	m	n	m	n
1	250.75	1456.3	234.54	704.01	232.82	234.94
2	198.38	1140.8	183.44	545.64	182.23	178.77
3	225.45	1303.8	209.81	627.40	208.32	207.79
4	171.40	978.50	157.24	464.26	156.34	149.79
5	179.13	1024.9	164.23	487.56	163.74	158.10
6	129.52	727.01	116.91	338.45	116.65	104.64

16 inch base, no overlay

MC	<u>50-53 inches</u>		<u>53-55 inches</u>		<u>55-57 inches</u>		<u>57-59 inches</u>	
	m	n	m	n	m	n	m	n
1	126.28	951.95	115.75	572.11	110.08	340.62	109.72	120.46
2	108.56	808.01	98.21	482.34	92.99	285.93	92.82	99.95
3	127.56	914.19	107.82	531.53	102.35	315.90	102.08	111.20
4	97.17	717.95	87.28	426.45	82.14	251.89	82.55	87.61
5	100.59	744.96	90.55	443.19	85.55	262.09	85.47	91.00
6	76.43	554.63	67.49	325.34	63.21	190.36	63.45	63.95

8 inch base, 3 inch overlay

MC	<u>50-53 inches</u>		<u>53-55 inches</u>	
	m	n	m	n
1	418.06	1884.1	401.27	629.89
2	309.10	1384.9	293.90	457.60
3	333.0	1565.9	316.75	566.90
4	242.36	1129.4	227.83	402.36
5	216.92	1120.2	201.76	469.46
6	155.14	787.30	141.99	321.91

8 inch base, 6 inch overlay

MC	<u>50-53 inches</u>		<u>53-55 inches</u>	
	m	n	m	n
1	287.63	1478.2	272.98	615.34
2	221.94	1133.2	208.50	467.40
3	221.17	1224.6	207.31	561.06
4	167.65	918.65	155.04	415.71
5	138.24	883.42	125.91	468.70
6	101.69	637.54	90.78	332.48

interval of 50-53 inches, is obtained by adding this slope to the stress at the first element centroid, located a unit distance away at 51 inches. Since there is a material (and thus stress) discontinuity between the base and the subgrade it is impossible to obtain the stress at the bottom of the base from the nearest subgrade element. It is thus necessary to assume something, and the above procedure is consistent with the concept of linearized stress distributions.

Mesh Considerations for Finite Element Runs

The sample mesh shown in Figure 12 is for a base of 8 inches, a surface of 3 inches, and a crack length of 3.5 inches (c/b of 0.4375). Also shown is an enlargement of a section of mesh in the base which is too fine to represent with the rest and an enlargement of the area immediately surrounding the crack element. This crack element and the area immediately surrounding it is common to all meshes. There is a mesh for each crack length in each base-overlay combination. The common crack element enables one to build one mesh from another quickly and easily and to be able to efficiently execute the analysis. As discussed in Chapter II, there are five crack lengths to be investigated for each base-overlay combination, and there are five base-overlay combinations targeted for analysis. Thus, there are 25 separate meshes to be considered and the efficiency afforded by a common crack element is essential.

The maximum aspect ratio in these meshes is 40:1. This occurs as far away from the crack element as possible. Near the crack, the aspect ratios are very nearly 1:1. Thus, near the crack where greater accuracy is required, the mesh is in its most accurate configuration, and far from the

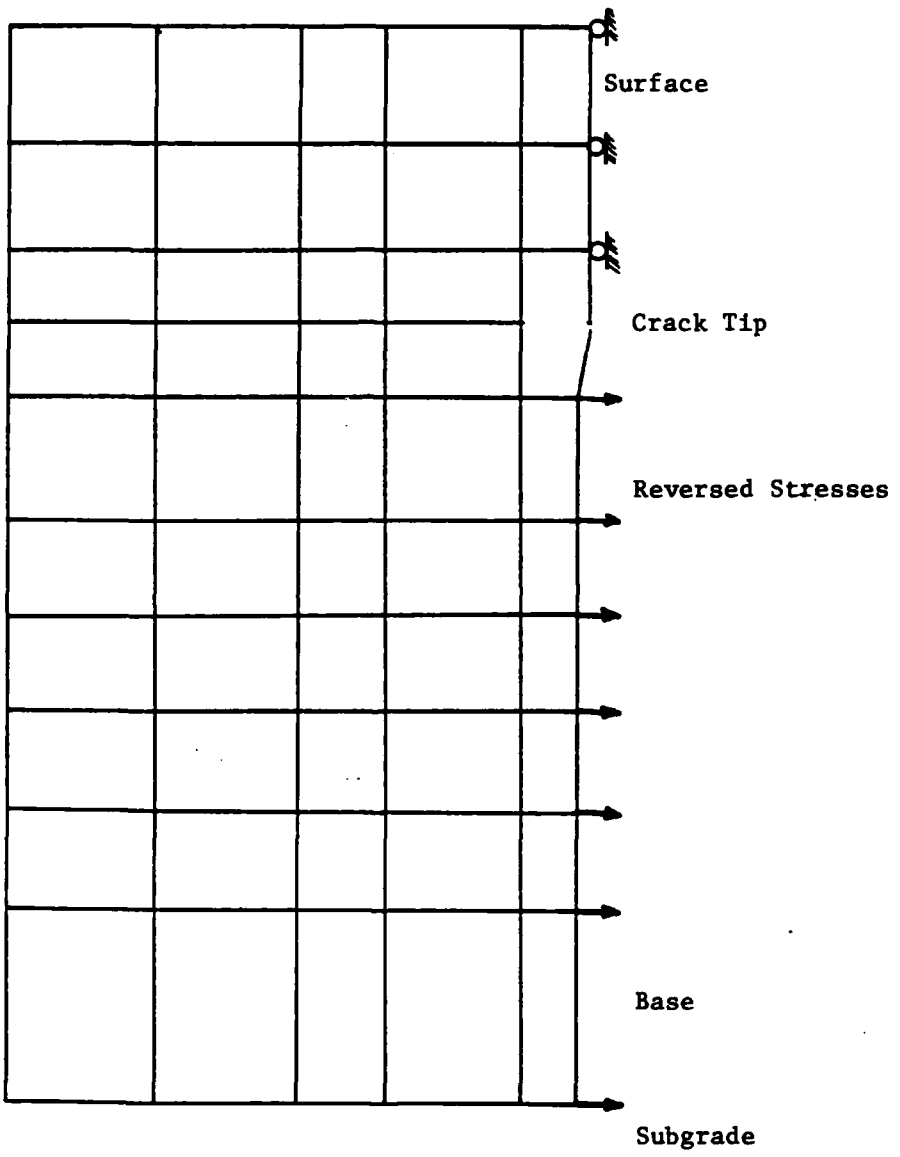


Figure 12. Illustration of Mesh Around Crack

crack where accuracy is not critical, the mesh is in its least accurate configuration.

The thickness of all the meshes of this section is one inch. Therefore, all stresses applied as loads transfer as tractions of the same magnitude.

The input file corresponding to Figure 11 is listed in Appendix B.

Applying Reverse Stresses to Crack Lengths

The linearized stresses shown above are applied to the meshes created above with a reverse sign. Note that there is one mesh for each base-surface combination and one linearized stress distribution for each modulus condition of each base-surface combination. Therefore, there are $25*6 = 150$ different files to be run in the finite element program. Reverse stress values calculated for the mesh shown in Figures 11 with modulus condition one are given in Table 6. These values also appear in the input file for the mesh in Figure 11 that is listed in Appendix B. Note that the values in the input file have units of force/length, not stress, but have the same magnitude as the stresses in Table 6. This is because the thicknesses of all meshes is one inch. A positive sign indicates a stress in the positive X direction.

Uncorrected K_I Values

Each of the 150 runs took between 1.50 and 3.00 minutes on a Harris 800 super mini-computer. The results are listed in Table 7. The values in the tables are uncorrected stress intensity factors in $\text{psi}/\sqrt{\text{inch}}$. The negative signs indicate that the reverse stresses act to close the crack. In actuality, these stress intensity factors are positive, because the crack is

Table 6. An Example of a Reverse Stress Profile for Figure 3, MC=1.

<u>Y COORDINATE, IN</u>	<u>REVERSE STRESS, PSI</u>
50.0	1884.1
50.833	1535.7
51.5	1257.0
51.833	1117.6
52.167	978.27
52.5	838.92
52.833	699.57
53.25	525.38

Table 7. Uncorrected Stress Intensity Factors, psi/ $\sqrt{\text{in}}$

MC	<u>8 inch base, no surface</u> <u>C/B</u>				
	1/12	1/8	1/6	7/16	1/2
1	-916.20	-1263.99	-1490.41	-2372.08	-2387.92
2	-653.28	-891.83	-1044.41	-1585.38	-1576.26
3	-778.18	-1068.65	-1256.70	-1959.78	-1962.35
4	-543.48	-735.67	-857.06	-1257.04	-1238.55
5	-573.83	-778.89	-908.91	-1347.53	-1331.49
6	-387.04	-512.59	-589.87	-801.68	-773.87

MC	<u>12 inch base, no surface</u> <u>C/B</u>				
	1/12	5/36	1/6	5/12	1/2
1	-798.13	-1147.78	-1216.62	-1490.31	-1388.27
2	-613.84	-878.07	-927.64	-1105.32	-1017.78
3	-709.19	-1017.63	-1077.19	-1304.38	-1209.25
4	-518.45	-738.42	-778.06	-906.79	-827.16
5	-545.82	-778.48	-820.98	-963.63	-881.70
6	-369.66	-520.76	-545.04	-601.43	-535.64

MC	<u>16 inch base, no surface</u> <u>C/B</u>				
	1/12	1/8	1/6	7/16	1/2
1	-603.00	-779.24	-913.42	-870.49	-783.82
2	-502.45	-647.50	-757.11	-704.63	-631.38
3	-572.40	-736.91	-860.32	-800.74	-725.99
4	-439.56	-565.24	-659.70	-602.85	-537.92
5	-458.43	-589.91	-688.91	-633.19	-535.64
6	-325.38	-416.05	-483.27	-420.69	-371.11

MC	<u>8 inch base, 3 inch surface</u> <u>C/B</u>				
	1/12	1/8	1/6	7/16	1/2
1	-763.07	-1165.89	-2161.30	-1962.77	-2009.58
2	-553.75	-837.89	-1540.76	-1360.62	-1382.10
3	-630.24	-957.27	-1758.64	-1593.91	-1633.61
4	-446.75	-669.68	-1218.07	-1066.60	-1082.68
5	-443.83	-664.67	-1198.61	-1083.01	-1110.89
6	-303.38	-444.61	-791.12	-682.53	-691.41

MC	<u>8 inch base, 6 inch surface</u> <u>C/B</u>				
	1/12	1/8	1/6	7/16	1/2
1	-596.74	-906.85	-1655.76	-1532.27	-1579.01
2	-452.21	-681.49	-1237.18	-1122.00	-1150.22
3	-490.88	-741.00	-1338.24	-1243.83	-1284.41
4	-362.56	-541.13	-970.67	-880.61	-903.77
5	-348.11	-517.56	-915.72	-855.82	-884.99
6	-245.00	-357.48	-627.08	-567.97	-582.97

opened by the loads on the pavement. However, as mentioned previously, the magnitudes of these numbers are correct.

A sample output file is given in Appendix B. This output file corresponds to the input file in Appendix B that was discussed previously.

Stress Intensity Correction Factors

The equation used to compute the correction factors is given by equation (2) of Chapter I. In this equation, σ_e is the stress in the vicinity of the crack tip that would be applied to the portion of the crack within the crack element, if that were allowed. Because the reverse stress distribution is assumed to be linear with depth, there is no one value of reverse stress in the vicinity of the crack tip. σ_e is then defined as the average value of the reverse stress that would be applied to the length of the crack within the crack element. The average reverse stress is the stress that would be applied halfway from the crack tip to the edge of the crack element. If Y is the vertical coordinate of the crack tip, then σ_e acts at $Y = Y - z/2$. The value of z , the length of crack within the crack element, is 1/4 inches.

A negative correction factor indicates that the reverse stresses to be applied act in a manner which closes the crack. They add with the negative stress intensity factors computed in the previous section to increase the magnitude of K_I . Positive correction factors add to decrease the magnitude of the stress intensity factor.

The computed correction factors are given in Table 8. The computed stress intensity factors are added to the correction factors in order to find the final values of K_I .

Table 8. Stress Intensity Correction Factors, psi/in

MC	<u>8 inch base, no surface</u> C/B				
	1/12	1/8	1/6	7/16	1/2
1	-1572.34	-1418.26	-1264.17	-262.62	-31.492
2	-1135.84	-1023.34	-910.85	-179.63	-10.889
3	-1342.77	-1210.58	-1078.38	-219.11	-20.821
4	-954.68	-859.39	-764.10	-144.72	-1.791
5	-1004.65	-904.65	-804.62	-154.40	-4.352
6	-697.21	-626.29	-555.36	-94.34	12.052

MC	<u>12 inch base, no surface</u> C/B				
	1/12	5/36	1/6	5/12	1/2
1	-986.86	-853.48	-786.79	-186.60	13.470
2	-771.70	-666.18	-613.42	-138.58	19.698
3	-882.84	-762.92	-702.96	-163.31	16.571
4	-661.04	-569.86	-524.28	-114.01	22.752
5	-692.72	-597.44	-549.08	-121.04	21.881
6	-489.65	-420.75	-386.30	-76.28	27.064

MC	<u>16 inch base, no surface</u> C/B				
	1/12	1/8	1/6	7/16	1/2
1	-637.80	-570.63	-503.46	-66.84	33.914
2	-540.04	-482.29	-424.59	-49.22	37.393
3	-606.45	-538.60	-470.75	-29.73	72.049
4	-479.16	-427.47	-375.79	-39.82	37.711
5	-497.41	-443.91	-390.40	-42.61	37.649
6	-368.85	-328.19	-287.53	-23.28	37.705

MC	<u>8 inch base, 3 inch surface</u> C/B				
	1/12	1/8	1/6	7/16	1/2
1	-1322.58	-1211.39	-1100.21	-382.52	-222.43
2	-971.40	-889.19	-806.98	-277.18	-159.93
3	-1105.49	-1016.92	-928.36	-357.55	-231.19
4	-796.42	-731.96	-667.50	-252.87	-161.98
5	-800.05	-742.36	-684.66	-314.21	-233.72
6	-561.14	-519.88	-478.62	-214.36	-157.72

MC	<u>8 inch base, 6 inch surface</u> C/B				
	1/12	1/8	1/6	7/16	1/2
1	-1055.15	-978.65	-902.15	-409.29	-300.39
2	-808.25	-749.22	-690.20	-310.55	-227.37
3	-881.48	-822.66	-763.83	-385.63	-302.93
4	-660.52	-615.93	-571.34	-285.30	-223.45
5	-645.12	-608.36	-571.59	-336.30	-286.07
6	-464.73	-437.69	-410.64	-238.12	-201.91

The final values of K_I are given in Table 9 and illustrated in Figure 13 through Figure 17. Note that the values of K_I are positive. The actual stress intensity factors are equal in magnitude but opposite in sign to the computed ones; that is, they indicate that the crack will open under load, not close.

From the tables and graphs it can be seen that the K_I values for the 8 inch base, no surface, are greater than those of the other pavements with no surfaces. The 16 inch base has the least K_I values of the above pavements. This is intuitively reasonable. Adding a 3 inch surface to the 8 inch base generally decreases the stress intensity factors, although the K_I values for $c/b = 1/6$ are greater. For the 6 inch surface, the K_I values are less than their counterparts in the no surface case for all the c/b values for which stress intensity factors are calculated.

Table 9. Corrected Stress Intensity Factors

<u>8 inch base, no surface</u> <u>C/B</u>					
<u>MC</u>	<u>1/12</u>	<u>1/8</u>	<u>1/6</u>	<u>7/16</u>	<u>1/2</u>
1	2488.5	2682.2	2754.6	2634.7	2419.4
2	1789.1	1915.2	1955.2	1765.0	1587.1
3	2120.9	2279.2	2335.1	2178.9	1983.2
4	1498.2	1595.1	1621.2	1401.8	1240.3
5	1587.5	1683.5	1713.5	1501.9	1335.8
6	1084.2	1138.9	1145.2	896.02	761.82

<u>12 inch base, no surface</u> <u>C/B</u>					
<u>MC</u>	<u>1/12</u>	<u>5/36</u>	<u>1/6</u>	<u>5/12</u>	<u>1/2</u>
1	1785.0	2001.3	2003.4	1676.9	1374.8
2	1385.5	1544.2	1541.1	1243.9	998.08
3	1592.0	1780.6	1780.2	1467.7	1192.7
4	1179.5	1308.3	1302.3	1020.8	804.41
5	1238.5	1375.9	1370.8	1084.7	859.81
6	859.31	941.51	931.34	677.71	508.57

<u>16 inch base, no surface</u> <u>C/B</u>					
<u>MC</u>	<u>1/12</u>	<u>1/8</u>	<u>1/6</u>	<u>7/16</u>	<u>1/2</u>
1	1240.8	1349.9	1416.9	937.34	749.90
2	1042.5	1129.8	1181.7	753.85	593.99
3	1178.8	1275.5	1331.1	830.47	653.94
4	918.72	992.71	1035.5	642.67	500.21
5	955.84	1033.8	1079.3	675.80	528.11
6	694.22	744.24	770.81	443.97	333.40

<u>8 inch base, 3 inch surface</u> <u>C/B</u>					
<u>MC</u>	<u>1/12</u>	<u>1/8</u>	<u>1/6</u>	<u>7/16</u>	<u>1/2</u>
1	2085.7	2377.3	3261.5	2354.3	2232.0
2	1525.2	1727.1	2347.7	1637.8	1542.0
3	1735.7	1974.2	2687.0	1951.5	1864.8
4	1243.2	1401.6	1885.6	1319.5	1244.7
5	1243.9	1407.0	1883.3	1397.2	1344.6
6	864.52	964.5	1269.7	896.89	849.13

<u>8 inch base, 6 inch surface</u> <u>C/B</u>					
<u>MC</u>	<u>1/12</u>	<u>1/8</u>	<u>1/6</u>	<u>7/16</u>	<u>1/2</u>
1	1651.9	1885.5	2557.9	1941.6	1879.4
2	1260.5	1430.7	1927.4	1432.5	1377.6
3	1372.4	1563.7	2102.1	1629.5	1587.3
4	1023.1	1157.1	1542.0	1165.9	1127.2
5	993.24	1125.9	1487.3	1192.1	1171.1
6	709.73	795.17	1037.7	806.09	784.90

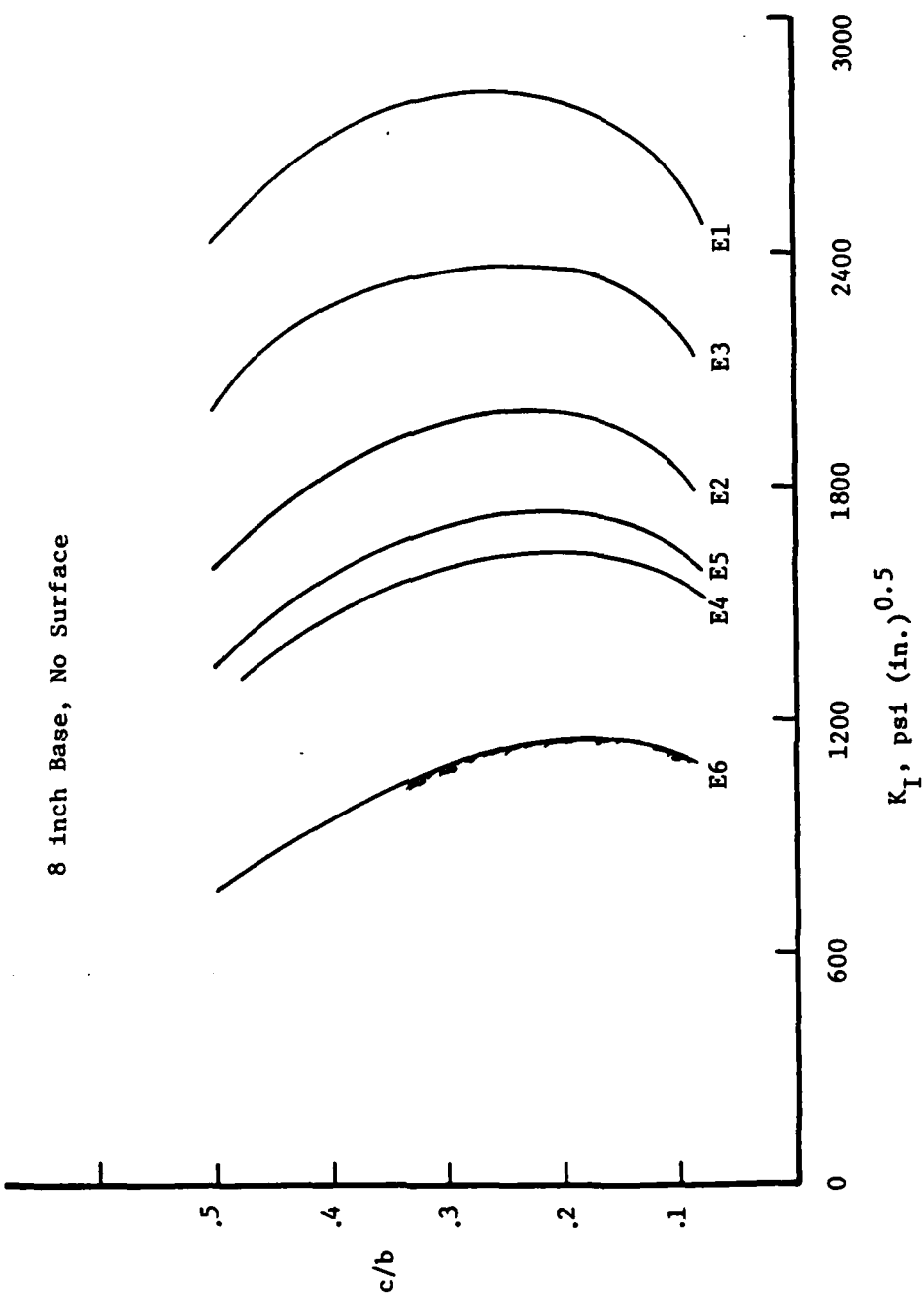


Figure 13. Distribution of Stress Intensity Factor

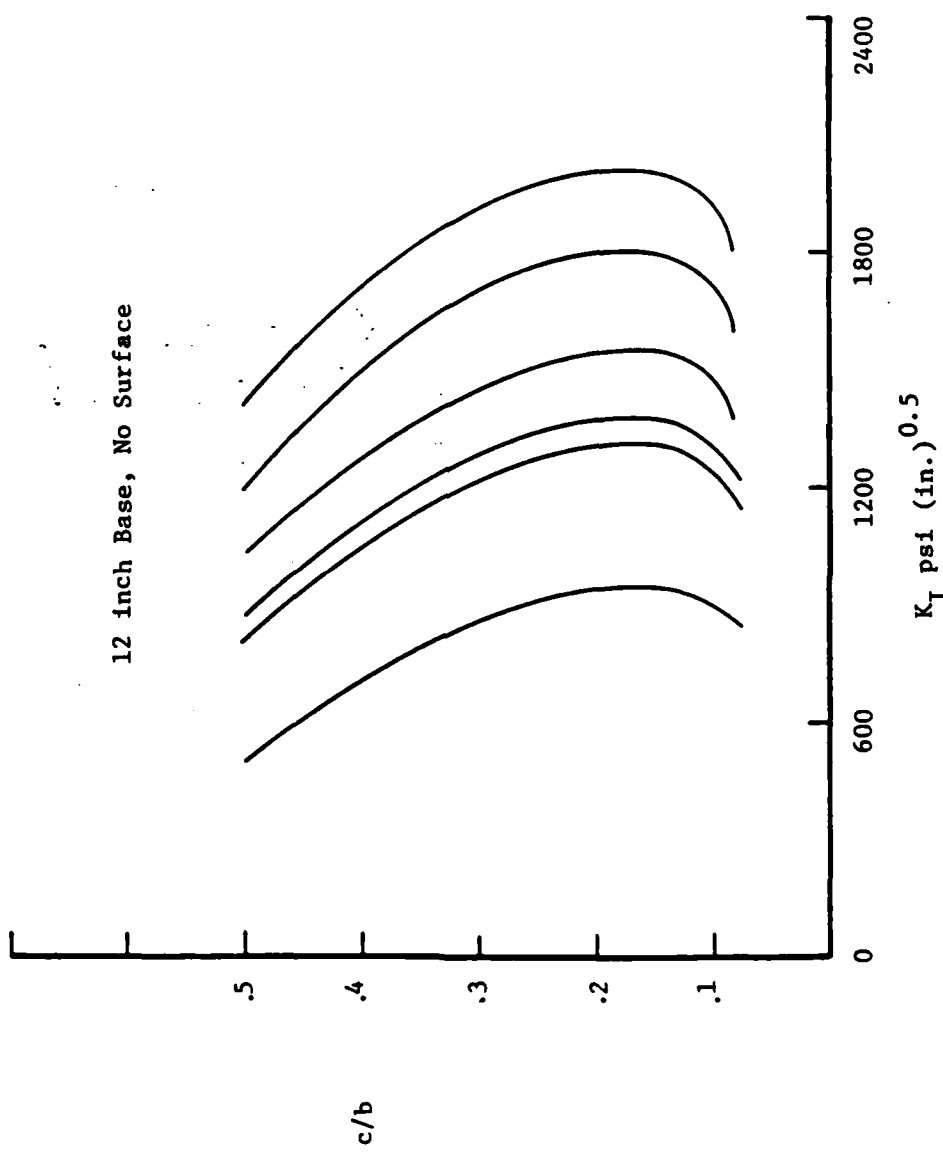


Figure 14. Distribution of Stress Intensity Factor

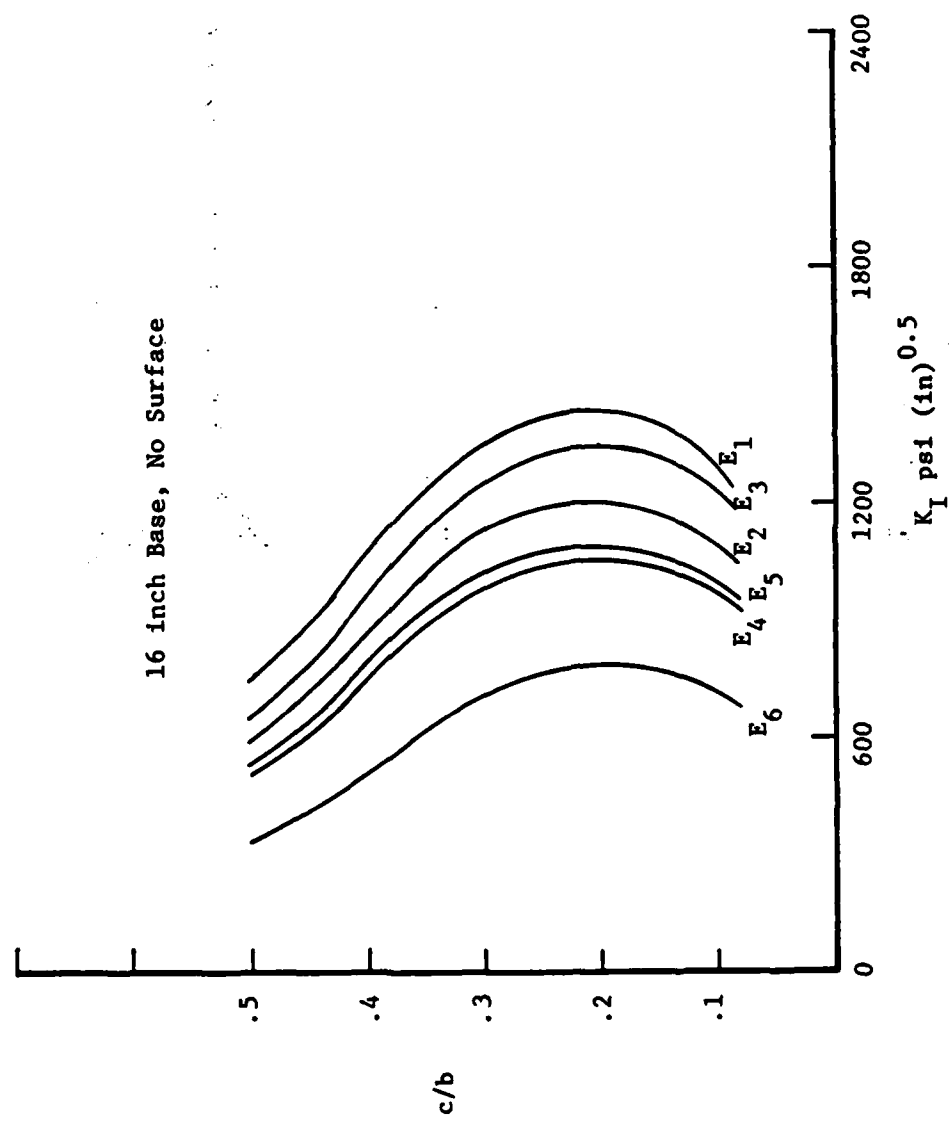


Figure 15. Stress Intensity Factor Distribution

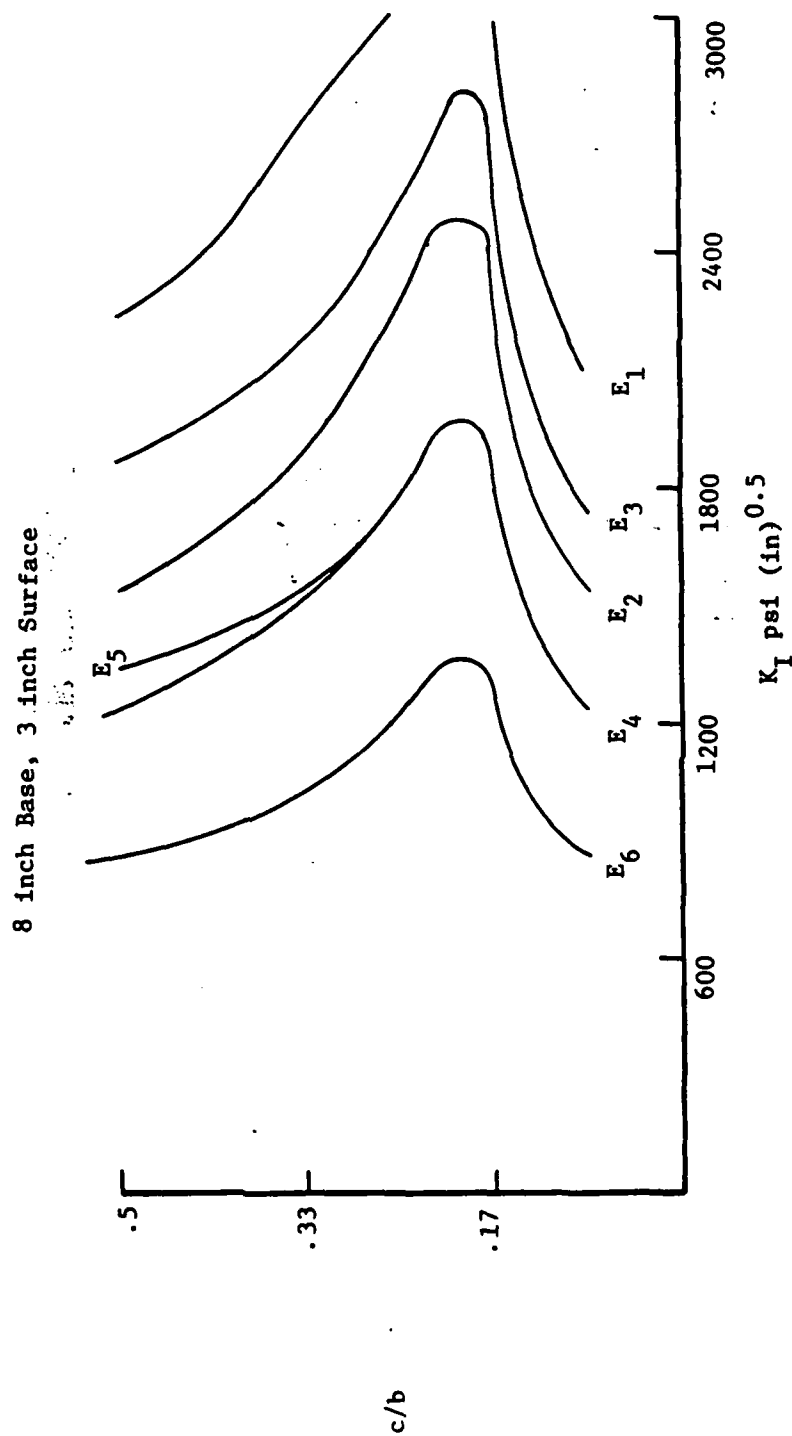


Figure 16. Stress Intensity Factor Distribution

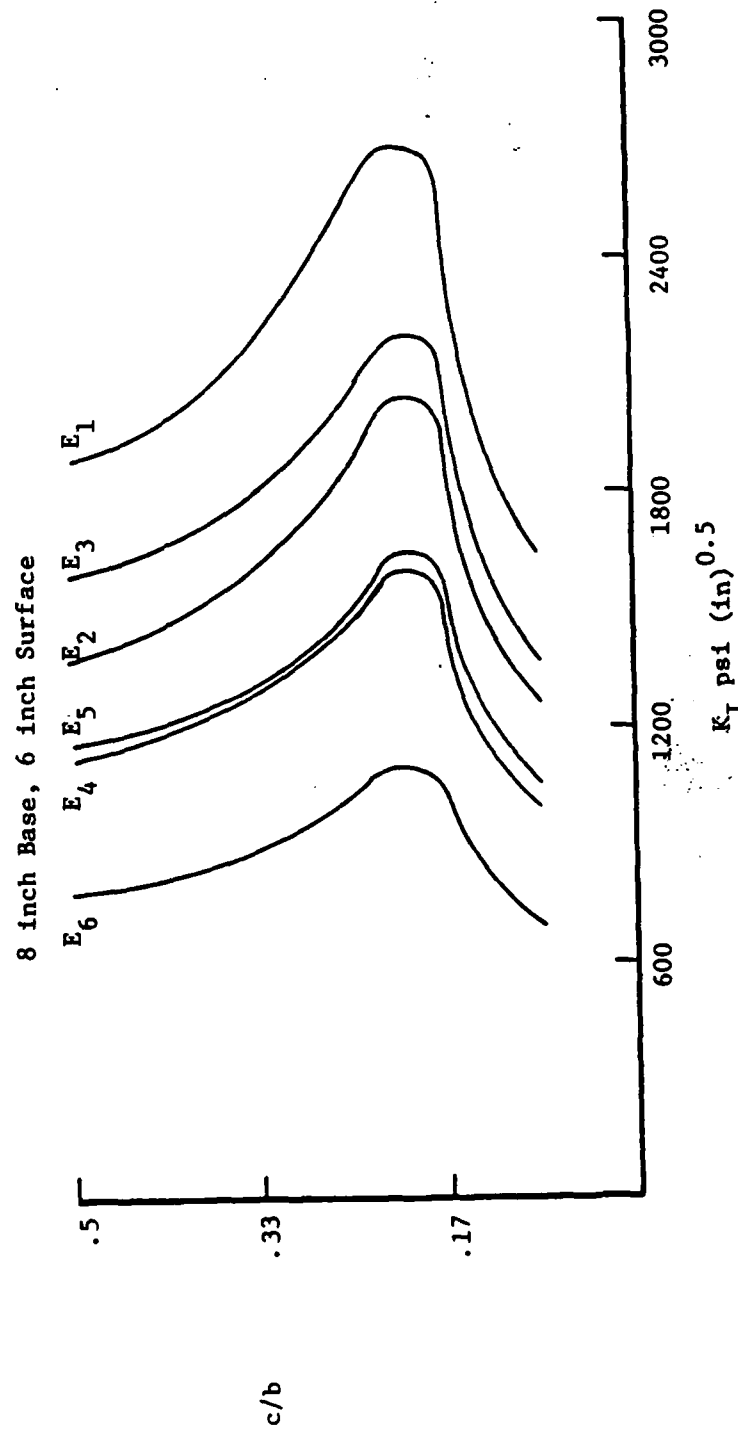


Figure 17. Stress Intensity Factor Distribution

CHAPTER IV: CALCULATING FRACTURE LIFE

Regression Equations for Stress Intensity Factors

In order to compute a fracture life for the pavement system the stress intensity factor distribution must be calculated for every combination of pavement and loading, and then this distribution must be used in the Paris equation. A simpler approach is to develop a series of regression equations to describe the distribution of the stress intensity factor. This eliminates the need to rerun the finite element program a large number of times to develop a series of stress intensity factors differing only slightly from each other. The equation must relate K_I to c/b .

Examining the graphs of the stress intensity factor distribution shown in the previous chapter, it is reasonable to assume a cubic distribution of K_I versus c/b , especially for the cases with no overlay. In order to define this assumed cubic relationship, regression techniques are used. A statistical package on the IBM personal computer was utilized to find the best fit coefficients to a cubic distribution. The results of the polynomial regression analysis are given in Table 10. The R^2 parameters of the regression are also listed. A value of $R^2 = 1.0$ denotes a perfect fit. Note that the fit is very good for the cases with no surface, and satisfactory for those with a surface. Plots of K_I versus c/b for both the cubic distribution and the distributions of the previous section are shown for representative cases in Figure 18 through Figure 22.

For reasons discussed previously, the range of c/b values for which stress intensity factors were computed extend from $1/12$ to $1/2$. For no c/b

Table 10. Regression Coefficients for Cubic Polynomial
Fit to Stress Intensity Distribution.

$$K = B_0 + B_1(C/B) + B_2(C/B)^2 + B_3(C/B)^3$$

MC	<u>8 inch base, no surface</u>				<u>R²</u>
	<u>B₀</u>	<u>B₁</u>	<u>B₂</u>	<u>B₃</u>	
1	2047.043	6567.108	-14172.16	5067.807	0.9861128
2	1490.105	4544.518	-10815.35	4237.885	0.9940159
3	1753.576	5513.253	-12415.28	4625.061	0.9903571
4	1260.895	3666.674	-9340.74	3857.532	0.9966238
5	1351.920	3600.485	-8792.111	3060.146	0.9971226
6	938.9210	2345.091	-6942.935	3093.236	0.9988023

MC	<u>12 inch base, no surface</u>				<u>R²</u>
	<u>B₀</u>	<u>B₁</u>	<u>B₂</u>	<u>B₃</u>	
1	1297.536	7693.483	-22383.32	14619.22	0.9951294
2	1019.034	5847.388	-17613.80	11676.70	0.9962779
3	1162.857	6804.254	-20087.00	13202.72	0.9957248
4	875.8471	4887.160	-15129.88	10145.02	0.9968587
5	916.8071	5163.552	-15845.97	10587.44	0.9966850
6	654.5362	3373.223	-11169.04	7681.451	0.9978152

MC	<u>16 inch base, no surface</u>				<u>R²</u>
	<u>B₀</u>	<u>B₁</u>	<u>B₂</u>	<u>B₃</u>	
1	808.9672	6928.043	-22642.82	17098.41	0.9999410
2	687.1326	5742.700	-19189.89	14661.88	0.9998762
3	776.4540	6547.792	-22345.70	17517.90	0.9998906
4	611.02611	5000.017	-16980.85	13073.25	0.9999341
5	633.80810	5223.816	-17649.63	13556.44	0.9999398
6	472.87540	3650.309	-12930.04	10141.79	0.9998798

MC	<u>8 inch base, 3 inch surface</u>				<u>R²</u>
	<u>B₀</u>	<u>B₁</u>	<u>B₂</u>	<u>B₃</u>	
1	-394.5381	37465.05	-117437.1	105884.90	0.8500299
2	-235.5056	26687.00	-84582.00	76535.600	0.8609347
3	-280.6712	30515.79	-96126.81	87240.120	0.8503666
4	-137.2445	20948.11	-66598.86	60381.990	0.8641640
5	-112.6183	20547.46	-64805.32	59002.900	0.8512328
6	-12.82105	13339.98	-42658.10	38802.090	0.8696607

MC	<u>8 inch base, 6 inch surface</u>				<u>R²</u>
	<u>B₀</u>	<u>B₁</u>	<u>B₂</u>	<u>B₃</u>	
1	-247.4966	28694.99	-89707.74	81544.99	0.8456994
2	-148.9915	21328.18	-67057.85	60936.81	0.8496895
3	-153.3865	23050.09	-71954.05	65549.56	0.8465933
4	-72.99951	16591.39	-52166.28	47507.98	0.8494838
5	-35.03687	15331.10	-48342.45	44153.58	0.8497349
6	17.19202	10486.71	-32985.49	30127.45	0.8487314

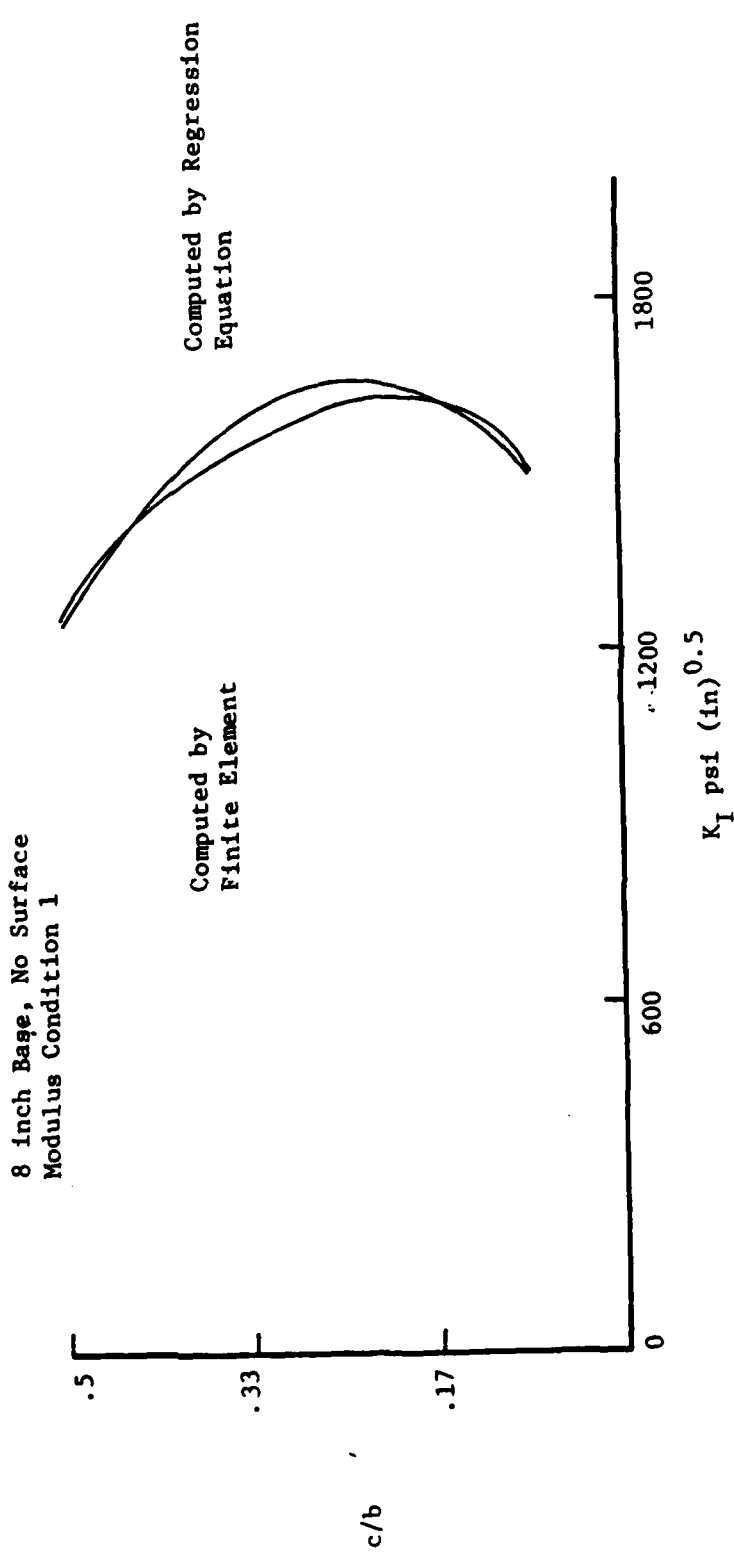


Figure 18. Comparison of Computed and Regression Stress Intensity Factors

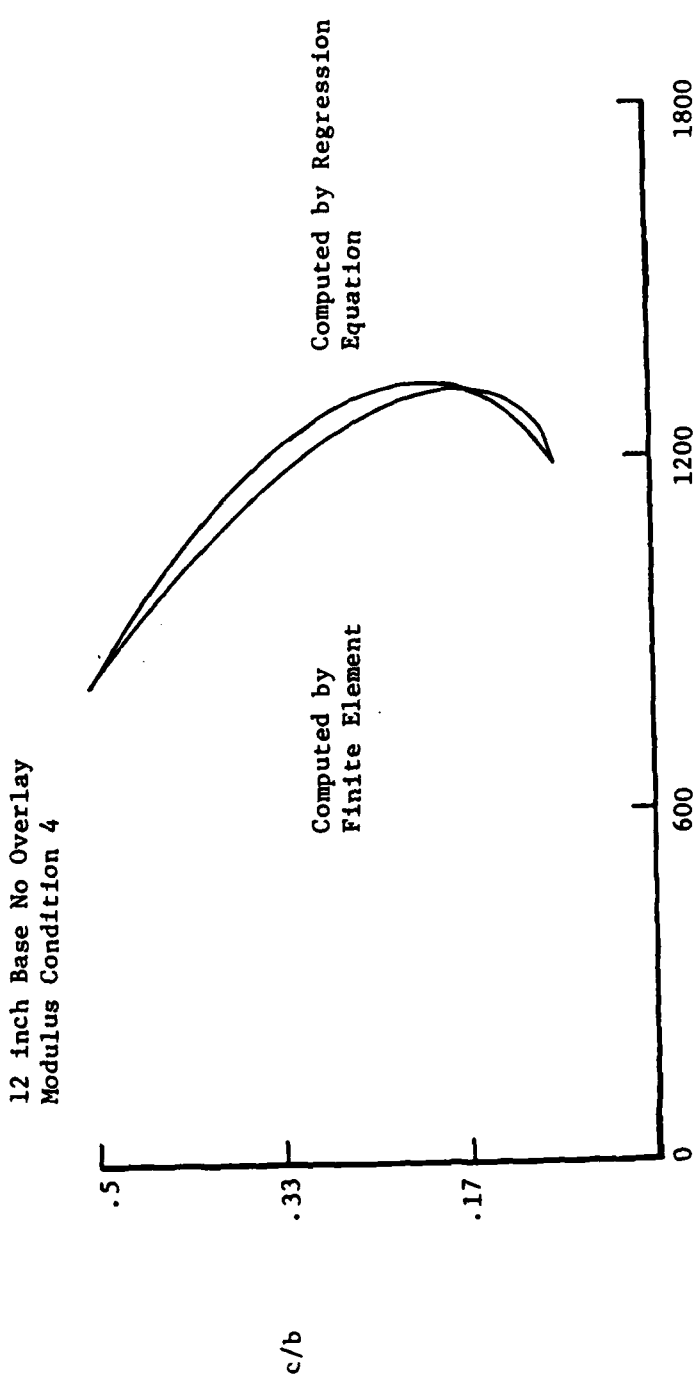


Figure 19. Comparison of Computed and Regression Stress Intensity Factors

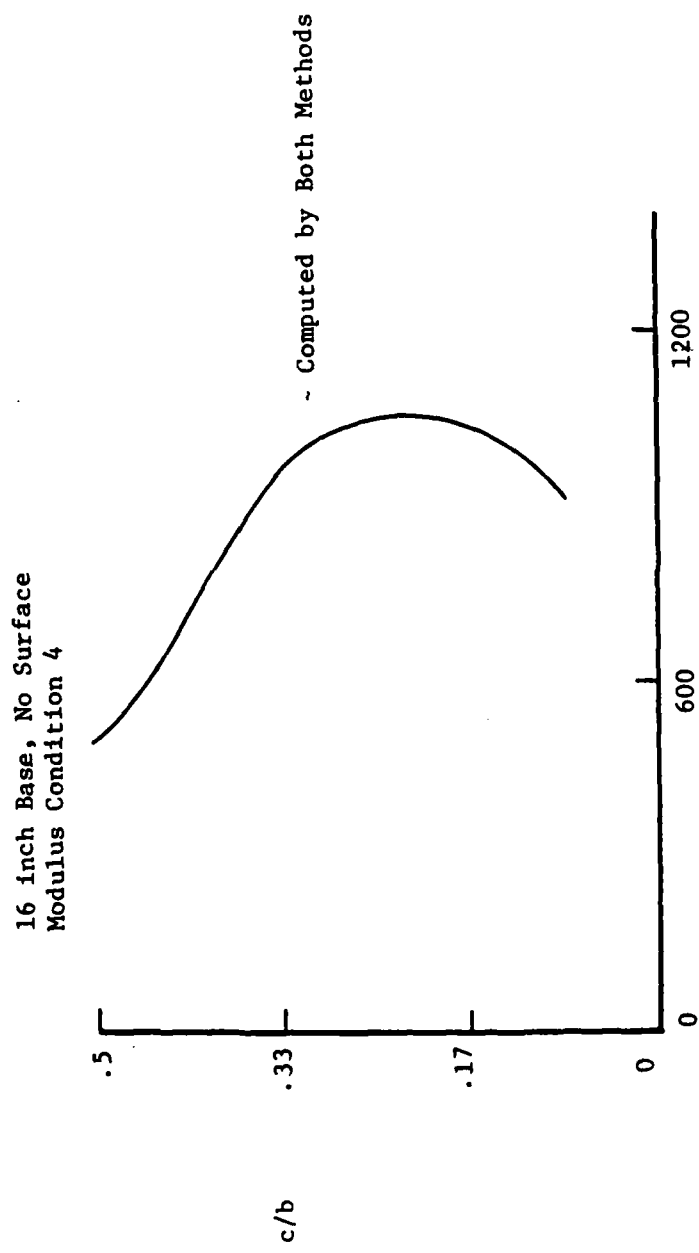


Figure 20. Stress Intensity Factor Distribution

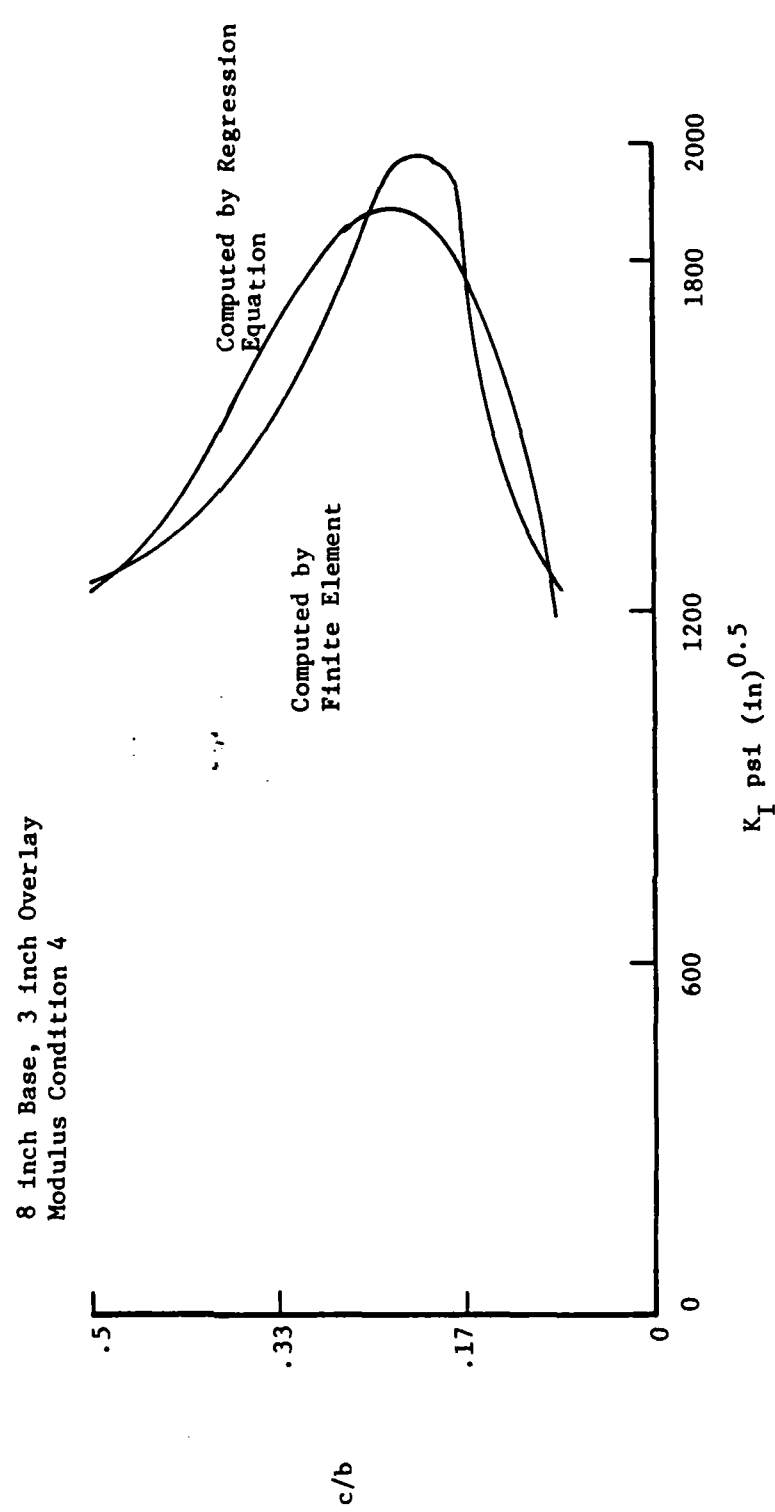


Figure 21. Distribution of Stress Intensity Factor

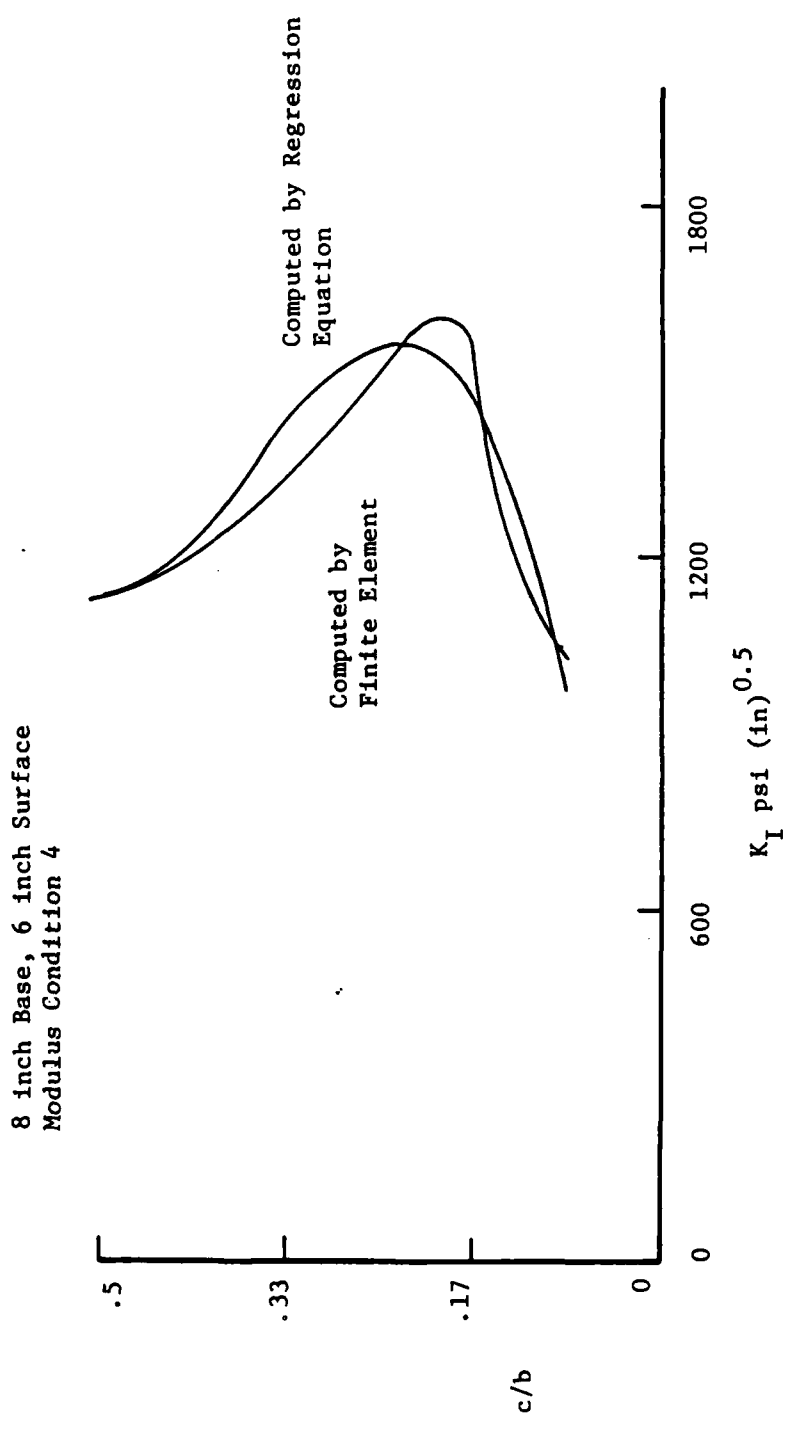


Figure 22. Distribution of Stress Intensity Factors

values greater than 1/2 were stress intensity factors calculated. Thus, for c/b greater than 1/2, the assumed cubic distributions give the only K_I values; they must be relied on exclusively. The graphs of the predicted distributions for c/b greater than 1/2 are shown in Figure 23 through 27. As can be seen, the plots for all cases get smaller directly after $c/b = 1/2$, and then double back and increase. For the 8 inch base, no surface, the K_I values go negative and never become positive again. For the rest of the cases, K_I is always positive past $c/b = 1/2$, and for the 8 inch base, 3 and 6 inch surface cases K_I gets very large at $c/b = 1$. In addition, noting that B_0 equals K_I at $c/b = 0$, it can be seen that for the 8 inch base, 3 and 6 inch surface cases K_I is negative at $c/b = 0$. The exception is modulus condition 6 of the 6 inch surface, where K_I manages to remain positive at $c/b = 0$.

The predicted K_I values at $c/b = 0$ cannot be checked (there is no crack length on which to apply reverse stresses), but for c/b greater than 1/2 the cubic values should be checked with calculated K_I values. It may be that the cubic distributions are misleading in this range, but these values have not been checked.

Computation of Crack Propagation Histories

To calculate the rate of crack propagation, the Paris equation described in Chapter II was coded into a Fortran program to allow easy application of stress intensity factors, pavement geometry and structural properties into a program that predicted the number of load cycles to failure. Up to this point, all the necessary input has been calculated except for the initial and final crack lengths for each modulus condition, base, and surface

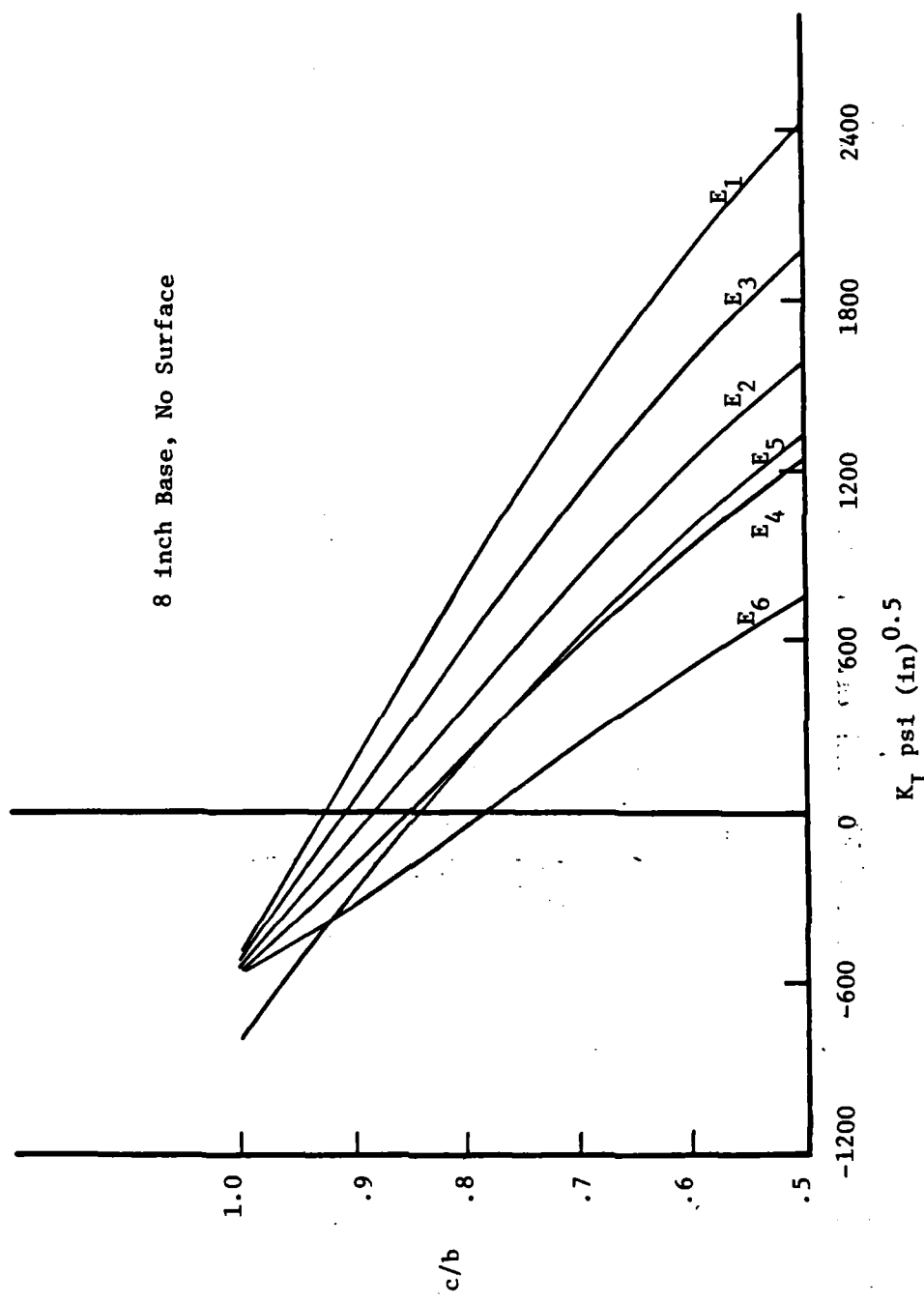


Figure 23. Distribution of Stress Intensity Factors Calculated by Regression Equation for Various Modulus Conditions

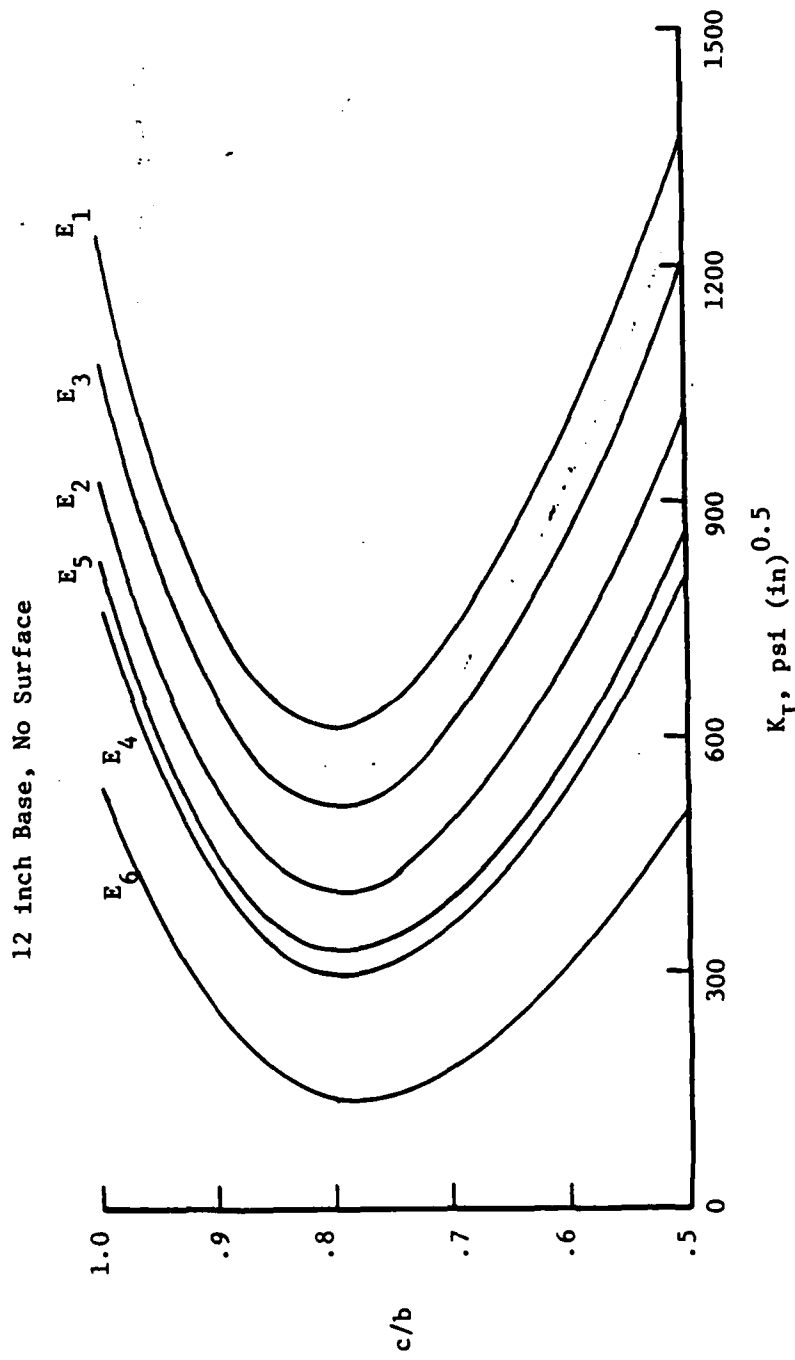


Figure 24. Distribution of Stress Intensity Factors Computed by Regression Equation for Various Modulus Conditions

16 inch Base, No Surface

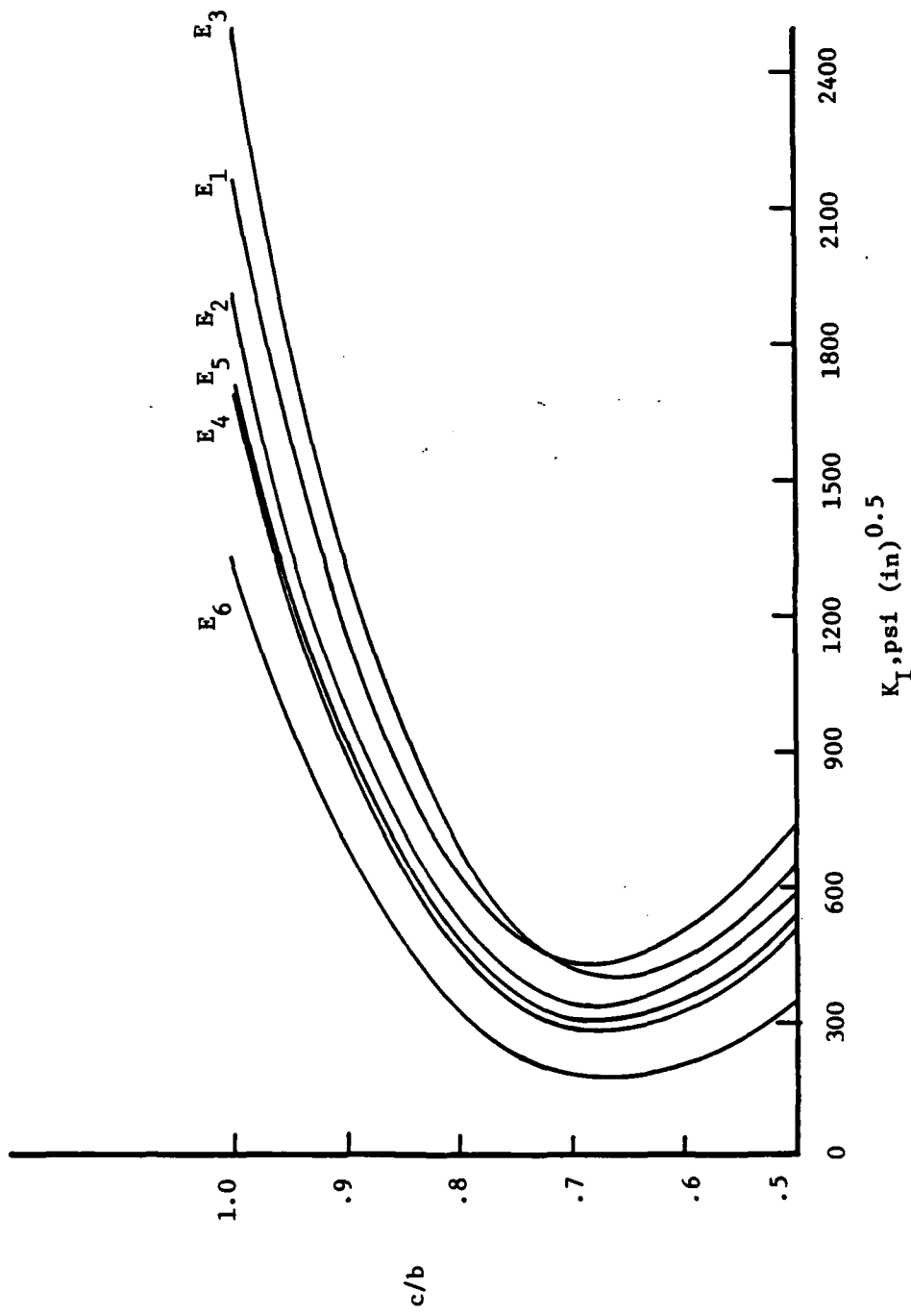


Figure 25. Distribution of Stress Intensity Factors Computed by Regression Equation for Various Modulus Conditions

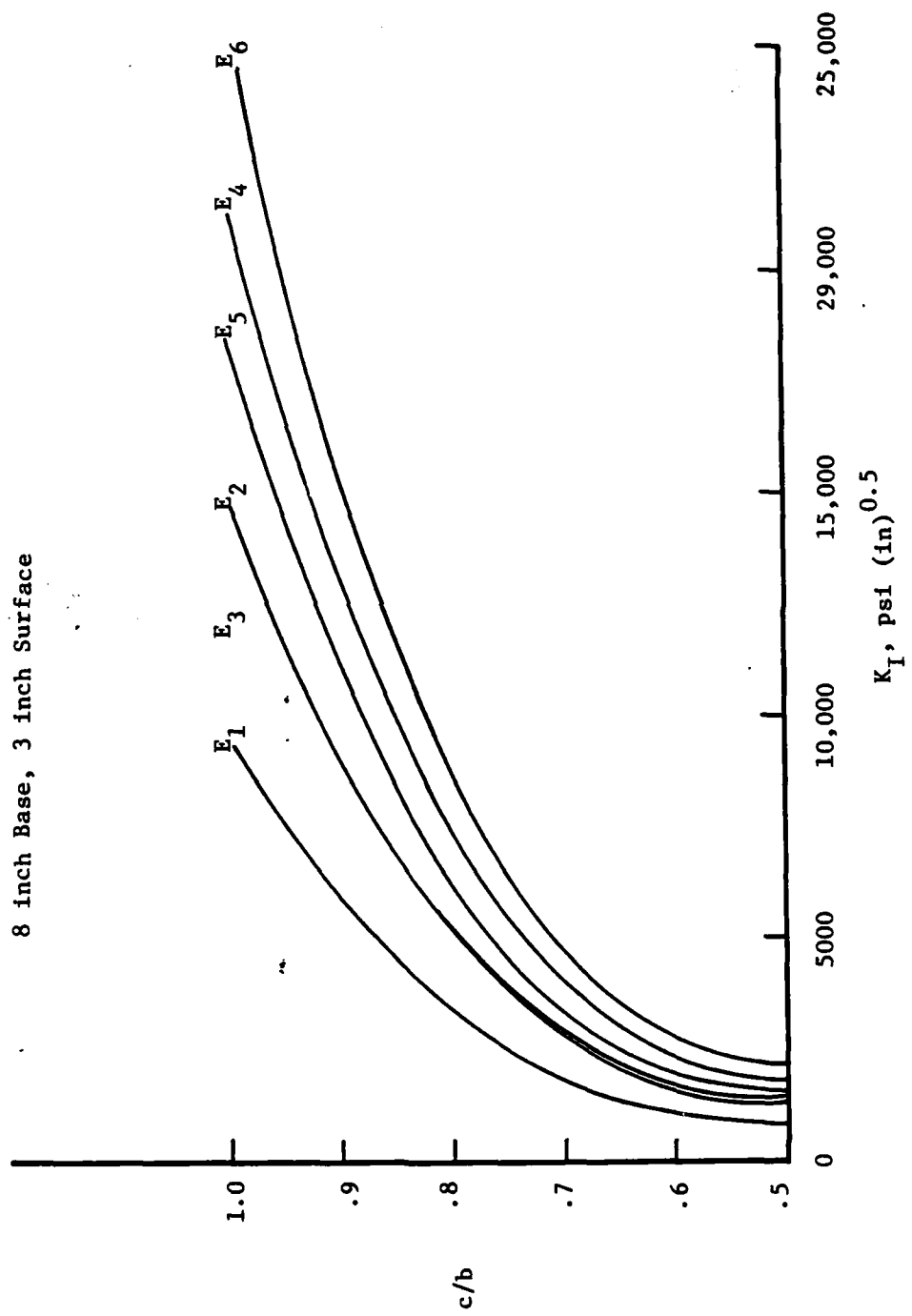


Figure 26. Distribution of Stress Intensity Factors Computed by Regression Equation for Various Modulus Conditions

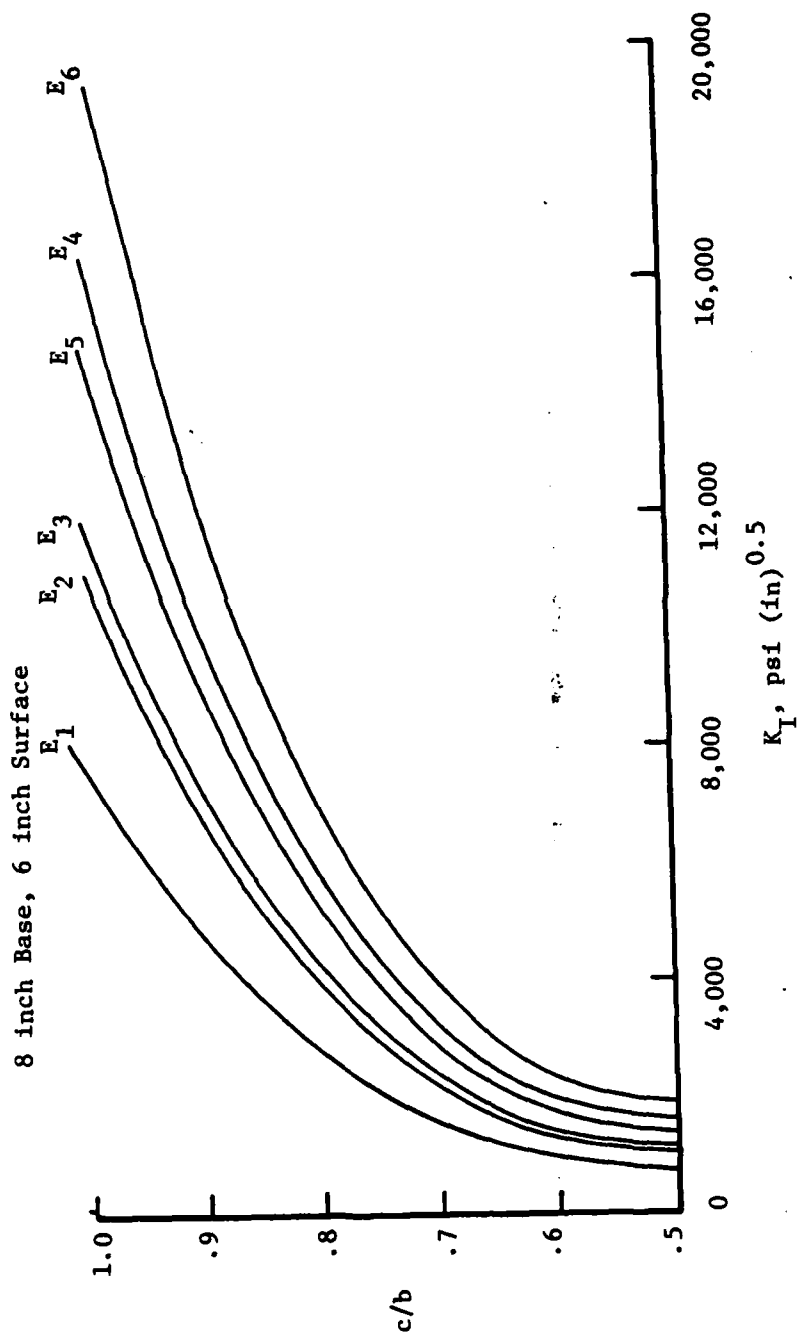


Figure 27. Distribution of Stress Intensity Factors Computed by Regression Equation for Various Moduli Conditions

combination. These are found by calculating the roots of the K_I cubic distributions. The first two roots in the range $0 \leq c/b \leq 1$ which define a positive region of K_I are the endpoints, as explained in Chapter 1. If K_I is positive in the range $0 \leq c/b \leq 1$, then the endpoints are 0 and 1. The endpoints found by using this procedure are shown in Table 11. When input, if the endpoint in question is a root, then it is modified slightly so that it does not assign a zero (or negative due to round-off errors) value to K_I and thus cause computational errors. If it is a right endpoint, it is made smaller, and if it is a left endpoint it is made larger so that K_I is always positive.

The crack propagation histories for modulus condition 4, all base and surface combinations, are given in Figure 28 through Figure 32. These histories correspond to arbitrarily selected values of A and n equal to 10^{-10} and 2.0 respectively. The numbers defining these graphs can be found in the output in Appendix B, as mentioned before. The histories graphed are typical in their relationship to each other for each modulus condition and A and n combination.

It appears from the graphs that of the pavements with no surface, the 8 inch base is the most critical, followed by the 12 and then 16 inch bases. Although the number of cycles required to traverse the last crack increment in the 8 inch base is five orders of magnitude greater than the total to failure of the 12 and 16 inch bases, the load cycles needed to reach near failure in the 8 inch base is significantly smaller than the aforementioned totals. It is reasonable to believe that in such a state of near failure some perturbation could advance the crack to failure. Besides, the 8 inch base is practically destroyed at near failure anyway.

Table 11. Endpoints For Crack Propagation Histories

8 inch base, no surface

MC	LEFT	RIGHT
----	------	-------

1	0.0	0.925978
2	0.0	0.880403
3	0.0	0.905504
4	0.0	0.849452
5	0.0	0.837094
6	0.0	0.784196

12 inch base, no surface

MC	LEFT	RIGHT
----	------	-------

1	0.0	1.0
2	0.0	1.0
3	0.0	1.0
4	0.0	1.0
5	0.0	1.0
6	0.0	1.0

16 inch base, no surface

MC	LEFT	RIGHT
----	------	-------

1	0.0	1.0
2	0.0	1.0
3	0.0	1.0
4	0.0	1.0
5	0.0	1.0
6	0.0	1.0

8 inch base, 3 inch surface

MC	LEFT	RIGHT
----	------	-------

1	0.010900	1.0
2	0.009084	1.0
3	0.009478	1.0
4	0.006693	1.0
5	0.005579	1.0
6	0.000964	1.0

8 inch base, 6 inch surface

MC	LEFT	RIGHT
----	------	-------

1	0.008869	1.0
2	0.007145	1.0
3	0.006798	1.0
4	0.004462	1.0
5	0.002302	1.0
6	0.0	1.0

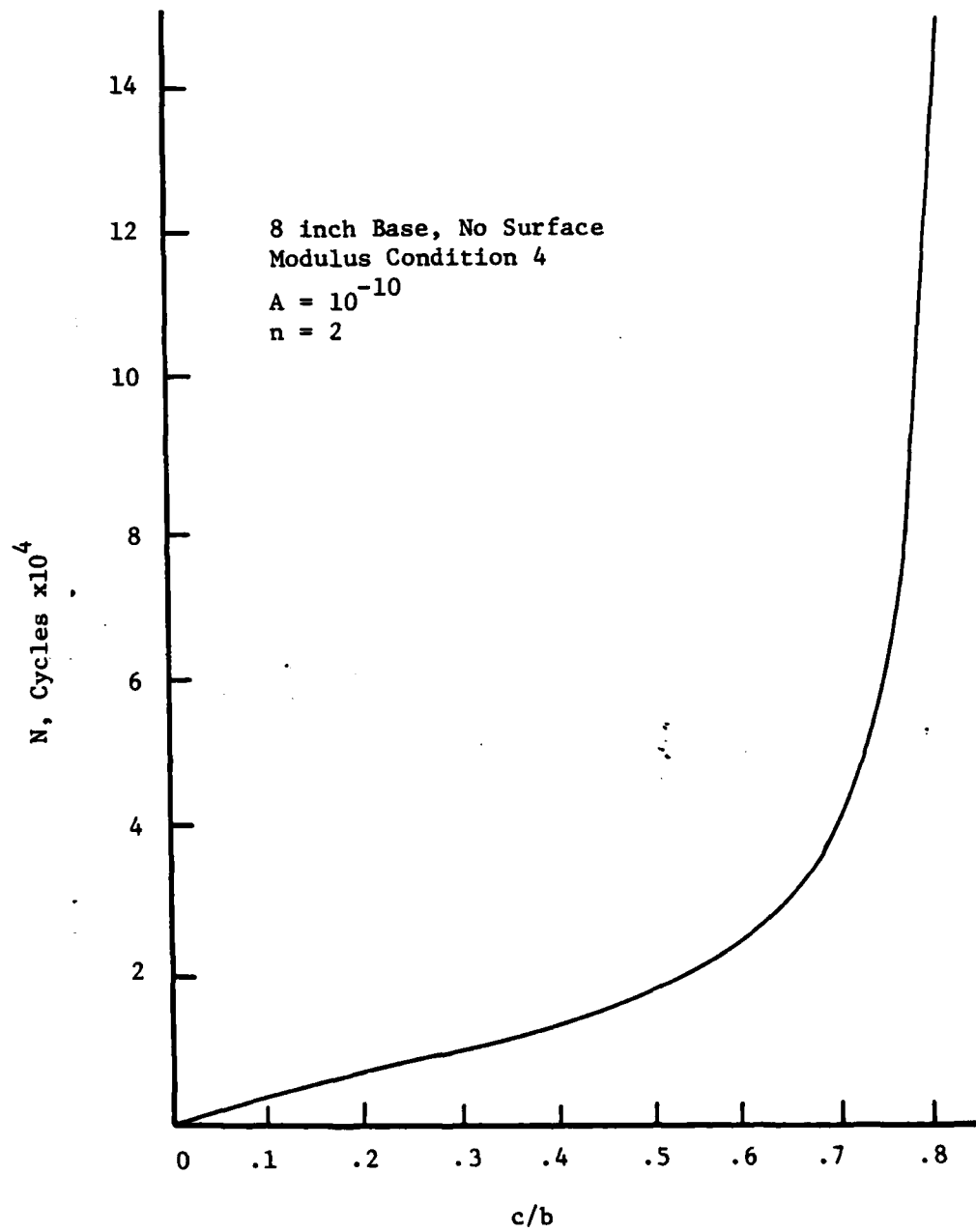


Figure 28. Progression of Crack (c) Through Base (b)
as a Function of Load Cycles, N

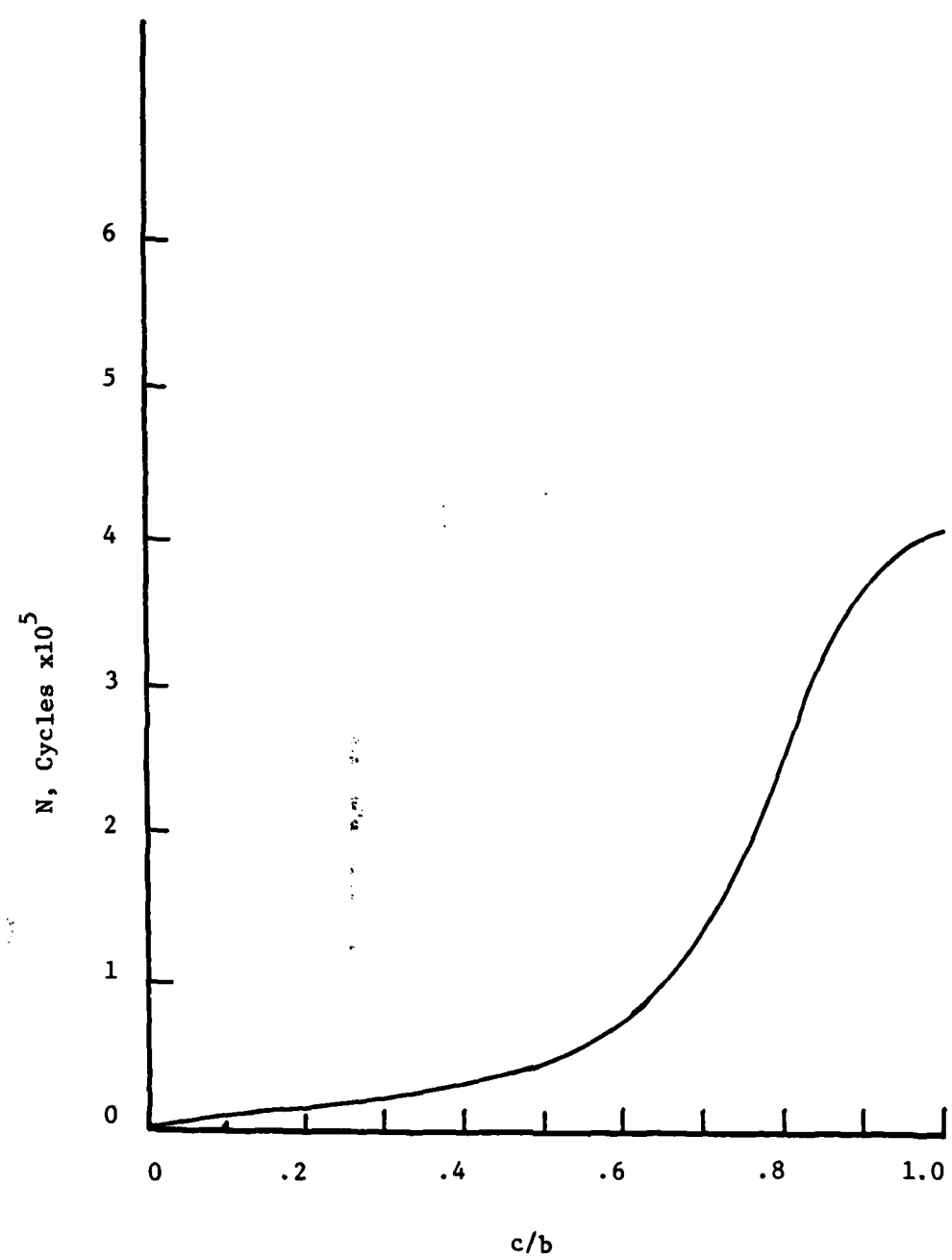


Figure 29. Progression of Crack (c) Through Base (b)
as a Function of Load Cycles, N

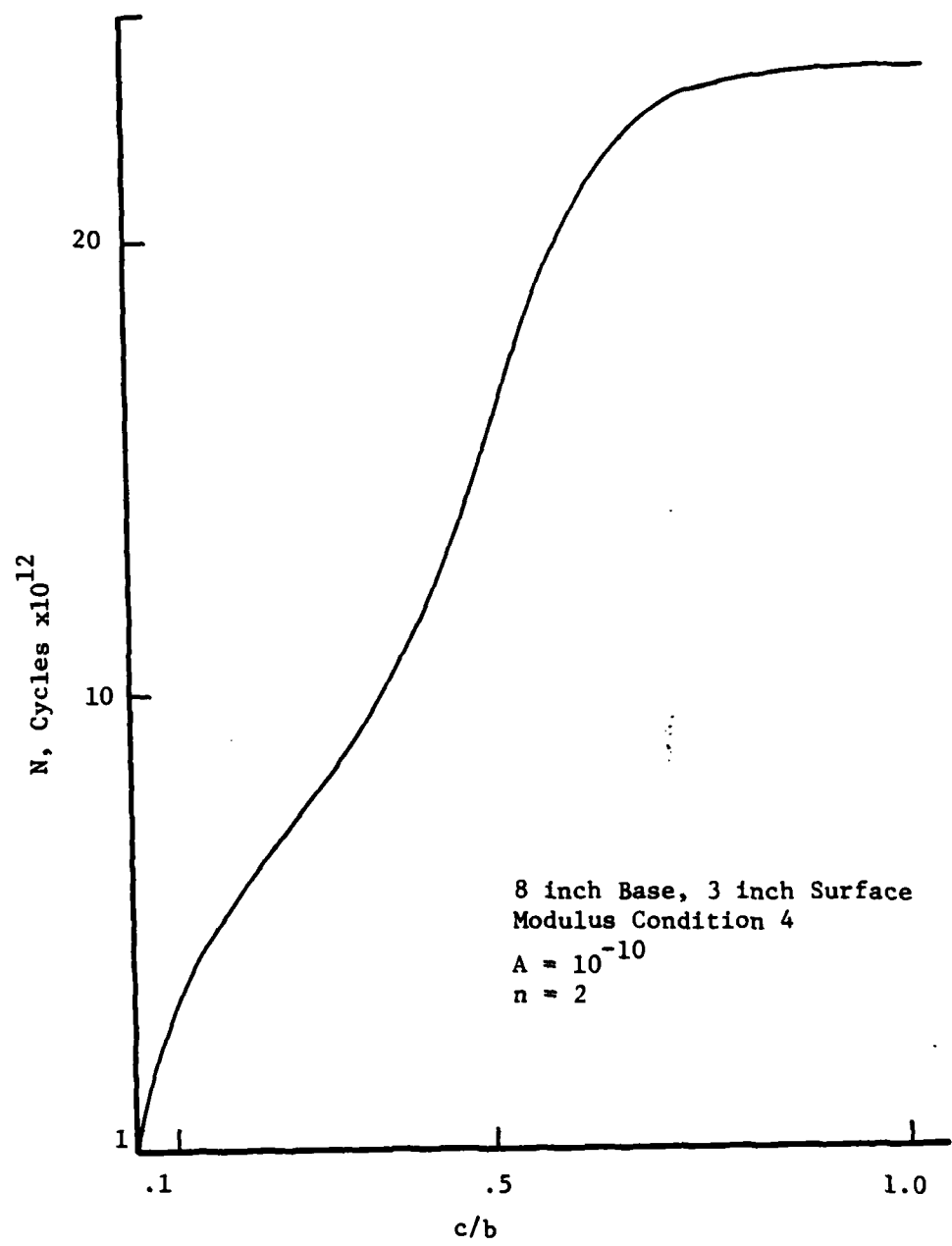


Figure 30. Progression of Crack (c) Through Base (b)
as a Function of Load Cycles, N

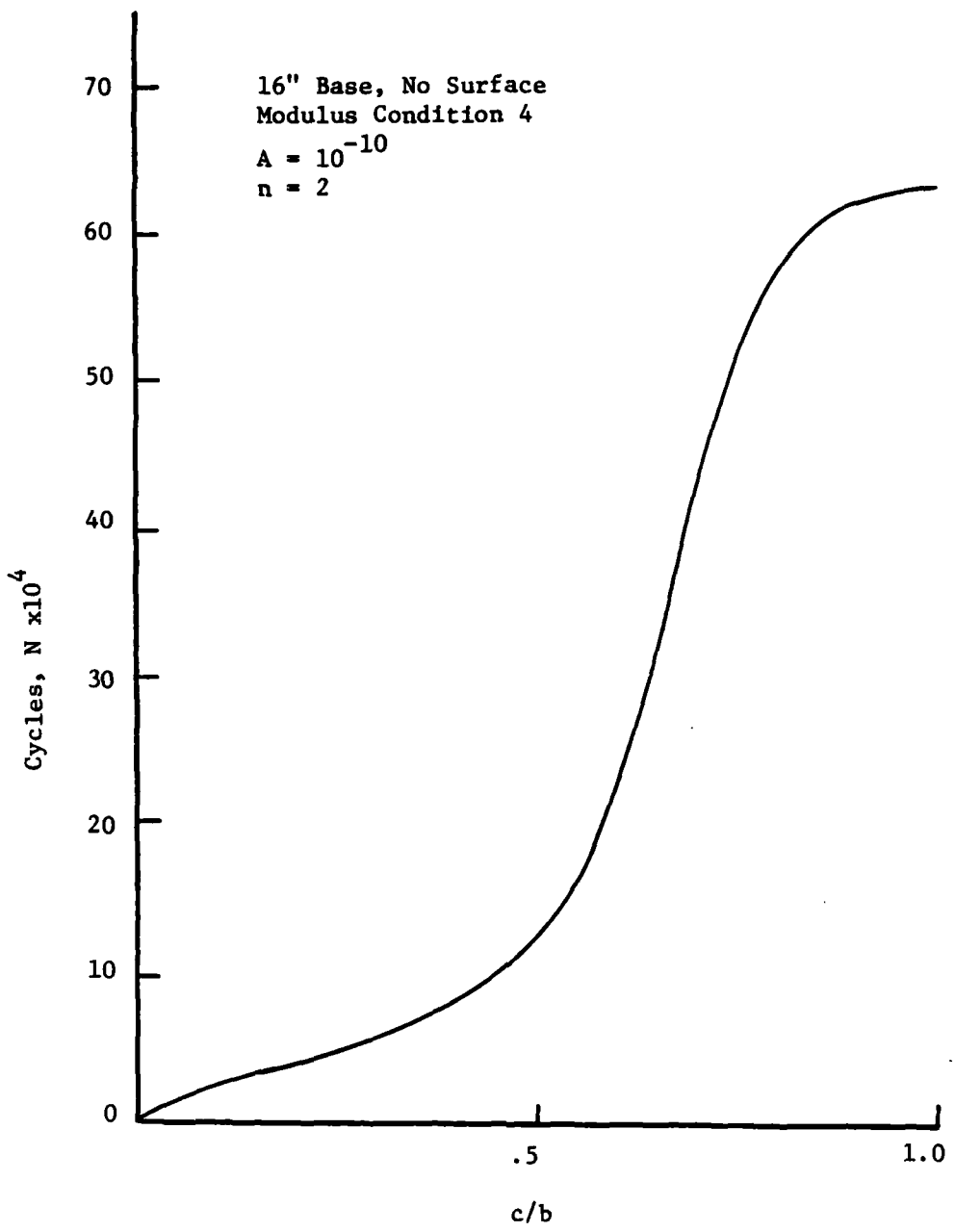


Figure 31. Progression of Crack (c) Through Base (b)
as a Function of Load Cycles, N

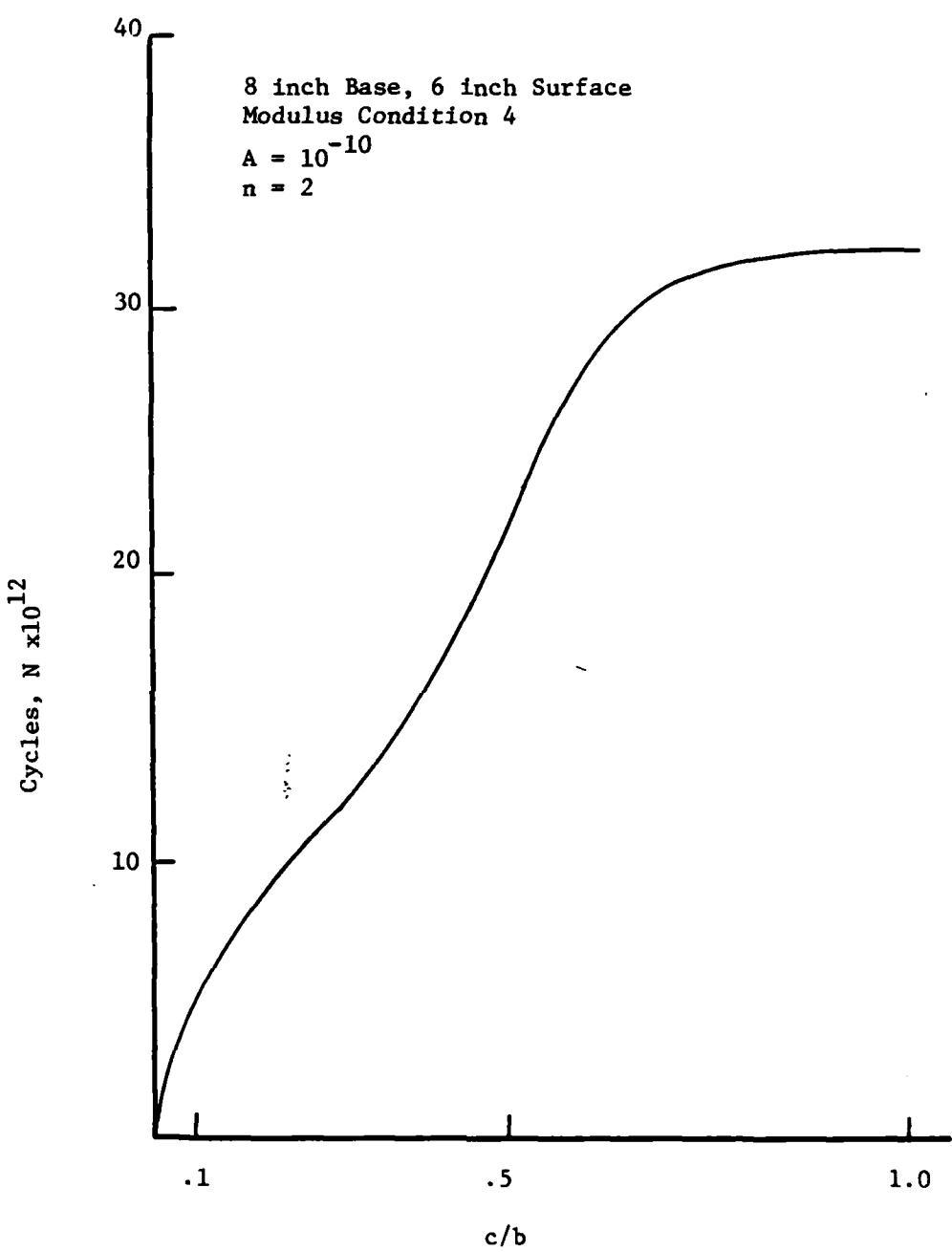


Figure 32. Progression of Crack (c) Through Base (b)
as a Function of Load Cycles, N

The 3 and 6 inch surfaces are added to the 8 inch base with the intent of increasing the fatigue life. From the graphs it is seen that theoretically they do, but perhaps realistically they won't. In both the 3 and 6 inch surface cases, it takes a tremendous amount of load cycles to advance the crack through the first increment of approximately 0.05 inches. After that, though, it takes less cycles to propagate the crack to failure than it does for the crack to reach near failure in the no surface case. Therefore, if the crack were somehow jumped past the initial increment in the 3 and 6 inch surface cases, due to say a starter flaw, which may typically have dimensions capable of doing this, those pavements would be more critical than the no surface case. It is certainly reasonable to think that the first increment could be jumped, as it is assumed that a zone of negative K_I is jumped to get to the first increment in the first place. In this case the negative zone is only about 0.01 inches at most, so that it is no great achievement to bypass it. So, in one sense, adding a surface will greatly postpone failure as long as the negative K_I zone and the first crack increment are not vaulted. In another sense, if the above were circumvented, adding a surface could hasten failure.

As would be expected, the 3 inch surface case requires more cycles to failure than the 6 inch surface case for the same pavement structure.

Calculations With Actual Laboratory Fracture Properties

Extensive laboratory studies conducted at Texas A&M University have indicated that the fracture parameters, A and n can be predicted from tests along with K_{Ic} for stabilized materials. These parameters are necessary to predict the fracture life of a material insitu. Typical values determined are as follows:

CEMENT LEVEL $E=355,600 \text{ psi}$ $v = 0.15$

10 % CREEP VALUES $A=8.12 \times 10^{-59}$

$K_{IC}=138.6$ $n=25.28$

 FATIGUE VALUES $A=15.4 \times 10^{-27}$

$n=10.0$

$E=597,600 \text{ psi}$ $v = 0.15$

15 % CREEP VALUES $A=1.45 \times 10^{-53}$

$K_{IC}=209.3$ $n=21.24$

 FATIGUE VALUES $A=10 \times 10^{-51}$

$n=22.0$

Comparison of these critical stress intensity factors indicates that the stress intensity factors calculated using the procedures outlined here are all larger than the critical stress intensity factors which means that fracture will proceed instantaneously. This indicates the inaccuracy of the pavement structure selected for modelling the stress intensity factors calculated.

CHAPTER V: CONCLUSIONS AND RECOMMENDATIONS

The analysis procedure presented in this report illustrates the complexities involved in calculating stress intensity factors, and applying them to a structure to predict cycles to failure. The stress intensity factors used in this analysis are not as accurate as may be desired, due to the use of plane strain, plane stress solutions used in the finite element procedure to calculate the initial stresses. The modification of more sophisticated programs to accept the fracture elements in an axi-symmetric analysis would increase the accuracy of the predictions of fracture in the cement stabilized base materials, or any material susceptible to fracture.

The methodology of applying the principles of fracture, as demonstrated in the development of this report are applicable to a design methodology, and indicate the modularized approach which must be taken to adequately characterize the pavements, their geometry, and the loading conditions which may be expected to occur in an actual airfield pavement.

The principles of fracture mechanics and crack propagation can be applied to pavement design life, to account for the gradual failure due to repeated loading over fracture susceptible materials. The parameters required to predict crack propagation are the material properties of A and n, as described in this report. A significant amount of testing has gone into evaluating these parameters for cement stabilized materials, and the influence of these material properties on fracture life was shown.

The predicted stress intensity factors were high, due directly to the level of structure modeled and the magnitude of loading investigated.

A broader range of loading conditions, and a thicker pavement structure would have produced more moderate stress intensity factors which would have shown a more pronounced effect on fracture life than was seen in this report.

1. The methodology developed in this study indicates the potential for considering fracture in pavement design methodology.
2. The stress calculation scheme can be refined and replaced by a general program to analyze an axisymmetric problem with multiple wheel loadings. This can be a simple elastic layer program, a stress dependent elastic layer program, or even a sophisticated stress dependent finite element program such as Illi-Pave.
3. The hybrid crack tip element provides a simple means of accurately evaluating the influence of loading on fracture life in fracture susceptible layers of a pavement system given the stresses present in the layers.
4. The modular approach developed to provide stress intensity factors using regression techniques to replace repetitive calculations with the finite element program is an accurate procedure to obtain the stress intensity factors in a manner applicable to design without extensive use of computer execution time.

REFERENCES

1. Chang, Hang-Sun, "Prediction of Thermal Cracking in West Texas," Masters Thesis, Texas A&M University, Department of Civil Engineering (1975).
2. Desai, C. S., and Abel, J. F., Introduction to the Finite Element Method, Van Nostrand Reinhold Company, 1972.
3. Pian, T.H.H., Tong, P., Luk, C. H., "Elastic Crack Analysis by a Finite Element Hybrid Method," (paper) 3rd Conf. Matrix Meth. Struct: Mech., Wright-Patterson AFB, Ohio (1971).
4. Pian, T.H.H., Tong, P., Lasry, S. J., "A Hybrid Element Approach to Crack Problems in Plane Elasticity," IJNME, Vol. 7, 1973, pp. 297-308.
5. Tong, P., Lin, K. Y., Orringer, O., "Effect of Shape and Size on Hybrid Crack-Containing Finite Elements," Computational Fracture Mechanics, ASME, 1975.

APPENDIX A: NOTATION AND CONVERSION FACTORS

SYMBOL	MEANINGS
A	regression constant in fracture equation; area in other cases
A_m	Element areas in finite element development
b	base course thickness in fracture analysis
c	crack length within a pavement layer
C_K	stress intensity correction factor
$C_{i,j,k,l}$	Elastic Compliance Tensor
e	2.71828
E	Young's modulus of elasticity
G	shear modulus
K	stress intensity factor
m	creep exponent
n	regression constant (exponent) in fracture equation
N	number of cycles in fracture
P	load
q	nodal displacements
R	statistical correlation coefficient
r	radius
S	Surface for integration
T	Traction vector normal to integration path
u	boundary displacement
x, y	x_1, y_1 directions respectively
ϵ	error in stress intensity predictions, strain
ζ	local coordinate axis
θ	angle
ν	Poisson's ratio
σ	stress
σ_3	principal stress
τ	shear stress
Σ	summation
$\sqrt{}$	square root
\ln	natural (Naperian) logarithm (base e)
δ	Strain energy release rate
ξ	coordinate distance from crack tip
σ_e	stress applied to crack tip

APPENDIX B : DESCRIPTION OF PROGRAM UNITS

Finite Element Fracture Program

A flow diagram of subroutines is shown in Figure B-1. The following is a brief description of each subroutine and the input data format follows.

DATAIN:

Reads and echo prints all data pertaining to the conventional elements. It also performs checks on this data.

ASEMBL:

Initializes and assembles the global stiffness matrix (including the crack element) and the global load vector. Modifies the above to reflect the geometric boundary conditions.

QUAD:

Computes the stress-strain matrix, stiffness matrix, body force vector, and strain-displacement matrix of either a 4-CST quadrilateral or a triangular element.

CST:

Computes the strain-displacement matrix, stiffness matrix, and body force vector of a CST element.

GEOMBC:

Applies prescribed displacement boundary conditions at a single, specified node.

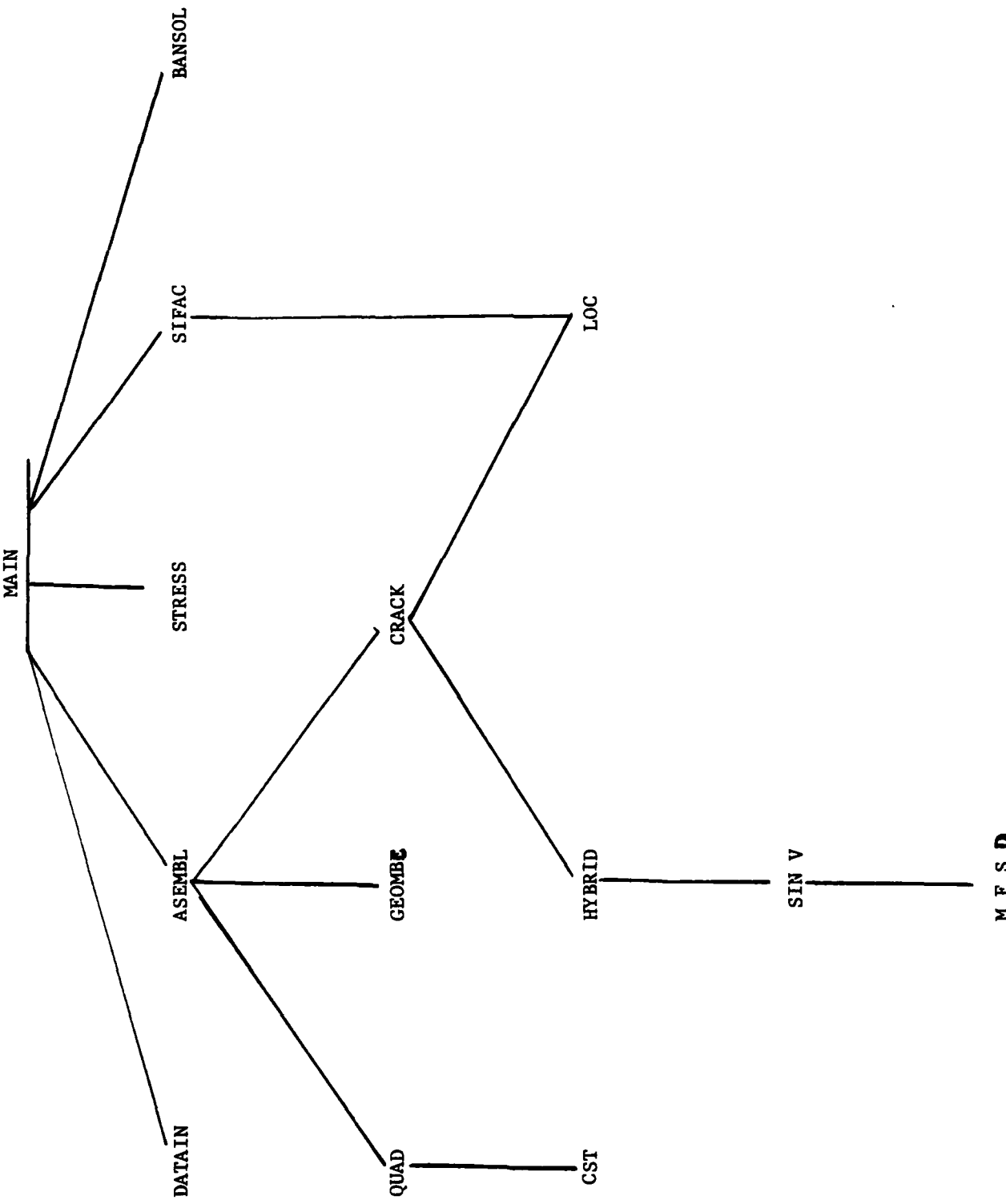


Figure B-1. Flow Diagram of Program for Finite Element Fracture Calculations

CRACK:

Reads the input data pertaining to the crack element. Computes the constants and of Section II. Incorporates the crack element stiffness matrix into the global stiffness matrix which had previously contained stiffnesses from only conventional elements.

HYBRID:

Computes the matrices [G] and [H] of Section II. Computes the crack element stiffness matrix. Computes the $(B_I)^T$ and $(B_{II})^T$ row vectors of Section II.

LOC:

The crack element stiffness matrix is not derived in two-dimensional array form but rather in vector form. Thus, in CRACK and SIFAC where this stiffness matrix is used in calculations and manipulations, some operator must be used to translate from two- to one-dimensional form. This operator is LOC. This is probably done to save memory.

MFSD:

Uses numerical methods to perform the integration implied by equations (16) and (17) of Section II.

SINV:

Performs the inversion of [H].

BANSOL:

Triangularizes the global banded stiffness matrix by symmetric Gauss-Doolittle decomposition and/or solves for the global displacement vector corresponding to a given load vector

STRESS:

Computes strains, stresses, and principal stresses for conventional elements. Computes the strain energy due to all the conventional elements which can be used to calculate stress intensity factors by energy methods, as mentioned in Section I. Prints stresses and principal stresses at element centroids, and the strain energy.

SIFAC:

Computes the stress intensity factors by equations (23) in Section II. Computes the crack element strain energy and the global strain energy, which can be used to compute stress intensity factors by energy methods, as in Section I. Prints the crack element strain energy.

Input Guide- Descriptions are included for each card.

IDENTIFICATION CARD:

One card per problem: Format (I5,3x,9A8)

cc 1-5 NPROB: The problem number. If NPROB = 0, execution of the program is halted.

cc 9-80 TITLE(I): Title of the problem. The vector has 9 elements, each of which contains 9 characters of the title.

Multiple problems can be handled, but as soon as the next problem is read the previous problem is lost, so a problem cannot be recalled.

BASIC PARAMETERS:

One card per problem: Format 615

cc 1-5 NNP: Number of nodal points

cc 6-10 NEL: Number of conventional elements

cc 11-15 NMAT: Number of different materials

cc 16-20 NLSC: Number of surface tractions

cc 21-25 NOPT: Option for stress state. 1 = plane strain, 2 = plane stress.

cc 26-30 NBODY: Option for body force. 0 = no weight, 1 = weight in the negative y direction.

cc 31-35 NCKEL: Number of crack elements.

MATERIAL PROPERTIES

NMAT cards per problem: Format 4F10.0

cc 1-10 E: Modulus of elasticity

cc 11-20 PR: Poisson's ratio

cc 21-30 RO: Density of the material

cc 31-40 TH: Thickness of the material

NODAL POINT DATA:

Up to NNP cards per problem: Format (215,4F10.0)

cc 1-5 M: Nodal point number

cc 6-10 KODE(I): Index of displacement and concentrated load conditions at node I. The values Kode can assume and the conditions assigned to each are given in Table IV-1.

cc 11-20 X: Horizontal coordinate of node I.

cc 31-30 Y: Vertical coordinate of node I.

cc 31-40 ULX: Concentrated load or displacement in X direction at node
I.

cc 41-50 ULY: Concentrated load or displacement in Y direction at node
I.

Usually one card is needed for each node. However, if some nodes fall on a straight line and are equidistant, data for only the first and last points of this group are needed. Intermediate nodal point data are automatically generated by linear interpolation. The nodal data must be entered in order from smallest to largest, leaving out those nodes which are to be interpolated. The nodes which are interpolated are assigned values of KODE = 0, ULX = 0, and ULY = 0. The signs of prescribed nodal displacements or forces follow the signs of the coordinate directions assigned by the user.

ELEMENT DATA:

Up to NEL cards per problem: Format 615.

cc 1-5 M: The element number

cc 6-10 IE(M,1): The index of the first node of a CST or 4-CST quadrilateral element.

cc 11-15 IE(M,2): The index of the second node of a CST or 4-CST quadrilateral element.

cc 16-20 IE(M,3): The index of the third node in a CST or 4-CST quadrilateral element.

cc 21-25 IE(M,4): The index of the fourth node in a CST or 4-CST quadrilateral element. If it is a CST element, the index of fourth node equals that of the third node; that is, IE(M,3) = IE(M,4).

cc 26-30 IE(M,5): Material type number corresponding to element M.

Usually, one card is needed for each element. However, if some elements are on a line in such a way that their corner node indexes each increase by one compared to the previous element, only the data for the first element on the line need be input. As the elements on the line are generated by adding one to each node of the preceding element, starting with the first element on the line, the last element on a line needn't be input. However, data for the last element in the assemblage must be input whether it could be generated or not. Also, please note that triangular elements cannot be generated from quadrilateral elements because the third and fourth indexes of a triangular element are equal. The same material type as the first element on a line is assigned to all elements generated on that line.

For a right-handed coordinate system, the nodal indices for an element must be input counter-clockwise around the element.

SURFACE TRACTIONS:

As many cards as needed: Format (215,4F10.0)

cc 1-5 ISC: I, the first node upon which tractions act.

cc 6-10 JSC: J, the second node upon which tractions act.

cc 11-20 SURX1: The intensity of the traction in the X direction acting at node I.

cc 21-30 SURX2: The intensity of the traction in the X direction acting at node J.

cc 31-40 SURY1: The intensity of the traction in the Y direction acting at node I.

cc 41-50 SURY2: The intensity of the traction in the Y direction acting at node J.

Surface tractions must be specified between two adjacent nodes only. The tractions in both the X and Y directions are assumed to vary linearly between the two nodes. Intensities are expressed in units of force/length so that pressures must be multiplied by the thickness before being input into the computer. The signs of the tractions follow the directions of the coordinate axes assigned by the user.

CRACK ELEMENT DATA:

There are NCKEL cards per problem for each of the two types of card which comprise the crack element data.

Card one: Format (215,2F10.0,15)

cc 1-5 KEY: The type of crack element. 1 = five node case, 2 = nine node case.

cc 6-10 MATYP: The type of material where the crack element is placed.

cc 11-20 XC: The horizontal coordinate of the crack tip.

cc 21-30 YC: The vertical coordinate of the crack tip.

cc 31-35 NCOT: Flag which determines which direction nodal indexes are to be counted around the crack element. For the five node case 1 = clockwise, 0 = counter-clockwise.

Card two: Format 1015

cc (5I-4)-5I KCRK(I): Nodal incidence for the Ith node of the crack element.

cc (5K+1)-5(K+1) MAXDIF: Maximum difference between the nodal incidences of the crack element. Used to compute the bandwidth after the addition of the crack element.

For the five node case there are five incidences input for the crack element ($K = 5$) and for the nine node case there are nine ($K = 9$). In either case the input for MAXDIF immediately follows the last incidence input. All crack element data is omitted if NCKEL = 0.

The listing of the finite element computer code is given on the following pages.

```

1 C PROGRAM FEGDI INPUT, OUTPUT, TAPES= INPUT, TAPEG= OUTPUT,
2 C *TEMP3, TEMP4, TEMP5, TEMP6,
3 C +TAPE1, TAPE2, TAPE3, TAPE4= TEMP3, TAPE4= TEMP4, TAPE8= TEMP8,
4 C IMPLICIT REAL*8(A, H, O-2)
5 C PROGRAM FEGD
6 C IMPLICIT REAL(A-H, O-Z)
7 C DIMENSION TITLE(9),
8 C COMMON /C01/, PR(10), RO(10), X(700), Y(700),
9 C COMMON /CONS/NNP, NEL, NMAT, NSLC, NOPT, NBODY, MTYP, NCCEL,
10 C COMMON/DIE/ QK(10,10), Q(10), B(3,10), C(3,3), BT(3,6), XQ(5), YA(5),
11 C COMMON/TRO/ IBAND, NEQ, R(1400), AK(1400), 100),
12 C COMMON/T1/ E(700, 5),
13 C DATA MAXEL, MAXNP, MAXMAT, MAXNL, MAXNP/700, 700, 10, 100/
14 C 15 C PROBLEM IDENTIFICATION AND DESCRIPTION
15 C 16 C READ(15, 100)NPROB, (TITLE(I), I=1, 9)
17 9999 READ(15, 100)NPROB, (TITLE(I), I=1, 9)
18 1020 WRITE(16, 200)NPROB, (TITLE(I), I=1, 9)
19 CALL DATTAIN(MAXEL, MAXNP, MAXMAT, MAXNL, MAXNP, 1STOP)
20 MAXDOF=2*MAXNP
21
22 C COMPUTE MAX, NODAL DIFFERENCE AND SEMI-BANDWIDTH, EQ. (6-1)
23 C MAXDIF=0
24 MAXDIF=0
25 DO 11=1, NEL
26 DO 12=1, 4
27 DO 1K=1, 4
28 LL=ABS((E(I,J)-E(I,K))
29 IF(LL.GT. MAXDIF)MAXDIF=LL
30 1 CONTINUE
31 1BAND=2*MAXDIF+1
32 NEQ=2*NNP
33 IF(1BAND.GT. MAXNBW)GOTO999
34 IF(1STOP.GT. 0)GOTO999
35 CALL ASENBL(1STOP)
36 IF(1STOP.GT. 0)GOTO999
37 C TRIANGULARIZE STIFFNESS MATRIX, EQ. (2-2), KKK=2
38 C SOLVE FOR DISPLACEMENTS CORRESP. TO LOAD VECTOR R, EQ. (2-3), KKK=2
39 C 40 C CALL BANSOL(AK, R, NEG, IBAND, MAXNBW)
40 C WRITE(16, 300)(1, R(2*I-1), R(2*I), I=1, NNP)
41 C CALL STRESS(WORK)
42 C WRITE(16, 605)
43 C 44 C FORMAT('1', 3X, 'NCCEL = ', I3)
44 C 45 DO 36 I=1, NCCEL
45 C TOTAL=D, D
46 C SUM=0.0
47 C IF(NCCEL.EQ. 0)GOTO645
48 C 49 C REWIND 12
49 C 50 C 51 C WRITE(16, 37)NCCEL
51 C 52 C FORMAT('0', 3X, 'NCCEL = ', I3)
52 C 53 DO 36 I=1, NCCEL
53 C 54 CALL SIFAC(I, TOTAL)
54 C 55 SUM=SUM+TOTAL
55 C 56 CONTINUE
56 C 57 645 CONTINUE
57 C ENERGY-SUM+WORK
58 C WRITE(16, 400)ENERGY
59 C 400 FORMAT(' -', 3X, '...TOTAL STRAIN ENERGY = ', G20, 8, ' . . . ')

```

RD-A167 106

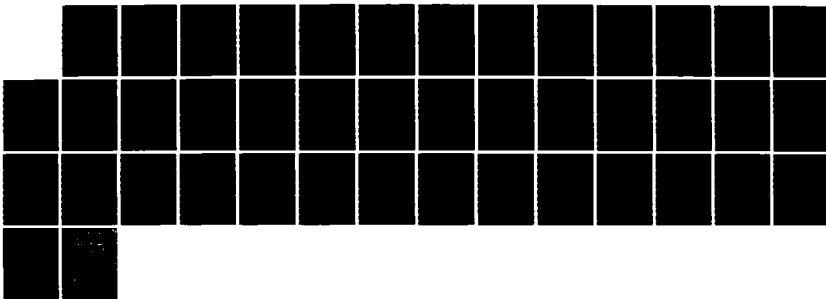
FRACTURE IN STABILIZED SOILS VOLUME 2(U) TEXAS
TRANSPORTATION INST COLLEGE STATION D N LITTLE ET AL.
31 DEC 85 AFOSR-TR-86-8242-VOL-2 F49620-82-K-0027

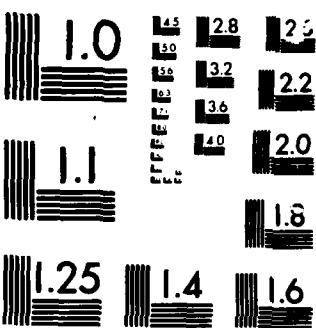
2/2

UNCLASSIFIED

F/G 8/13

NL





MICROCOM[®]

CHART

```

121      Y(N)=Y(N-1)+RY
122      ULX=0.0
123      VLY=0.0
124      GOTO 6
125      442  ULX=ULX
126      VLY=VLY
127      KODE=KODE
128      6  WRITE(16,52)N,KODE,X(N),Y(N),ULX,VLY
129      WRITE(14)N,KODE,ULX,VLY
130      N=N+1
131      IF(M-N).LT.0  GO TO 9
132      9  IF(N.LE.NNP)GO TO 3
133      C  READ AND PRINT ELEMENT PROPERTIES, TABLE 6-4
134      C  WRITE(16,106)
135      13  L=0
136      14  READ(15,15)M,((IE(M,1),I=1,5)
137      16  L=L+1
138      17  IF(M-L).LT.17,18
139      18  WRITE(16,117,17,18
140      19  WRITE(16,116)M
141      20  WRITE(16,53)M,(IE(M,1),I=1,5)
142      21  ISTOP=1
143      22  GOTO 14
144      23  IE(L,1)=IE(L-1,1)+1
145      24  IE(L,2)=IE(L-1,2)+1
146      25  IE(L,3)=IE(L-1,3)+1
147      26  IE(L,4)=IE(L-1,4)+1
148      27  IE(L,5)=IE(L-1,5)
149      28  WRITE(16,53)L,(IE(L,I),I=1,5)
150      29  IF(M-L).GT.20,16
151      30  IF(NEL.L).GT.21,14
152      31  21  CONTINUE
153      C  READ AND PRINT SURFACE LOADING(TRACTION) CARDS
154      C  IF(NSLC.EQ.0)GOTO 999
155      32  WRITE(16,900)ISTOP
156      33  WRITE(16,108)
157      34  DO 40 L=1,NSLC
158      35  READ(15,41)ISC,JSC,SURX1,SURX2,SURY1,SURY2
159      36  WRITE(16,42)ISC,JSC,SURX1,SURX2,SURY1,SURY2
160      37  40  WRITE(16,42)ISC,JSC,SURX1,SURX2,SURY1,SURY2
161      38  31  IF(ISTOP.EQ.0)GOTO 999
162      39  WRITE(16,900)ISTOP
163      C
164      1  FORMAT(715)
165      100 FORMAT(10,"INPUT TABLE 1. BASIC PARAMETERS",//5X,
166      " NUMBER OF NODAL POINTS.",15/5X,
167      " NUMBER OF ELEMENTS.",15/5X,
168      " NUMBER OF DIFFERENT MATERIALS.",15/5X,
169      " NUMBER OF SURFACE LOAD CARDS.",15/5X,
170      " 1 - PLANE STRAIN, 2 - PLANE STRESS.",15/5X,
171      " BODY FORCES(1 = IN - Y DIREC., 0 = NONE) - 15")
172      200 FORMAT("0",6X,"NUMBER OF CRACK ELEMENTS.",15)
173      251 FORMAT(10,"//",100," TOO MANY NODAL POINTS, MAXIMUM = ",15)
174      252 FORMAT(10,"//",100," TOO MANY ELEMENTS, MAXIMUM = ",15)
175      253 FORMAT(10,"//",100," TOO MANY MATERIALS, MAXIMUM = ",15)
176      255 FORMAT(10,"//",100," EXECUTION HALTED BECAUSE OF",15," FATAL ERRORS")
177      2  FORMAT(4F10.0)
178      101 FORMAT(10,"INPUT TABLE 2. MATERIAL PROPERTIES",//5X,
179      "MODULUS OF",6X,"ELASTICITY",6X," RATIO",6X,"DENSITY",6X,
180      "NUMBER",5X,"POISSON'S",7X,"MATERIAL",7X," MATERIAL",5X,
181      "FOR LOAD",6X,"OR LOAD")
```

```

241 DO 10001, NEL
242   IF(I<M,5),GT,0.0)GOTO701
243   ISTOP=1STOP+1
244   GOTO 10
245   CALL QUAD(N, AREA)
246   IF(AREA.GT.0.0)GOTO7016
247   ISTOP=1STOP+1
248   WRITE(15,201H
249   C
250   C STORE ELEMENT STIFFNESS MATRIX TO COMPUTE STORED ENERGY
251   C LIM=16 IF(I<M,3),EQ,IE(M,4))GOTO201
252   C
253   LIM=10
254   GOTO 205
255   201 LIM=6
256   205 WRITE(13)LIM,(OK((I,J),J=1,LIM),I=1,LIM)
257   C CONDENSE ELEMENT STIFF. FROM 10X10 TO 6X6. EQ. (5-64). AND ELEMENT
258   C LOADS FROM 10X1 TO 6X1. EQ. (5-64D). (REF. 2)
259   C
260   IF(I<M,3),EQ,IE(M,4))GOTO226
261   DO 31 J=1,2
262   IJ=10-J
263   IK=IJ
264   PIVOT=OK(IK,IK)
265   DO 32 K=1,IJ
266   F=OK(IK,K)/PIVOT
267   OK(IK,K)=F
268   DO 33 IK=1,IJ
269   OK(IJ,IK)=OK(IJ,IK)-F*OK(IK,IK)
270   33 OK(K,IK)=OK(K,IK)
271   32 Q(OK)=OK(IK,K)=0.0
272   31 Q(IK)=Q(IK)/PIVOT
273   C STORE MULTIPLIERS, PIVOTS, CONDENSED LOADS, STRAIN-DISP. AND STRESS-STR
274   C MATRICES ON SCRATCH TAPE NO. 1 (TO BE USED LATER TO COMPUTE STRAINS A
275   C STRESSES)
276   C
277   26 WRITE(11)((OK((I,J),J=1,10),*9,10),Q((9),Q(10),(B(I,J),J=1,10),I=
278   *1,3),(C(I,J),J=1,3),I=1,3),XQ(5),YQ(5))
279   C ASSEMBLE STIFF. AND LOADS . DIRECT STIFF. METHOD. SEC. 6-5.
280   C
281   C
282   LIM=8
283   IPI(1EM,3),EQ,IE(M,4))LIM=M
284   DO 40 I=2,LIM,2
285   IJ=1/2
286   LP(I,-1)*2*IE(M,IJ)-1
287   40 LP(I,1/2)*2*IE(M,IJ)
288   DO 50 ILL=1,LIM
289   I=LPI(ILL)
290   R(I)=OK(I)*Q(ILL)
291   DO 50M=1,LIM
292   J=LP(1M)-1+1
293   IF(J,LE,0)GOTO800
294   AK(I,J)=AK(I,J)+Q(ILL,MM)
295   50 CONTINUE
296   10 IF(NCKEL,EQ,0)GOTO835
297   DO 14 I=1,NCKEL
298   14 CALL CRACK
299   35 CONTINUE
300
301 C ADD EXTERNALLY APPL. CONIC. NODAL LOADS TO R
302 C
303 DO 55N=1,NNP
304 READ(14,N,1)KODE,ULX,VLY
305 IF(KODE,EQ,3)GOTO65
306 K=2*N
307 IF(KODE,EQ,1)GOTO57
308 RIK=1)RIK(-1)*ULX
309 IF(KODE,NE,0)GOTO55
310 RIK)=RIK(K)*VLY
311 57 CONTINUE
312 C CONVERT LINEARLY VARYING SURFACE TRACCTIONS TO STATIC EQUIVALENTS.
313 C AND ADD TO OVERALL LOAD VECTOR R. EQ. (5-61A).
314 C
315 IF(NSLC,EQ,0)GOTO660
316 DO 61LL=1,NSLC
317 READ(18,LL)SC,JSC,SURX1,SURY1,SURX2,SURY2
318 I=ISC
319 J=JSC
320 IJ=2*I
321 JJ=2*J
322 OK=X(IJ)-X(LL)
323 OY(Y,IJ)V(LL)
324 EL=SQR(TDXDX+DY*DY*2)
325 PXI=SURX1*EL
326 PYJ=SURX2*EL
327 PYJ=SURY1*EL
328 RIJ=1)*R(JJ-1)*PXI/3.0+PYJ/6.0
329 RIJ=1)*R(JJ-1)*PXI/6.0+PYJ/3.0
330 RIJ=1)*R(JJ-1)*PYI/3.0+PYJ/6.0
331 RIJ=1)*R(JJ-1)*PYI/6.0+PYJ/3.0
332 RIJ=1)*R(JJ-1)*PYI/6.0+PYJ/3.0
333 61 CONTINUE
334 C INTRODUCE KINEMATIC CONSTRAINTS (GEOMETRIC BOUNDARY CONDITIONS).
335 C
336 C EQ.(16-18).
337 C
338 60 CONTINUE
339 REMIND 14
340 DO 70P=1,NNP
341 READ(14,N,1)KODE,ULX,VLY
342 IF(KODE,GE,0.AND.KODE.LE,3)GOTO72
343 ISTOP=1STOP+1
344 QET(70)
345 72 IF(KODE,EQ,0)GOTO70
346 IF(KODE,EQ,2)GOTO71
347 CALL GEOMBC(ULX,2*M-1)
348 IF(KODE,EQ,1)GOTO70
349 71 CALL GEOMBC(VLY,2*M)
350 70 CONTINUE
351 ENDFILE11
352 ENDFILE12
353 ENDFILE13
354 ENDFILE14
355 ENDFILE15
356 ENDFILE16
357 FILESTOP, EQ, 0)GOTO801
358 WRITE(16,100)1STOP
359 20 FORMAT(5X," AREA OF ELEMENT ",16," IS NEGATIVE ")
360 100 FORMAT(5X," SOLUTION WILL NOT BE PERFORMED BECAUSE OF ",16,
361 +," DATA ERRORS ")

```

```

361   61 RETURN
362   END
363 C SUBROUTINE QUAD(M, TOTALA)
364 C   IMPLICIT REAL(A-H,0-2)
365 C   IMPLICIT REAL(A-H,0-2)
366 C   IMPLICIT REAL(MNP, NEL, MAT, NSLC, NOPT, NBODY, MTYP, NCKEL
367 C   COMMON/CONS/NMP, NEL, MAT, NSLC, NOPT, NBODY, MTYP, NCKEL
368 C   COMMON/ONE/PR(10), RO(10), TH(10), X(700), Y(700)
369 C   COMMON/TWO/GK(10,10), G(10,10), S(10,10), C(3,3), BT(3,6), XQ(5), YQ(5)
370 C   COMMON/T1/IE(1400), AK(1400, 100)
371 C   TOTALA=0.0
372 C   I=IE(M, 1)
373 C   J=IE(M, 2)
374 C   K=IE(M, 3)
375 C   L=IE(M, 4)
376 C   MYP=IE(M, 5)
377 C   TOTALA=0.0
378 C CONSTRUCT STRESS-STRAIN MATRIX C, EQ. (3-18C), FOR PLANE STRAIN
379 C NOPT=1, AND M. ST. 1.00705
380 C ISOTROPIC MATERIALS
381 C IF INPUT EQ. 1, AND M. ST. 1.00705
382 C IF INPUT EQ. 2, GO TO 382
383 C P=1.0*PR(MTYP)/(1.0-PR(MTYP))=((1.0-2.0)*PR(MTYP)))
384 C P=1.0*PR(MTYP)/(1.0-PR(MTYP))
385 C C1(1,1)=CF*(1.0-PR(MTYP))
386 C C1(1,2)=CF*(1.0-PR(MTYP))
387 C C1(2,1)=CF*(1.0-2.0)
388 C C1(2,2)=CF*(1.0-2.0)
389 C C1(3,3)=CF*((1.0-2.0)*PR(MTYP))/2.0
390 C GOTO 5
391 C IF(E(MTYP)/(1.0-PR(MTYP))=PR(MTYP))
392 C C1(1,1)=CF
393 C C1(1,2)=PR(MTYP)*CF
394 C C1(2,1)=CF*(1.0-2.0)
395 C C1(2,2)=CF
396 C C1(3,3)=CF*(1.0-PR(MTYP))/2.0
397 C LIM=4
398 C IF(K.EQ.L) LIM=3
399 C XQ(5)=0.0
400 C YQ(5)=0.0
401 DO 10 NH=LIM
402 NH=IE(P, NH)
403 XQ(NH)=X(NH)
404 YQ(NH)=Y(NH)
405 XQ(5)=XQ(5)+X(NH)/FLOAT(LIM)
406 YQ(5)=YQ(5)+Y(NH)/FLOAT(LIM)
407 C INITIALIZ QUAD STIFFNESS, LOAD VECTOR AND STRAIN-DISPLACEMENT VECTOR
408 C   DO 131 J=1,10
409 Q(1,1)=0.0
410 DO 12 J=1,10
411 DO 11 J=1,10
412 DO 10 K=1,3
413 DO 13 JJJ=1,3
414 B(JJJ,1)=0.0
415 IF(K.NE.1) B(JJJ,1)=1.0
416 CALL CST(1,2,3, TOTALA)
417 GOTO 999
418 CALL CST(1,2,5, AREA)
419 TOTALA=TOTALA+AREA
420 CALL CST(2,3,5, AREA)
421 TOTALA=TOTALA+AREA
422 CALL CST(3,4,5, AREA)
423 TOTALA=TOTALA+AREA
424 CALL CST(4,1,5, AREA)
425 TOTALA=TOTALA+AREA
426 999 RETURN
427 END
428 SUBROUTINE CST(1,J,K, AREA)
429 C   IMPLICIT REAL(A-H,0-2)
430 C   IMPLICIT REAL(A-H,0-2)
431 DIMENSION CB(3,6), LC(6), LT(3), TK(6,6)
432 C
433 COMMON/CONS/NMP, NEL, MAT, NSLC, NOPT, NBODY, MTYP, NCKEL
434 COMMON/ONE/PR(10), RO(10), TH(10), X(700), Y(700)
435 COMMON/TWO/GK(10,10), G(10,10), S(10,10), C(3,3), BT(3,6), XQ(5), YQ(5)
436 COMMON/T1/BAND, NEQ, RL(1400), AK(1400, 100)
437 LT(1)=J
438 LT(2)=J
439 LT(3)=K
440 C COMPUTE STRAIN-DISPLACEMENT MATRIX B FOR TRIANGLE, EQ. (5-35A)
441 BT(1,1)=YQ(JJ)-YQ(K)
442 BT(1,2)=YQ(K)-YQ(L)
443 BT(1,3)=YQ(L)-YQ(J)
444 BT(2,4)=XQ(K)-XQ(L)
445 BT(2,5)=XQ(L)-XQ(K)
446 BT(2,6)=XQ(J)-XQ(K)
447 BT(3,1)=BT(2,4)
448 BT(3,2)=BT(2,5)
449 BT(3,3)=BT(2,6)
450 BT(3,4)=BT(1,1)
451 BT(3,5)=BT(1,2)
452 BT(3,6)=BT(1,3)
453 AREA=(BT(2,4)*BT(1,3)-BT(2,6)*BT(1,1))/2.0
454 C COMPUTE C,B
455 DO 101 J=1,3
456 DO 102 JJ=1,6
457 DO 103 JJ=1,6
458 CB(1,J,J)=0.0
459 DO 104 KK=1,3
460 DO 105 JJ=1,3
461 DO 106 JJ=1,3
462 C COMPUTE (B+B)*C=B, EQ. (5-45A)
463 DO 121 J=1,6
464 DO 122 JJ=1,6
465 TK(1,J,J)=0.0
466 DO 123 KK=1,3
467 DO 124 JJ=1,3
468 C ADD TRIANGLE STIFFNESS TO QUADRILATERAL STIFFNESS, EX. (6-2),
469 C ADD TRIANGLE STRAIN-DISPLACEMENT MATRIX TO QUADRILATERAL STRAIN-
470 C DISPLACEMENT MATRIX
471 C
472 DO 151 J=1,3
473 DO 152 JJ=1,3
474 DO 153 JJ=1,3
475 DO 301 J=1,6
476 LL=LC(J)
477 FK=1.0/14.0*AREA
478 FB=2.0*FK
479 DO 201 JJ=1,6
480 MM=LC(JJ)

```

```

481      20 OK(LL,MM)=OK(LL,MM)+TK(11,JJ)+TH(MTYP)+FK
482      30 BI(JJ,LL)=BI(JJ,LL)+BT(JJ,LL)+BT(JJ,11)=FB
483      C DEVELOP BODY FORCE VECTOR, EQ, (5-61B)
484      C IF (NBODY.EQ.0) GOTO999
485      TBODYF=AREARO(MTYP)=TH(MTYP)
486      BODYF=.7BODYF/3.0
487      DO 351=1,3
488      JJ=2*L1(11)
489      35 QIJJJ=QIJJJ+BODYF
490      999 RETURN
491      END
492      SUBROUTINE CRACK
493      IMPLICIT REAL*8 (A-H,O-Z)
494      COMMON/CON/ NNP,NEL,NHAT,NSLC,NOPT,NDDY,MTYP,NCNL
495      COMMON/CON1/ PR10, TH10, TH110, TH1100, Y1700
496      COMMON/TDO/IBAND,NEO,R11400,AK11400,100
497      COMMON/NT3/BCR(2,18),EK(12),XY(18),KCRK(9),LP(18)
498      READ(15,12)KEY,MTYP,XC,YC,NCNT
499      12 FORMAT(12I5,2F10.0,1B)
500      503 IF (KEY.EQ.1) GOTO10
501      503 NODE=9
502      504 NODE=18
503      505 GOTO 20
504      506 NODE=5
505      507 NODE=10
506      508 NODE=10
507      509 READ(15,2)(KCRK(1),I=1,NOOE),MAXDIF
508      2 FORMAT(10I5)
509      510 K=2*(MAXDIF)
510      511 IPIK.LE.1BAND)GOTO91
511      L1BAND+1
512      L1BAND
513      DO 100I=1,NEQ
514      100I=L,K
515      AK(I,J)=0.
516      1BAND)MAXD1BAND,K)
517      91 CONTINUE
518      DO 30I=1,NOE
519      XXY(2*I-1)X(KCRK(1))
520      30 XXY(2*I)=Y(KCRK(1))
521      DO 31I=1,NOE
522      31 WRITE(16,321),XXY(1)
523      32 FORMAT(10.5X,(2*X1,13,")",G20.6)
524      SMU=EMATYP)/(2*(1,1.+PRIMATYP))
525      IF (NOPT.EQ.1) GOTO40
526      ETA=1.35*SMU,ETA
527      GOTO 80
528      40 ETA=3.-4.*PRIMATYP)
529      80 CONTINUE
530      35 FORMAT(10.5X,"SMU,ETA",2G20.6)
531      CALL HYBRID(KEY,SMU,ETA,XC,YC,NCNT)
532      36 FORMAT(10.5X,"SMU,ETA",2G20.6)
533      DO 60I=1,NOE
534      LP(2*I-1)=2*KCRK(1)-1
535      60 LP(2*I)=2*KCRK(1)
536      DO 36I=1,NOE
537      36 WRITE(16,331),LP(1)
538      33 FORMAT(10.5X,"LP (",13,")",15)
539      34 DO 70I=1,NOE

```

```

541      70 LPILL)
542      543      DG 70MM=1,NOE
543      JFLP (MM)=1
544      IF (J.LE.0) GOTO70
545      CALL LOC(LI,MM,I,J,NOE,NOE,1)
546      AK(I,J)=AK(I,J);EK(I,J,1,J,AK(I,J)
547      WRITE(16,841)J,EK(I,J,1,J,AK(I,J)
548      84 FORMAT("0.5X, "EK(" ,4,":"),G20.6,"AK(",13,".",",13,")",G20.6)
549      70 CONTINUE
550      WRITE(16,34)NODE,NOE,MTYP,XC,YC
551      34 FORMAT("0.5X,"NODE,NOE,MTYP,XC,YC",,314,2015,5)
552      KK=(NOE-1)/2
553      WRITE(12)KK,NOE,NOE,KEY,ILP(1),I=1,NOE,(EK(1),I=1,KK),(BCR(1),
554      *J),I=1,KEY),J=1,NOE),XC,YC,MTYP,(KCRK(1),I=1,NOE)
555      RETURN
556      END
557      SUBROUTINE LOC(I,J,IR,N,M,MS)
558      IX=I
559      JX=J
560      IF (MS=1110,20,30
561      10 IR=NI*(JX-1)+IX
562      60TO 36
563      20 IF (IX-JX)>22,24,24
564      22 IX=IX+(JX-IX)/2
565      60TO 36
566      24 IX=IX-(IX-1X)/2
567      60TO 36
568      30 IX=0
569      1F(IX-JX)36,32,36
570      32 1R=IX
571      36 IR=IX
572      RETURN
573      END
574      SUBROUTINE HYBRID(KEY,SMU,ETA,XC,YC,NCNT),
575      60 IMPLICIT REAL*8(A,B,D-H,O-Y),COMPLEX*16(Z,C)
576      60 IMPLICIT REAL(A,B,D-H,O-Y),COMPLEX(Z,C)
577      COMPLEX SINT,SINT
578      COMPLEX 16 ZET1,Z,DCPLX,DCON16,F1,F2,F3,FF2(32),FF3(32),XY
579      COMPLEX ZET1,Z,DCPLX,DCON16,F1,F2,F3,FF2(32),FF3(32),XY
580      COMPLEX 16 ZETK,CZK,ZETT,CZK,ZET4,ZE,ZD,ZC,ZA,ZB,C1,CDSORT
581      COMPLEX 16 ZETK,CZK,ZETT,CZK,ZET4,ZE,ZD,ZC,ZA,ZB,C1,CDSORT
582      DIMENSION ZETK,CZK,ZETT,CZK,ZET4,ZE,ZD,ZC,ZA,ZB,C1,CDSORT
583      *VB(136),W(16)
584      COMMON/T3/BCR(2,18),EK(17),XXY(18),KCRK(9),LP(18)
585      EQUIVALENCE(ZETT,UXX),CZK,UXX
586      EQUIVALENCE(V(1,1),V(1,1))
587      DATA W/-2369269,-4786287,5686868,47866287,-2369269/
588      DATA Y/-9061799,-5384693,0,...,5384693,.9061799/
589      DATA NNT//,
590      60 IF (KEY.EQ.1)NDE=10
591      60 CI=CMPLX(0.0,1.0)
592      60 IF (KEY.EQ.2)NDE=16
593      60 ELO=1.0
594      60 NT=KEY*INT
595      60 NMPE=NDE/2
596      60 IF (NCNT.EQ.0)GOTOS5
597      60 DO 61*I,NMPE
598      60 12=1*2
599      60 XY(12)=XY(12)
600      60 CONTINUE

```

```

601      NNN=(NNPE-1)/2
602      NTT=(NNNT+NNNT-NNNT)/2
603      DO 11=1,NTT
604      VA(1)=0.
605      1
606      VB(1)=0.
607      DO 41=1,1
608      DO 41=1,1,NDPE
609      VBL(J)=0.
610      4
611      C
612      *INTEGRATION COEFFICIENTS
613      1
614      ISIDE=NNEPE/KEY*KEY/2
615      ES=SORI((XXY(1))-YC)*2*(XXY(2))-YC)*2*
616      UXX((XXY(2))-YC)/ES
617      UY=(XXY(1))-YC)/ES
618      11=1+1
619      XXY(11-1)=(XXY(11-1))-AC)/ES
620      XTY-XXY(11-1)*UY+XXY(11)*UX
621      XXY(11)-XXY(11-1)*UX+XXY(11)*UY
622      XXY(11-1)*XT
623      440
624      ISIDE=NNEPE/KEY*KEY/KEY
625      DO 41IS1=1,1SIDE
626      IY=IS1+1
627      UX-XXY(IY+2)-XXY(IY)
628      UY=XXY(IY-1)-XXY(IY+1)
629      DO 4111=1,5
630      XX-XXY(IY-1)*(1-X(IY+1))+XXY(IY+1)*X(IY)
631      YY*XX(IY)*(1-X(IY+1))+XXY(IY+2)*X(IY)
632      Z=CHPLXXX,YY
633      ZET=CSORT(ZETT)
634      ZET=ZETT-ZETT
635      C2Z=CONJG(ZETT)
636      ZETK1-/ZETT
637      KK=1
638      IF (KEY .EQ. 2) GOTO 0101
639      DO 101OK=1,NNT
640      FF2(K)=0.
641      ZETK=ZETK*ZET
642      C2Z=CONJG(ZETK)
643      KK=KK
644      IF (UY .EQ. 0.) GOTO 1009
645      ZD=C2K*C2Z-KK*ZETK*ZETT
646      2C-2ETK1*(C2Z-ZETT)
647      FF2(K)*0.5K*(K-2)*ZC*K=2D
648      FF2(K)*FF2(K)*UY*.5
649      1009 2E-C2K*C2Z-(C2Z-ZETT)
650      FF3(K)=ETA*ZETK*ZETT+KK*C2K=CONJG(ZETT)+.S*K*ZE
651      FF3(K)*FF3(K)*.25
652      1F(UX .EQ. 0.) GOTO 01010
653      IB-K=2*K*KK
654      ZA1K*(K-2)*ZETK-2.*C2K
655      FF2(K)*K=(C2Z-ZA1B*ZETK*ZETT)+CI*.25*UX+FF2(K)
656      1010 CONTINUE
657      GOTO 2000
658      1011  DO 1012K=1,NNT
659      FF2(K)=0.
660      FF2(K)*NNNT=0.
661      ZETK=ZETK*ZET
662      C2Z=CONJG(ZETK)
663      KK=-KK
664      IF (UY .EQ. 0.) GOTO 1014
665      2D=C2K*C2Z-KK*ZETK*ZETT
666      2C=ZETK*(C2Z-ZETT)
667      FF2(K)*.5K*(K-2)*ZC*K=2D
668      FF2(K)*FF2(K)*UY*.6
669      FF2(K)*NNNT=(FF2(K)*K*ZDUY)+CI
670      1014 2E-C2K*C2Z-(C2Z-ZETT)
671      FF3(K)=ETA*ZETK*ZETT+KK*C2K=CONJG(ZETT)+.S*K*ZE
672      FF3(K)*FF3(K)*.25
673      IF (UX .EQ. 0.) GOTO 01012
674      IB-K=2*K*KK
675      ZA1K*(K-2)*ZETK-2.*C2K
676      FF2(K)*K=(C2Z-ZA1B*ZETK*ZETT)+CI*.25*UX+FF2(K)
677      1B=K*2-KK-KK
678      2A1(K-2)*ZETK*2.*C2K
679      FF2(K)*NNNT=K*(C2Z-ZA1B*ZETK*ZETT)*.25*UX+FF2(K*NNNT)
680      1012 CONTINUE
681      2000 KJ=0
682      DO 41K=1,NNT
683      L=2*1S1-1
684      DO 40J=1,KEY
685      L=J>NNNT-NNT*PK
686      SINT=FF2(1)*X(1)
687      SINT=FF2(1)-SINT
688      SJNT=F2(1)-SINT
689      VQ(1,L)*VQ(1,L)*Q(1)*A*IMAG(SJNT)
690      VQ(1,L)*VQ(1,L+1)*Q(1)*C(1)*REAL(SJNT)
691      VQ(1,L+2)*VQ(1,L+2)*Q(1)*A*IMAG(SINT)
692      VQ(1,L+3)*VQ(1,L+3)*Q(1)*REAL(SINT)
693      DO 41J=1,K
694      SINT=FF2(K*FF3(J))+FF2(J)*FF3(K)
695      KJ=KJ+1
696      VA(KJ)=VA(KJ)+Q(1)*A*IMAG(SINT)/SMU
697      IF (KEY .EQ. 1) GOTO 041
698      I=K*NNNT
699      SINT=FF2(1)*FF3(L)+FF2(L)*FF3(1)
700      VQ(KJ)*VQ(KJ)*Q(1)*A*IMAG(SINT)/SMU
701      CONTINUE
702      41
703      IF (KEY .EQ. 1) GOTO 064
704      DO 500 I=1,NNT
705      VQ(1,1)*Q(1)*C(1)
706      VQ(1,1,2)*2.*VG(1,1,1)
707      VQ(1,1,2)*2.*VG(1,1,2)
708      VQ(1,1,2)*2.*VG(1,1,2)
709      VQ(1,1,2)*2.*VG(1,1,2)
710      455
711      CONTINUE
712      DO 501 I=1,NNN
713      JL=NNPE-1-J
714      VQ(1,1,2*JL-1)*VG(1,1,2*JL-1)
715      VQ(1,1,2*JL)*-VG(1,1,2*JL)
716      VQ(1,1,2*JL-1)*-VG(1,1,2*JL-1)
717      500
718      DO 501 I=1,NNP
719      501
720      VQ(NNT/2,1)*Q(1)
    DO 631=1,NNT

```

```

721   83   VA(1)=VA(1)*2.
722   VB(1)=VB(1)*2.
723   VB(2)=0.
724   VB(3)=1.
725   DO 621=3,NNT
726   62   VB((I=1,J=1)/2*2)=0.
727   *4  CONTINUE
728   CALL SIN(VA,NNT,1E-05,IER)
729   IF(KEY.EQ.2)CALL SIN(VB,NNT,.1E-05,IER)
730   DO 110J=1,NOPE
731   110  I=10J,NNT
732   I=(I+1)/2
733   BK((I,J))=0
734   DO 110K=1,NNT
735   IK=11*K
736   BK(I,J)*IK=(K*K-K)/2+1
737   110  BK(I,J)=BK(I,J)+VB(IK)*VI(K,J)
738   IF(KEY.EQ.1)GO TO 111
739   I=NNT+1
740   DO 121=11,NNT
741   I=I-NNT
742   IJ=(IJ+IJ-1)/2
743   BK(I,J)=0.
744   DO 122K=1,NNT
745   IK=11*K
746   IF(K.GT.1-NNT)IK=(K*K-K)/2+1-NNT
747   121  BK((I,J))=BK((I,J))+VB((IK))*VI(K+NNT,J)
748   111  CONTINUE
749   IJ=0
750   DO 112I=1,NOPE
751   DO 113J=1,1
752   IJ=IJ+1
753   EK(IJ)=0.
754   DO 112K=1,NNT
755   112  EK(IJ)*EK(IJ)*BK(K,J)*VI(K,I)
756   ELO=SOR(T2/ES)
757   DO 113J=1,NOPE
758   BCR(2,J)=0.
759   IF(KEY.EQ.2)BCR(2,J)=ELO=BK(10,J)
760   113  BCR(1,J)=ELO=BK(1,J)
761   RETURN
762   END
763   SUBROUTINE SIFACM(TOTAL)
764   IMPLICIT REAL*8(A-H,O-Z)
765   IMPLICIT REAL(A-H,O-Z)
766   REAL*8 K1,K2
767   REAL K1,K2
768   COMMON/TWO/1BAND,NEO,R(1400),AK(1400,100)
769   COMMON/T3/BCR(2,171),EK(171),KCK(9),LP(10)
770   WRITE(16,35)H
771   35  FORMAT("0",5X,"CKEL",15,"")
772   READ(12)KK, NODE, NOE, KEY, (LP(I), I=1,NOE), ((BCR(I,J),
773   *I=1,KEY,J=1,NOE), XC,YC,MATP, (KCK(I), I=1,NOE))
774   TOTAL=0.
775   K1=0.
776   K2=0.
777   DO 201=1,NOE
778   K1=K1+BCR(1,I)*R(LP(I))
779   IF(KEY.EQ.1)GO TO 20
780   K2=K2+BCR(2,I)*R(LP(I))

```

```

841      WRITE(16,300)
842      WORK=0.0
843      NOLINE=47
844      C      RETRIEVE MULTIPLIERS, PIVOTS, MATRICES B AND C, AND CENTROIDAL COORD.
845      C      READ(SH1,NEL)
846      C      FOR ELEMENT
847      DO 541 SH1=1,NEL
848      READ(11)((OK(1,1),J1=1,10),I1=1,2),(Q1(1),J=1,10),((B(1,J),J=1,10),I=1,
849      +3),(C(1,J),J=1,3),XC,YC
850      C      SELECT MODAL DISPLACEMENTS FOR THE ELEMENT
851      LIM=4
852      IF(IEM(1)=LIM) EQ. IE(M,4) LIM=3
853      DO 101 I,LIN
854      101 =2+I
855      JJ=2*IUM,1
856      Q(I1,I)=R(JJ-1)
857      10 Q(I1,I)=R(JJ)
858      C      RECOVER CONDENSED DISPLACEMENTS FOR THE QUADRILATERAL. EQ. (5-64G)
859      C      IF(LIM EQ. 3) GOTO 616
860      DO 15 K=1,2
861      JK=K+6
862      IK=JK-1
863      DO 15 L=1,IK
864      15 Q(IJK)=Q(JK-Q(K,L)+Q(L)
865      C      COMPUTE ELEMENT STRAINS. EQ. (5-35A)
866      C      LIM=10
867      FAC=0.25
868      GOTO 17
869      16 LIM=6
870      FAC=1.0
871      17 DO 20 I=1,3
872      E(I)=0.0
873      DO 20 J=1,3
874      E(I,J)=0.0
875      DO 20 K=1,LIM
876      20 E(I,J)=E(I,J)+Q(I,J)*FAC
877      C      COMPUTE STRAIN ENERGY IN EACH ELEMENT
878      READ(13)KK,((OK(1,J),J=1,KK),I=1,KK)
879      C      READ(13)KK,((OK(1,J),J=1,KK),I=1,KK)
880      DO 40 I=1,KK
881      RQ(I)=0.0
882      DO 40 J=1,KK
883      40 RQ(I)=RQ(I)+0.5*Q(J)*OK(I,J)
884      W=0.0
885      DO 50 I=1,KK
886      50 W=W+RQ(I)*Q(I)
887      WORK=WORK+W
888      C      COMPUTE ELEMENT STRESSES . EQ. (5-35B)
889      C      DO 30 I=1,3
890      SIG(I)=0.0
891      DO 30 I=1,3
892      SIG(I)=SIG(I)*E(I)
893      DO 30 I=1,3
894      30 SIG(I)=SIG(I)*E(I)*E(I)
895      C      COMPUTE PRINCIPAL STRESSES AND THE ANGLE WITH THE POSITIVE X AXIS
896      SP=(SIG(1)+SIG(2))/2.0
897      SM=(SIG(1)-SIG(2))/2.0
898      DS=SIGN(SIG(1)-SIG(2))
899      SIG(4)=SP*DS
900      SIG(5)=SP-DS
901      SIG(6)=0.0
902      IF(SIG(3).NE.0.0.AND.SH.NE.0.0) S1=S1(SIG(6))=28.648*ATAN2(SIG(3),SH)
903      C      PRINT STRESSES, 50 LINES PER PAGE
904      IF(NOLINE.GT.0) GOTO 654
905      WRITE(16,1000)
906      NOLINE=49
907      54 NOLINE=NOLINE-1
908      5 WRITE(16,1010)M,XC,YC,(SIG(I),I=1,6)
909      5 WRITE(16,21)WORK
910      21 FORMAT(16.5X,"STRAIN ENERGY W/O CKEEL",G20.6,"")
911      ENDFILE1
912      300 FORMAT("OUTPUT TABLE 2 - STRESSES AT ELEMENT CENTROIDS"/1X,
913      "ELEMENT",9X,"X",9X,"Y",9X,"SIGMAX",4X,"SIGMAY",4X,
914      "+TAUX(X,Y)",4X,"SIGMA(1)",4X,"SIGMA(2)",7X,ANGLE")
915      1000 FORMAT("1 - ELEMENT",9X,"X",9X,"Y",4X,"SIGMA(X)",4X,
916      "+SIGMA(Y)",4X,"TAUX(X,Y)",4X,"SIGMA(1)",4X,"SIGMA(2)",7X,
917      "+ANGLE")
918      1010 FORMAT(16.2F10.2,1P6E12.4)
919      RETURN
920      END
921      SUBROUTINE BANSOL(A,B,NEQ,NBAND,MAXDOF,MAXBW)
922      C      IMPLICIT REAL*8 (A-H,O-Z)
923      C      IMPLICIT REAL(A-H,O-Z)
924      DIMENSION A(MAXDOF,MAXBW),B(1)
925      DO 100 I=1,NEQ
926      I=N
927      DO 20 L=2,NBAND
928      I=I+1
929      IF(A(I,N,L).EQ.0.) GOTO 20
930      C=A(I,N,L)/A(I,N,1)
931      J=0
932      DO 30 K=L,NBAND
933      J=J+1
934      IF(A(I,N,K).EQ.0.) GOTO 30
935      A(I,J)=A(I,J)-C*A(I,N,K)
936      30 CONTINUE
937      A(N,L)=C
938      C      REDUCE LOAD VECTOR
939      61(I)=B(I)-C*B(N)
940      20 CONTINUE
941      10 B(N)=B(N)/A(N,1)
942      C      BACK SUBSTITUTION
943      N=NEQ
944      35 N=N-1
945      IF(N.LE.0) GOTO 43
946      L=N
947      DO 40 K=2,NBAND
948      L=L+1
949      IF(A(I,N,K).EQ.0.) GOTO 40
950      B(N)=B(N)-A(N,K)*B(L)
951      40 CONTINUE
952      GOTO 35
953      43 RETURN
954      END
955      C      SUBROUTINE SINVA(N,EPS,IER)
956      REAL*B(A(1)),APS,DIN,WORK
957      REAL(A(1)),APS,DIN,WORK
958      CALL MFSD(A,N,EPS,IER)
959      IF(IER)<9,1,1
960      1 IPIV=N-(N+1)/2

```

```

961      IND=IPIV
962      DO 61=1,N
963      DIN=1,EO/DBLE(A(IPIV))
964      A(IPIV)=DIN
965      MIN=N
966      KEND=I-1
967      LANF=N-KEND
968      IF(KEND<5,2
2      J=IND
970      DO 4K=1,KEND
971      WORK=0.EO
972      MIN=MIN-1
973      LHOR=IPIV
974      LVER=J
975      DO 3L=LANF,MIN
976      LVER=LVER+1
977      LHOR=LHOR+L
978      WORK=WORK+DBLE(A(LVER))*A(LHOR)
979      A(IJ)=WORK+DIN
980      IJ=MIN
981      IPIV=IPIV-MIN
982      IND=IND-1
983      DO 8I=1,N
984      IPIV=IPIV+I
985      J=IPIV
986      DO 8K=1,N
987      WORK=0.EO
988      LHOR=J
989      DO 7LSK,N
990      LHOR=LHOR+K-1
991      WORK=WORK+DBLE(A(LHOR))*A(LVER)
992      LHOR=LHOR+L
993      A(IJ)=WORK
994      J=J+K
995      RETURN
996      END SUBROUTINE MFSDA(N,EPS,IER)
997      REAL=8 A(1),EPS,TOL
998      C
999      REAL A(1),EPS,TOL
1000      C
1001      REAL DPIV,DSUM
1002      IF(N-1)12,1,1
1003      IER=0
1004      KPIV=0
1005      DO 11K=1,N
1006      KPIVK=KPIV*K
1007      IND=KPIV
1008      LEND=K-1
1009      TOL=ABS(EPS*A(KPIV))
1010      DO 111=K,N
1011      DSUM=0.EO
1012      IF(LEND)12,4,2
2      DO 3L=1,LEND
1013      LANFK=KPIV-L
1014      LIND=LIND-L
1015      3      DSUM=DSUM+DBLE(A(LANF)*A(LIND))
1016      4      DSUM=DSUM-A(IND)
1017      5      IF((K)10,5,10
1018      5      IF(DSUM)-TOL,6,9
1019      6      IF(DSUM)12,12,7

```

Sample Input for Finite Element Fracture Program- The following pages contain the input cards necessary to run the finite element program.

		PHASE	2	MESH,	TIP=	53.5
1	615	565	3	7	1	0
1	2	3	4	5	6	7
2	3	4	5	6	7	8
3	3	3	3	3	3	3
4	3	3	3	3	3	3
5	3	3	3	3	3	3
6	3	3	3	3	3	3
7	3	3	3	3	3	3
8	3	3	3	3	3	3
9	3	3	3	3	3	3
10	3	3	3	3	3	3
11	3	3	3	3	3	3
12	3	3	3	3	3	3
13	3	3	3	3	3	3
14	3	3	3	3	3	3
15	3	3	3	3	3	3
16	3	3	3	3	3	3
17	3	3	3	3	3	3
18	3	3	3	3	3	3
19	3	3	3	3	3	3
20	3	3	3	3	3	3
21	3	3	3	3	3	3
22	3	3	3	3	3	3
23	3	3	3	3	3	3
24	3	3	3	3	3	3
25	3	3	3	3	3	3
26	3	3	3	3	3	3
27	3	3	3	3	3	3
28	3	3	3	3	3	3
29	3	3	3	3	3	3
30	3	3	3	3	3	3
31	3	3	3	3	3	3
32	3	3	3	3	3	3
33	3	3	3	3	3	3
34	3	3	3	3	3	3
35	3	3	3	3	3	3
36	3	3	3	3	3	3
37	3	3	3	3	3	3
38	3	3	3	3	3	3
39	3	3	3	3	3	3
40	3	3	3	3	3	3
41	3	3	3	3	3	3
42	3	3	3	3	3	3
43	3	3	3	3	3	3
44	3	3	3	3	3	3
45	3	3	3	3	3	3
46	3	3	3	3	3	3
47	3	3	3	3	3	3
48	3	3	3	3	3	3
49	3	3	3	3	3	3
50	3	3	3	3	3	3
51	3	3	3	3	3	3
52	3	3	3	3	3	3
53	3	3	3	3	3	3
54	3	3	3	3	3	3
55	3	3	3	3	3	3
56	3	3	3	3	3	3
57	3	3	3	3	3	3
58	3	3	3	3	3	3
59	3	3	3	3	3	3
60	3	3	3	3	3	3

0	58.0	28.0
0	66.0	28.0
0	68.0	28.0
0	69.0	28.0
0	69.3	28.0
1	69.75	28.0
1	69.95	28.0
1	3.0.0	34.0
1	24.0	34.0
1	42.0	34.0
1	58.0	34.0
1	66.0	34.0
1	68.0	34.0
1	69.0	34.0
1	69.3	34.0
1	69.75	34.0
1	69.95	34.0
1	0	34.0
1	3.0.0	40.0
1	24.0	40.0
1	42.0	40.0
1	58.0	40.0
1	66.0	40.0
1	68.0	40.0
1	69.0	40.0
1	69.3	40.0
1	69.75	40.0
1	69.95	40.0
1	0	44.0
1	24.0	44.0
1	42.0	44.0
1	58.0	44.0
1	66.0	44.0
1	68.0	44.0
1	69.0	44.0
1	69.3	44.0
1	69.75	44.0
1	69.95	44.0
1	0	46.0
1	24.0	46.0
1	42.0	46.0
1	58.0	46.0
1	66.0	46.0
1	68.0	46.0
1	69.0	46.0
1	69.3	46.0
1	69.75	46.0
1	69.95	46.0
1	0	48.0
1	24.0	48.0
1	42.0	48.0
1	58.0	48.0
1	66.0	48.0
1	68.0	48.0
1	69.0	48.0
1	69.3	48.0
1	69.75	48.0
1	69.95	48.0
1	0	49.0
1	24.0	49.0
1	42.0	49.0
1	58.0	49.0
1	66.0	49.0
1	68.0	49.0
1	69.0	49.0
1	69.3	49.0
1	69.75	49.0
1	69.95	49.0

23	0	58.0	49.0
22	0	66.0	49.0
23	0	68.0	49.0
24	0	69.0	49.0
25	0	69.3	49.0
26	0	69.75	49.0
27	0	69.95	49.0
28	3	0.0	50.0
29	24.6	0	50.0
30	24.9	0	50.0
31	25.3	0	50.0
32	25.7	0	50.0
33	25.9	0	50.0
34	26.1	0	50.0
35	26.2	0	50.0
36	26.3	0	50.0
37	26.4	0	50.0
38	26.5	3	0.0
39	26.8	0	50.833
40	27.1	0	50.833
41	27.5	0	50.833
42	27.9	0	50.833
43	28.1	0	50.833
44	28.3	0	50.833
45	28.4	0	50.833
46	28.5	0	50.833
47	28.6	0	50.833
48	28.7	3	0.0
49	29.0	0	51.5
50	29.3	0	51.5
51	29.7	0	51.5
52	30.1	0	51.5
53	30.3	0	51.5
54	30.5	0	51.5
55	30.6	0	51.5
56	30.7	0	51.5
57	30.8	0	51.5
58	30.9	3	0.0
59	31.2	0	51.833
60	31.5	0	51.833
61	31.9	0	51.833
62	32.3	0	51.833
63	32.5	0	52.167
64	32.7	0	52.167
65	32.8	0	52.167
66	32.9	0	52.167
67	33.0	0	52.167
68	33.1	3	0.0
69	33.4	0	52.5
70	33.7	0	52.5
71	34.1	0	52.5
72	34.5	0	52.5
73	34.7	0	52.5
74	34.9	0	52.5
75	35.0	0	52.5
76	35.1	0	52.5
77	35.2	0	52.5
78	35.3	0	52.5
79	35.6	0	52.0
80	35.9	0	52.0

181	182	363	367	369	0	58.0
183	184	371	372	0	66.0	
185	186	373	374	0	68.0	
187	188	375	376	0	69.0	
189	190	378	381	0	70.0	
191	192	385	389	0	71.0	
193	194	391	393	0	72.0	
195	196	394	395	0	73.0	
197	198	396	397	0	74.0	
199	200	398	400	0	75.0	
201	202	399	403	0	76.0	
203	204	400	407	0	77.0	
205	206	401	411	0	78.0	
207	208	402	413	0	79.0	
209	210	403	415	0	80.0	
211	212	404	425	0	81.0	
213	214	405	429	0	82.0	
215	216	406	438	0	83.0	
217	218	407	443	0	84.0	
219	220	408	446	0	85.0	
221	222	409	450	0	86.0	
223	224	410	454	0	87.0	
225	226	411	456	0	88.0	
227	228	412	462	3	0.0	
229	230	413	465	0	24.0	
231	232	414	468	0	42.0	
233	234	415	472	0	58.0	
235	236	416	476	0	66.0	
237	238	417	478	0	68.0	
239	240	418	481	0	69.0	
			482	0	69.75	
			483	3	0.0	
			484	0	70.0	
			487	0	74.0	
			490	0	74.5	
			494	0	76.0	

22222

301	43	63	65	66	66	67	67	2
302	303	64	67	68	90	89	2	2
304	84	87	88	110	109	2	2	2
305	85	89	90	112	111	2	2	2
306	105	109	110	132	131	2	2	2
307	106	111	112	134	133	2	2	2
308	126	131	132	154	153	2	2	2
309	127	133	134	156	155	2	2	2
310	147	153	154	176	175	2	2	2
311	148	155	156	178	177	2	2	2
312	168	175	176	198	197	2	2	2
313	169	177	178	200	199	2	2	2
314	189	197	198	220	219	2	2	2
315	190	199	200	222	221	2	2	2
316	210	219	220	242	241	2	2	2
317	211	221	222	244	243	2	2	2
318	231	241	242	264	263	2	2	2
319	232	243	244	266	265	1	1	1
320	252	263	264	286	285	1	1	1
321	253	265	266	298	287	1	1	1
322	273	285	286	308	307	1	1	1
323	274	287	288	310	309	1	1	1
324	294	307	308	330	329	1	1	1
325	295	309	310	332	331	1	1	1
326	315	329	330	352	351	1	1	1
327	316	331	332	354	353	1	1	1
328	336	351	352	374	373	1	1	1
329	337	353	354	376	375	1	1	1
330	357	373	374	396	395	1	1	1
331	358	375	376	398	397	1	1	1
332	378	395	396	416	417	1	1	1
333	379	397	398	420	419	1	1	1
334	398	416	417	439	438	1	1	1
335	399	419	420	441	440	1	1	1
336	418	438	439	460	459	1	1	1
337	419	440	441	463	462	1	1	1
338	439	460	461	483	482	1	1	1
339	440	462	463	485	484	1	1	1
340	460	482	483	505	504	1	1	1
341	461	484	485	507	506	1	1	1
342	481	504	505	527	526	1	1	1
343	482	506	507	529	528	1	1	1
344	502	526	527	549	548	1	1	1
345	503	528	529	551	550	1	1	1
346	523	548	549	571	570	1	1	1
347	524	550	551	573	572	3	3	3
348	544	570	571	593	592	3	3	3
349	545	572	573	595	594	3	3	3
350	565	592	593	615	614	3	3	3
351	264	286	1129	44	927	743	0	0
352	286	308	927	743	765	90	0	0
353	308	330	765	90	685	113	0	0
354	330	352	685	113	604	327	0	0
355	352	374	604	327	523	54	0	0
356	374	396	523	54	442	753	0	0
357	396	418	442	753	341	77	0	0
358	1	1	70	0	53	5	0	0
359	417	418	461	460	439	44	0	0
360	0							

Sample Outupt From Finite Element Fracture Program - The following pages contain the output from the finite element program run using the sample data.

PROBLEM 1.. PHASE MESH, P= 53.

INPUT TABLE 1.. BASIC PARAMETERS

NUMBER OF NODAL POINTS.	615
NUMBER OF ELEMENTS.	565
NUMBER OF DIFFERENT MATERIALS	3
NUMBER OF SURFACE LOAD CARDS	7
1 = PLANE STRAIN, 2 = PLANE STRESS	1
BODY FORCES(1 = IN -Y DIREC., 0 = NONE)	0

NUMBER OF CRACK ELEMENTS. 1

INPUT TABLE 2.. MATERIAL PROPERTIES

MATERIAL NUMBER	MODULUS OF ELASTICITY	POISSON'S RATIO	MATERIAL DENSITY	MATERIAL THICKNESS
1	0.8000E+06	0.3500E+00	0.0000E+01	0.1000E+01
2	0.9000E+04	0.3500E+00	0.0000E+01	0.1000E+01
3	0.3500E+06	0.3500E+00	0.0000E+01	0.1000E+01

INPUT TABLE 3. NODAL POINT DATA

107

e_X

INPUT TABLE 4. ELEMENT DATA

ELEMENT	GLOBAL INDICES OF ELEMENT	NODES	4	MATERIAL
1	1	2	3	2
1	1	2	24	23
2	2	3	25	24
3	3	4	26	25
4	4	5	27	26
5	5	6	28	27
6	6	7	29	28
7	7	8	30	29
8	8	9	31	30
9	9	10	32	31
10	10	11	33	32
11	11	12	34	33
12	12	13	35	34
13	13	14	36	35
14	14	15	37	36
15	15	16	38	37
16	16	17	39	38
17	17	18	40	39
18	18	19	41	40
19	19	20	42	41
20	20	21	43	42
21	21	22	44	43
22	22	23	45	44
23	23	24	46	45
24	24	25	47	46
25	25	26	48	47
26	26	27	49	48
27	27	28	50	49
28	28	29	51	50
29	29	30	52	51
30	30	31	53	52
31	31	32	54	53
32	32	33	55	54
33	33	34	56	55
34	34	35	57	56
35	35	36	58	57
36	36	37	59	58
37	37	38	60	59
38	38	39	61	60
39	39	40	62	61
40	40	41	63	62
41	41	42	64	63
42	42	43	65	64
43	43	44	66	65
44	44	45	67	66
45	45	46	68	67
46	46	47	69	68
47	47	48	70	69
48	48	49	71	70
49	49	50	72	71
50	50	51	73	72
51	51	52	74	73
52	52	53	75	74
53	53	54	76	75
54	54	55	77	76
55	55	56	78	77
56	56	57	79	78
57	57	58	80	79
58	58	59	81	80

↓
X_c

537	563	564	564	565	565	566	566	567	567	568	568	569	569	570	570	571	571	573	573	574	574	575	575	576	576	577	577	578	578	579	579	580	580	581	581	582	582	583	583	584	584	585	585	586	586	587	587	588	588	589	589	590	590	591	591	592	592	593	593	594	594	595	595	596	596	597	597	598	598	599	599	600	600	601	601	602	602	603	603	604	604	605	605	606	606	607	607	608	608	609	609	610	610	611	611	612	612	613	613	614	614	615	615	616	616
585	586	586	587	587	588	588	588	588	589	589	589	589	590	590	591	591	592	592	593	593	594	594	595	595	596	596	597	597	598	598	599	599	600	600	601	601	602	602	603	603	604	604	605	605	606	606	607	607	608	608	609	609	610	610	611	611	612	612	613	613	614	614	615	615	616	616																																							
586	587	587	588	588	588	588	588	589	589	589	589	590	590	591	591	592	592	593	593	594	594	595	595	596	596	597	597	598	598	599	599	600	600	601	601	602	602	603	603	604	604	605	605	606	606	607	607	608	608	609	609	610	610	611	611	612	612	613	613	614	614	615	615	616	616																																								
587	588	588	589	589	589	589	589	590	590	590	590	591	591	592	592	593	593	594	594	595	595	596	596	597	597	598	598	599	599	600	600	601	601	602	602	603	603	604	604	605	605	606	606	607	607	608	608	609	609	610	610	611	611	612	612	613	613	614	614	615	615	616	616																																										

INPUT TABLE 5.. SURFACE LOADING DATA

		SURFACE LOAD INTENSITIES AT NODES		
NODE	J	XI	XJ	YI
264	286	0.1129E+04	0.9277E+03	0.0000E+01
286	308	0.9277E+03	0.7659E+03	0.0000E+01
308	330	0.7659E+03	0.6851E+03	0.0000E+01
330	352	0.6851E+03	0.6043E+03	0.0000E+01
352	374	0.6043E+03	0.5235E+03	0.0000E+01
374	396	0.5235E+03	0.4428E+03	0.0000E+01
396	418	0.4428E+03	0.3418E+03	0.0000E+01
XXY(1)=		69.7500		
XXY(2)=		53.2500		
XXY(3)=		69.9500		
XXY(4)=		53.2500		
XXY(5)=		70.0000		
XXY(6)=		53.7500		
XXY(7)=		69.7500		
XXY(8)=		53.7500		
XXY(9)=		69.7500		
XXY(10)=		53.5000		
SMU ETA =		296296.	1.60000	
LP (1)=		833		
LP (2)=		834		
LP (3)=		835		
LP (4)=		836		
LP (5)=		921		
LP (6)=		922		
LP (7)=		919		
LP (8)=		920		
LP (9)=		877		
LP (10)=		878		
EK(1)=		417700.	AK(833, 1)=	0.228690E+07
EK(2)=		184875.	AK(833, 2)=	-62038.5
EK(4)=		-588078.	AK(833, 3)=	-0.147536E+07

```

EK(  7)=      684789.    AK(833,   4)=      586023.
EK( 11)=     -837088.    AK(833,   89)=     -837088.
EK( 16)=      299415.    AK(833,   90)=      299415.
EK( 22)=     -59503.0    AK(833,   87)=     -59503.0
EK( 29)=     -212898.    AK(833,   88)=     -212898.
EK( 37)=      45405.0    AK(833,   45)=     -16180.3
EK( 46)=     -174474.    AK(833,   46)=     -75708.6
EK(  3)=      957870.    AK(834,   1)=      0.274957E+07
EK(  5)=     -215972.    AK(834,   2)=     -117207.
EK(  8)=      877590.    AK(834,   3)=      766150.
EK( 12)=     -358996.    AK(834,   86)=     -358996.
EK( 17)=      36150.5    AK(834,   89)=      36150.5
EK( 23)=      5510.71    AK(834,   86)=      5510.71
EK( 30)=      3410.25    AK(834,   87)=      3410.25
EK( 38)=     -44951.4    AK(834,   44)=     -143717.
EK( 47)=     -52300.7    AK(834,   45)=     -800582.
EK(  6)=      968673.    AK(835,   1)=      0.192701E+07
EK(  9)=     -0.123052E+07AK(835,   2)=     -983604.
EK( 13)=      0.150160E+07AK(835,   87)=      0.150160E+07
EK( 18)=     -672270.    AK(835,   88)=     -672270.
EK( 24)=      62758.4    AK(835,   85)=      62758.4
EK( 31)=      382421.    AK(835,   86)=      382421.
EK( 39)=     -203353.    AK(835,   43)=     -203353.
EK( 48)=      338999.    AK(835,   44)=      338999.
EK( 10)=      0.296001E+07AK(836,   1)=      0.337935E+07
EK( 14)=     -0.227816E+07AK(836,   86)=     -0.227816E+07
EK( 19)=      0.128738E+07AK(836,   87)=      0.128738E+07
EK( 25)=     -123993.    AK(836,   84)=     -123993.
EK( 32)=     -835522.    AK(836,   85)=     -835522.
EK( 40)=      409269.    AK(836,   42)=      409269.

```

```

EK( 49)=          -678742.    AK(836, 43)=      -678742.
EK( 15)=          0.304262E+07AK(921, 1)=      0.370452E+07
EK( 20)=          -0.136613E+07AK(921, 2)=     -0.161304E+07
EK( 21)=          994082.    AK(922, 1)=       0.143286E+07
EK( 26)=          17294.2    AK(919, 3)=       -536778.
EK( 27)=          92972.3    AK(919, 4)=       191738.
EK( 28)=          220480.    AK(919, 1)=       0.175314E+07
EK( 35)=          -4516.77   AK(919, 2)=       242397.
EK( 33)=          807875.    AK(920, 2)=       709109.
EK( 34)=          -649759.    AK(920, 3)=       -629988.
EK( 36)=          633420.    AK(920, 1)=       0.251987E+07
EK( 41)=          -694315.    AK(877, 45)=     -694315.
EK( 42)=          312595.    AK(877, 46)=     312595.
EK( 43)=          -6956.74   AK(877, 43)=     -68542.1
EK( 44)=          -186293.    AK(877, 44)=     -87527.8
EK( 45)=          380178.    AK(877, 1)=       0.121665E+07
EK( 54)=          -131997.    AK(877, 2)=     -131997.
EK( 50)=          565610.    AK(878, 44)=     565610.
EK( 51)=          -385751.    AK(878, 45)=     -385751.
EK( 52)=          -70180.5   AK(878, 42)=     -168946.
EK( 53)=          209317.    AK(878, 43)=     -538965.
EK( 55)=          316467.    AK(878, 1)=       0.197764E+07
NODE NOE MATYP XC,YC = 5 10 1 70.000 53.500

```

OUTPUT TABLE 1. NODAL DISPLACEMENTS

NODE	$U = X\text{-DISP.}$	$V = Y\text{-DISP.}$
1	0.0000000E+01	0.0000000E+01
2	0.0000000E+01	0.0000000E+01
3	0.0000000E+01	0.0000000E+01
4	0.0000000E+01	0.0000000E+01
5	0.0000000E+01	0.0000000E+01
6	0.0000000E+01	0.0000000E+01
7	0.0000000E+01	0.0000000E+01
8	0.0000000E+01	0.0000000E+01
9	0.0000000E+01	0.0000000E+01
10	0.0000000E+01	0.0000000E+01
11	0.0000000E+01	0.0000000E+01
12	0.0000000E+01	0.0000000E+01
13	0.0000000E+01	0.0000000E+01
14	0.0000000E+01	0.0000000E+01
15	0.0000000E+01	0.0000000E+01
16	0.0000000E+01	0.0000000E+01
17	0.0000000E+01	0.0000000E+01
18	0.0000000E+01	0.0000000E+01
19	0.0000000E+01	0.0000000E+01
20	0.0000000E+01	0.0000000E+01
21	0.0000000E+01	0.0000000E+01
22	0.0000000E+01	0.0000000E+01
23	-0.29459278E-03	-0.28193287E-03
24	-0.44878650E-03	-0.43177822E-03
25	-0.51457460E-03	-0.58366282E-03
26	-0.51170654E-03	-0.68915919E-03
27	-0.47060586E-03	-0.78535081E-03
28	-0.40061687E-03	-0.86495271E-03
29	-0.34372909E-03	-0.90640712E-03
30	-0.28343639E-03	-0.93907456E-03
31	-0.2265075E-03	-0.96365586E-03
32	-0.16326207E-03	-0.98131581E-03
33	-0.13475132E-03	-0.98804972E-03
34	-0.10679104E-03	-0.99339968E-03
35	-0.79320687E-04	-0.99748519E-03
36	-0.52242535E-04	-0.10003954E-02
37	-0.38937255E-04	-0.10014255E-02
38	-0.25682929E-04	-0.10021573E-02
39	-0.19088827E-04	-0.10024125E-02
40	-0.12501123E-04	-0.10025926E-02
41	-0.85532066E-05	-0.10026646E-02
42	-0.26302938E-05	-0.10027219E-02
43	-0.77187055E-03	-0.14035886E-02
44	0.0000000E+01	0.0000000E+01
45	0.0000000E+01	0.0000000E+01
46	-0.38157881E-03	-0.42538909E-03
47	-0.65292158E-03	-0.78945290E-03
48	-0.77454617E-03	-0.11485390E-02
49	-0.77187055E-03	-0.16307741E-02
50	-0.69960538E-03	-0.18103427E-02
51	-0.57774340E-03	-0.18977547E-02
52	-0.48162371E-03	-0.19608413E-02
53	-0.38343408E-03	-0.20456273E-02
54	-0.28984585E-03	-0.2093368E-02
55	-0.20482598E-03	-0.20385736E-02
56	-0.16618953E-03	-0.19297512E-02
57	-0.12975121E-03	-0.19045627E-02

$\rightarrow e^x$

598	0. 225433114E-02	-0. 54546608E-02
599	0. 25694593E-02	-0. 68603169E-02
600	0. 23651390E-02	-0. 79864856E-02
601	0. 20386126E-02	-0. 84418006E-02
602	0. 15607427E-02	-0. 85685298E-02
603	0. 91011823E-03	-0. 82453191E-02
604	0. 97091072E-04	-0. 73450069E-02
605	-0. 38923418E-03	-0. 65925266E-02
606	-0. 83608933E-03	-0. 56247722E-02
607	-0. 11483184E-02	-0. 44416935E-02
608	-0. 11743366E-02	-0. 31315278E-02
609	-0. 10270291E-02	-0. 25424788E-02
610	-0. 76199918E-03	-0. 20472161E-02
611	-0. 59469481E-03	-0. 18627626E-02
612	-0. 40683914E-03	-0. 17251853E-02
613	-0. 28889666E-03	-0. 1680948E-02
614	-0. 10311623E-03	-0. 16194794E-02
615	0. 00000000E+01	-0. 16124230E-02

OUTPUT TABLE 2.. STRESSES AT ELEMENT CENTROIDS

ELEMENT	X	Y	SIGMA(X)	SIGMA(Y)	TAU(X, Y)	SIGMA(1)	SIGMA(2)	ANGLE	
			-4.00	-4.0300E-01	-3.9773E-01	-1.2011E-01	-2.8023E-01	-4.5629E+01	
1	4.00	4.00	-4.8615E-01	-7.1928E-01	-1.8609E-01	-3.8313E-01	-8.2230E-01	-2.8969E+01	
2	12.00	4.00	-5.5301E-01	-9.4870E-01	-2.3234E-01	-4.4569E-01	-1.0560E+00	-2.4793E+01	
3	20.00	4.00	-6.1528E-01	-1.1472E+00	-2.4311E-01	-5.2091E-01	-1.2416E+00	-2.1215E+01	
4	27.00	4.00	-6.6730E-01	-1.3045E+00	-2.3137E-01	-5.9216E-01	-1.3797E+00	-1.7993E+01	
5	33.00	4.00	-7.1798E-01	-1.4445E+00	-2.0362E-01	-6.6481E-01	-1.4977E+00	-1.4636E+01	
6	39.00	4.00	-7.5836E-01	-1.5438E+00	-1.7234E-01	-7.2221E-01	-1.5800E+00	-1.1847E+01	
7	44.00	4.00	-7.8825E-01	-1.6074E+00	-1.4427E-01	-7.6358E-01	-1.6321E+00	-9.7018E+00	
8	48.00	4.00	-8.1519E-01	-1.6586E+00	-1.1568E-01	-7.9961E-01	-1.6742E+00	-7.6693E+00	
9	52.00	4.00	-8.3824E-01	-1.6981E+00	-8.7757E-02	-8.2938E-01	-1.7070E+00	-5.7681E+00	
10	56.00	4.00	-8.5437E-01	-1.7225E+00	-6.7698E-02	-8.4913E-01	-1.7277E+00	-4.4325E+00	
11	61.00	4.00	-8.6224E-01	-1.7344E+00	-5.4780E-02	-8.5881E-01	-1.7379E+00	-3.5798E+00	
12	63.00	4.00	-8.6859E-01	-1.7439E+00	-4.2178E-02	-8.6657E-01	-1.7459E+00	-2.7523E+00	
13	65.00	4.00	-8.7341E-01	-1.7510E+00	-2.9834E-02	-8.7240E-01	-1.7520E+00	-1.9448E+00	
14	69.15	4.00	-8.7974E-01	-1.7591E+00	-2.5421E-03	-8.7977E-01	-1.7559E+00	-1.3500E+00	
15	66.50	4.00	-8.7701E-01	-1.7555E+00	-2.0713E-02	-8.7653E-01	-1.7592E+00	-1.6561E+01	
16	67.25	4.00	-8.7824E-01	-1.7572E+00	-1.4682E-02	-8.7799E-01	-1.7575E+00	-9.5667E-01	
17	68.25	4.00	-8.7920E-01	-1.7584E+00	-1.0178E-02	-8.7908E-01	-1.7585E+00	-6.6318E-01	
18	68.75	4.00	-8.7950E-01	-1.7588E+00	-7.1617E-03	-8.7944E-01	-1.7589E+00	-4.6790E-01	
19	69.15	4.00	-8.7974E-01	-1.7591E+00	-4.7864E-03	-8.7971E-01	-1.7592E+00	-3.1184E-01	
20	69.53	4.00	-8.7978E-01	-1.7592E+00	-2.5421E-03	-8.7977E-01	-1.7592E+00	-1.6561E-01	
21	69.85	4.00	-8.7989E-01	-1.7593E+00	-5.9856E-04	-8.7989E-01	-1.7593E+00	-3.8997E-02	
22	4.00	12.00	-6.8017E-01	-4.5820E-01	-1.6548E-01	-3.6993E-01	-7.6844E-01	-6.1924E+01	
23	12.00	6.2777E-01	-6.5922E-01	-1.6771E-01	-4.7507E-01	-6.1197E-01	-4.2318E+01		
24	20.00	6.1765E-01	-9.2396E-01	-2.0314E-01	-5.1640E-01	-1.0252E+00	-2.6493E+01		
25	27.00	12.00	-6.1521E-01	-1.1513E+00	-2.0851E-01	-5.4366E-01	-1.2229E+00	-1.8939E+01	
26	33.00	12.00	-6.2180E-01	-1.3347E+00	-1.9174E-01	-5.7351E-01	-1.3830E+00	-1.4138E+01	
27	39.00	12.00	-6.3960E-01	-1.4924E+00	-1.5660E-01	-6.1175E-01	-1.5202E+00	-1.0084E+01	
28	44.00	12.00	-6.6521E-01	-1.5997E+00	-1.1932E-01	-6.5021E-01	-1.6147E+00	-7.1630E+00	
29	48.00	12.00	-6.9245E-01	-1.6633E+00	-8.9458E-02	-6.8427E-01	-1.6715E+00	-5.2208E+00	
30	52.00	12.00	-7.2321E-01	-1.7107E+00	-6.2651E-02	-7.1925E-01	-1.7146E+00	-3.6160E+00	
31	56.00	12.00	-7.5397E-01	-1.7441E+00	-4.0979E-02	-7.5227E-01	-1.7457E+00	-2.3660E+00	
32	59.00	12.00	-7.7665E-01	-1.7640E+00	-2.1669E-02	-7.8683E-01	-1.7648E+00	-1.6548E+00	
33	61.00	12.00	-7.8962E-01	-1.7731E+00	-2.1669E-02	-7.8914E-01	-1.7736E+00	-1.2616E+00	
34	63.00	12.00	-7.9959E-01	-1.7803E+00	-1.5829E-02	-7.9934E-01	-1.7805E+00	-9.2447E+00	
35	65.00	12.00	-8.0726E-01	-1.7855E+00	-1.0785E-02	-8.0714E-01	-1.7857E+00	-6.3156E+00	
36	66.50	12.00	-8.1332E-01	-1.7894E+00	-7.3716E-03	-8.1326E-01	-1.7894E+00	-4.3269E+00	
37	67.50	12.00	-8.1527E-01	-1.7907E+00	-5.1834E-03	-8.1524E-01	-1.7907E+00	-3.0447E+00	
38	68.25	12.00	-8.1695E-01	-1.7917E+00	-3.5814E-03	-8.1694E-01	-1.7917E+00	-2.1051E-01	
39	68.75	12.00	-8.1743E-01	-1.7920E+00	-2.5200E-03	-8.1742E-01	-1.7920E+00	-1.4815E-01	
40	69.15	12.00	-8.1785E-01	-1.7923E+00	-1.6792E-03	-8.1784E-01	-1.7923E+00	-9.8732E-02	
41	69.53	12.00	-8.1790E-01	-1.7923E+00	-8.9318E-04	-8.1789E-01	-1.7923E+00	-5.2518E-02	
42	69.85	12.00	-8.1810E-01	-1.7925E+00	-2.0823E-04	-8.1810E-01	-1.7925E+00	-1.2245E-02	
43	4.00	19.00	-7.6347E-01	-4.7406E-01	-2.0083E-01	-3.7123E-01	-8.6629E-01	-6.2888E+01	
44	12.00	19.00	-7.1854E-01	-6.4419E-01	-2.1050E-01	-4.6761E-01	-8.9512E-01	-5.0008E+01	
45	20.00	19.00	-6.5778E-01	-9.0472E-01	-2.3254E-01	-5.1797E-01	-1.0445E+00	-3.1017E+01	
46	27.00	19.00	-6.1373E-01	-1.1639E+00	-2.2811E-01	-5.3145E-01	-1.2462E+00	-1.9834E+01	
47	33.00	19.00	-5.8915E-01	-1.3760E+00	-1.9533E-01	-5.4333E-01	-1.4218E+00	-1.3202E+01	

↓ e^{1c}

ELEMENT	X	Y	SIGMA(X)	SIGMA(Y)	TAU(X,Y)	SIGMA(1)	SIGMA(2)	ANGLE
538	66.50	58.75	-1.2728E+01	4.9650E+00	7.0390E+01	-7.4826E+01	4.8582E+01	
539	67.50	58.75	1.0436E+01	-1.3283E+01	6.8006E+01	6.7610E+01	-7.0456E+01	4.0054E+01
540	68.25	58.75	2.7765E+01	-2.9699E+01	5.7093E+01	6.2948E+01	-6.4882E+01	3.1643E+01
541	68.75	58.75	3.8928E+01	-3.8991E+01	4.4427E+01	5.9058E+01	-5.9121E+01	2.4376E+01
542	69.15	58.75	4.6020E+01	-4.5326E+01	3.1820E+01	5.6012E+01	-5.5317E+01	1.7433E+01
543	69.53	58.75	5.0431E+01	-4.8837E+01	1.8259E+01	5.3663E+01	-5.2089E+01	1.0099E+01
544	69.88	58.75	5.2578E+01	-5.0865E+01	4.8212E+00	5.2802E+01	-5.1089E+01	2.6627E+00
545	4.00	60.25	5.0753E+01	1.4270E+01	-4.6237E+00	5.1330E+01	1.3693E+01	-7.1116E+00
546	12.00	60.25	3.6270E+01	-1.8187E+00	-4.7763E-01	3.6276E+01	-1.8247E+00	-7.1834E-01
547	20.00	60.25	2.6229E+01	3.2224E-02	-2.0418E+00	2.6387E+01	-1.2596E-01	-4.4301E+00
548	27.00	60.25	1.5221E+01	-1.5222E-01	-1.9310E+00	1.5460E+01	-3.9106E-01	-7.0510E+00
549	33.00	60.25	3.4321E+00	2.0267E-01	-2.2143E+00	4.5579E+00	-9.2315E-01	-2.6950E+01
550	39.00	60.25	-1.0424E+01	-7.1816E-02	-2.4162E+00	4.6435E+01	-1.0960E+01	-7.7489E+01
551	44.00	60.25	-2.7063E+01	-8.9174E-01	-2.4098E+00	-6.7170E-01	-2.7283E+01	-8.4783E+01
552	48.00	60.25	-4.0146E+01	1.6554E-01	-3.2820E+00	4.3100E-01	-4.0412E+01	-8.5376E+01
553	52.00	60.25	-5.5168E+01	3.4740E-02	-3.5934E+00	2.6766E-01	-5.5401E+01	-8.6292E+01
554	56.00	60.25	-7.0142E+01	7.4205E-02	-2.6765E+00	-7.7608E-01	-7.0244E+01	-8.7821E+01
555	59.00	60.25	-8.2451E+01	-8.2955E-01	9.9843E-01	-8.1734E-01	-8.2463E+01	8.9300E+01
556	61.00	60.25	-7.7362E+01	1.5862E+00	4.7301E+00	1.8685E+00	-7.7644E+01	8.6584E+01
557	63.00	60.25	-5.7162E+01	2.2114E+00	1.3690E+01	5.2162E+00	-6.0166E+01	7.7622E+01
558	65.00	60.25	-1.2926E+01	4.0496E+00	2.5963E+01	2.2877E+01	-3.1753E+01	5.4052E+01
559	66.50	60.25	3.5522E+01	2.9363E+00	3.0149E+01	5.3499E+01	-1.5040E+01	3.0806E+01
560	67.50	60.25	7.0942E+01	-2.2983E+00	2.9547E+01	8.1376E+01	-1.2732E+01	1.9449E+01
561	68.25	60.25	9.4457E+01	-5.8944E+00	2.4019E+01	9.9909E+01	-1.1347E+01	1.2790E+01
562	68.75	60.25	1.0719E+02	-8.0856E+00	1.8544E+01	1.1010E+02	-1.0995E+01	8.9175E+00
563	69.15	60.25	1.1428E+02	-9.7672E+00	1.3108E+01	1.1565E+02	-1.1137E+01	5.9663E+00
564	69.53	60.25	1.1937E+02	-1.0105E+01	7.5472E+00	1.1981E+02	-1.0543E+01	3.3249E+00
565	69.88	60.25	1.2090E+02	-1.0697E+01	2.0391E+00	1.2094E+02	-1.0929E+01	8.8613E-01

STRAIN ENERGY W/O CKEL = 9.28372

NCKEL = 1
CKEL = 1

... STRESS INTENSIYY FACTOR ... 1

OPENING MODE K1 = -1066.60
SHEARING MODE K2 = 0.00000
CRACK TIP XC = 70.0000 YC = 53.5000 AT MATERIAL 1
THE SNODES = 417 418 461 460 439
STRAIN ENERGY = 0.425538

... TOTAL STRAIN ENERGY = 9.7092569

Crack Propagation Calculation Program

Figure B-2 shows the program flow diagram. The following is a brief description of the main program and each subroutine.

CRACK:

Main program. Sets values of necessary parameters and reads in necessary data. Iterates from problem to problem, reading in data specific to the problem and calling NVSC. Writes out modulus values, A, and n for each modulus condition considered.

NVSC: Calculates and applies crack increments. Computes N_f values for each increment. Computes N_f for each crack increment. Prints the

base and overlay thicknesses and the modulus condition of the pavement being analyzed.

TRAPRLE:

Given the left and right limits of the crack increment, numerically integrates the Paris equation using the trapezoidal rule, producing N_f . Iterates until the percent difference is below 10^{-3} or to a limit of 15 iterations.

SIMPRLE:

Performs exactly as does TRAPRLE except that Simpson's rule is used for the numerical integration.



Figure B-2. Flow Diagram of Program for Solution of Paris Equation

PARIS:

Determines the value of K_I for a given value of (c/b) according to equation (6), Section I. Computes the integrand of equation (4), Section I, including the base thickness term. Paris is a function which returns as its value the above integrand.

Input Guide- The input parameters and formats are explained here.

BASIC PARAMETERS:

One Card: Format 2I5

cc 1-5 **Nmodcon:** The number of modulus conditions considered for the problem.

cc 6-10 **K:** A value of $K = 0$ indicates that the trapezoidal rule will be used. Any other 5 digit integer, normally 1, indicates that Simpson's rule will be used.

Nmodcon cards: Format 4F10.0

cc 1-10 **Evalues(I,1):** Modulus of elasticity of the base corresponding to modulus condition 1.

cc11-20 **Evalues(I,2):** Modulus of elasticity of the overlay corresponding to modulus condition 1

cc 21-30 **AA(I):** Values of the parameter A in the Paris equation corresponding to modulus condition 1.

cc 31-40 **NN(I):** Value of the parameter n in the Paris equation corresponding to modulus condition 1.

PROBLEM PARAMETERS:

One card per problem: Format 3I5

cc 1-5 Nprob: The problem number of the current problem. If the value is 0, execution of the program is halted.

cc 6-10 Base: Thickness of the base.

cc 11-15 Olay: Thickness of the overlay.

Nmodcon cards per problem: Format 6F10.0

cc 1-10 B₀: Coefficient B₀ in equation (6), Section I.

cc 11-20 B₁: Coefficient B₁ in equation (6), Section I.

cc 21-30 B₂: Coefficient B₂ in equation (6), Section I.

cc 31-40 B₃: Coefficient B₃ in equation (6), Section I.

cc 41-50 Left: Initial crack length for a pavement with given base and overlay thicknesses and modulus condition.

cc 51-60 Right: Final crack length for a pavement with given base and overlay thicknesses and modulus condition.

The computer code listing for the paris equation calculation scheme is given on the following pages.

```

PROGRAM CRACK(INPUT,OUTPUT,TAPES=INPUT,TAPE6=OUTPUT)
  IMPLICIT INTEGER (A-Z)
  REAL LEFT, RIGHT, TEST, AA(20), NN(20), EVALUES(20,2), OBASE
  REAL BO,B1,B2,B3
  COMMON/INTCON/ BASE,OLAY,BO,B1,B2,B3,AA,NN
  COMMON/PARAM/ IN,OUT,TEST,Z,EVALUES
  DATA TEST/0.001/,2/15/,IN/5/,OUT/6/,OBASE/350000.0/
  READ (IN,100) NMODCON,K
  10 C
  11 WRITE(OUT,500)
  12 C
  DO 10 I=1,NMODCON
  13   READ (IN,200) EVALUES(I,1),EVALUES(I,2),AA(I),NN(I)
  14   WRITE(OUT,600) I,EVALUES(I,1),EVALUES(I,2),OBASE,AA(I),NN(I)
  15   CONTINUE
  16   10
  17 C
  18   READ (IN,300) NPROB,BASE,OLAY
  19 C
  20   IF (NPROB.EQ.0) GO TO 40
  21 C
  DO 30 I=1,NMODCON
  22   READ (IN,400) BO,B1,B2,B3,LEFT,RIGHT
  23   CALL NVSC(LEFT,RIGHT,I,K)
  24   CONTINUE
  25   30
  26 C
  27   IF (NPROB.NE.0) GO TO 20
  28 C
  29   100 FORMAT(2I5)
  30   200 FORMAT(4F10.0)
  31   300 FORMAT(3I5)
  32   400 FORMAT(6F10.0)
  33   500 FORMAT(//35X,'MODULUS',7X,'BASE',8X,'SUBGRADE',6X,'OVERLAY',/
  34   +34X,'CONDITION',5X,'MODULUS',2(6X,'MODULUS'),9X,'A',12X,'N'/30X,
  35   +6(4X,'-----'))
  36   600 FORMAT(34X,15,8X,F9.1,6X,F6.1,6X,F8.1,4X,F9.4,6X,F5.2)
  37 C
  38   40 STOP
  39   40 END
  40 C
  41 C
  42 C
  SUBROUTINE TRAPRLE(CL,CR,MODCON,DNF,FLAG,DIFF)
  IMPLICIT REAL (A-Z)
  INTEGER YOMAMA,NDIV,I,J,MODCON,IN,OUT,Z
  LOGICAL FLAG
  COMMON/PARAM/ IN,OUT,TEST,Z,EVALUES
  43   40
  44   40
  45   40
  46   40
  47   40
  48 C
  49 C
  50   40
  51   40
  52   40
  53   40
  54   40
  55 C
  56 C
  H=(CR-CL)/NDIV
  INTSUM=PARIS(CL+2*X,H,MODCON)
  ENDSUM=PARIS(CL,MODCON)+PARIS(CR,MODCON)
  57   40
  58   40
  59   40
  60 C

```

```

61 C
62 DO 10 I=1,2
63 LIM=NDIV-1
64 C
65 DO 20 J=1,LIM,2
66 ODDSUM=ODDSUM+PARIS(CL+J*H,MODCON)
67 CONTINUE
68 C
69 INTSUM=INTSUM+ODDSUM
70 NEWVAL=H/2*ENDSUM+H*INTSUM
71 DIFF=ABS(NEWVAL-OLDVAL)/NEWVAL
72 C
73 C
74 IF(DIFF.LT.TEST) THEN
75 YOMAMA=1
76 GO TO 30
77 ELSE
78 OLDVAL=NEWVAL
79 NDIV=NDIV*2
80 ODDSUM=0.0
81 H=(CR-CL)/NDIV
82 END IF
83 10 CONTINUE
84 C
85 30 IF(YOMAMA.EQ.0) THEN
86 FLAG=.TRUE.
87 DNF=NEWVAL
88 ELSE
89 DNF=NEWVAL
90 END IF
91 C
92 C
93 RETURN
94 END
95 C
96 C
97 C
98 REAL FUNCTION PARIS(X,E)
99 IMPLICIT REAL (A-Z)
100 INTEGER E,BASE,OUT
101 DIMENSION AA(20),NN(20)
102 COMMON/LINTCON/ BASE,OLAY,B0,B1,B2,B3,AA,NN
103 COMMON/PARAM/ IN,OUT,TEST,Z,EVALUES
104 C
105 A=AA(E)
106 N=NN(E)
107 KI=BO+B1*X+B2*(X**2)+B3*(X**3)
108 IF(KI.LE.0.0) THEN
109 WRITE(OUT,100) X
110 STOP
111 END IF
112 POWER=-N
113 KN=KI**POWER
114 PARIS=(KN/A)*BASE
115 C
116 C
117 100 FORMAT(1X,'>>>>>>>>',KI IS NEGATIVE FOR C/B= ,F6.4)
118 C
119 C
120 999 RETURN

```

```

121      END
122      C
123      C
124      C
125      SUBROUTINE NVSC(LEFT,RIGHT,MODCON,K)
126      IMPLICIT REAL (A-Z)
127      INTEGER NINC,I,OUT
128      LOGICAL FLAG
129      COMMON /PARAM/ IN,OUT
130      COMMON /INTCON/ BASE,OLAY
131      C
132      C
133      NF=0.0
134      NINC=20
135      C
136      DC=(RIGHT-LEFT)/NINC
137      CL=LEFT
138      C
139      WRITE(OUT,100) BASE,OLAY,MODCON
140      WRITE(OUT,200)
141      C
142      DO 10 I=1,NINC
143      CR=CL+DC
144      IF(K.EQ.0) THEN
145      CALL TRAPRL(CL,CR,MODCON,DNF,FLAG,DIFF)
146      ELSE
147      CALL SIMPRL(CL,CR,MODCON,DNF,FLAG,DIFF)
148      END IF
149      NF=NF+DNF
150      C
151      WRITE(OUT,300) CL,CR,DNF,NF
152      IF(FLAG) THEN
153      WRITE(OUT,400) DIFF
154      END IF
155      C
156      10  CONTINUE
157      C
158      C
159      100  FORMAT('///42X,'DEPTH OF BASE',15//42X,
160      +'DEPTH OF OVERLAY.....',15//42X,'MODULUS CONDITION',
161      +15)
162      200  FORMAT('///39X,'INITIAL',9X,'CURRENT',6X,'INCREMENTAL',7X,
163      +'CURRENT',33X,2(4X,'C/B RATIO'),2(5X,'LOAD CYCLES'),/
164      +'33X,4(4X,'-----'))
165      300  FORMAT(30X,2(10X,F6.4),8X,E10.5)
166      400  FORMAT(35X,'>>>>>', 'ERROR: THE PRECEDING LOAD',
167      +' CYCLES INCREMENT DID',35X,'>>>>>',6X,'NOT CONVERGE',
168      +' THE VALUE OF X DIFFERENCE',35X,'>>>>>',6X,'AFTER 15',
169      +' ITERATIONS IS ',E10.5)
170      C
171      C
172      RETURN
173      END
174      C
175      C
176      C
177      SUBROUTINE SIMPRL(CL,CR,MODCON,DNF,FLAG,DIFF)
178      IMPLICIT REAL (A-Z)
179      INTEGER YODADY,NDIV,I,J,MODCON,IN,OUT,Z
180      LOGICAL FLAG

```

```

181      COMMON/PARAM/ IN,OUT,TEST,Z
182      C
183      C
184      FLAG=.FALSE.
185      YODADY=0
186      NDIV=4
187      C
188      H=(CR-CL)/NDIV
189      EVENTS=PARIS(CL+2*H,MODCON)
190      ODDS=PARIS(CL+H,MODCON)+PARIS(CL+3*H,MODCON)
191      ENDSUM=PARIS(CL,MODCON)+PARIS(CR,MODCON)
192      OLDVAL=H/3.0*(ENDSUM+4*ODDS+2*EVENTS)
193      C
194      DO 10 I=2,Z
195      NDIV=2*NDIV
196      H=(CR-CL)/NDIV
197      EVENTS=EVENTS+ODDS
198      ODDS=0.0
199      LIM=NDIV-1
200      DO 20 J=1,LIM,2
201      ODDS=ODDS+PARIS(CL+J*H,MODCON)
202      CONTINUE
203      NEWVAL=H/3.0*(ENDSUM+4*ODDS+2*EVENTS)
204      DIFF=ABS(NEWVAL-OLDVAL)/NEWVAL
205      IF(DIFF.LT.TEST) THEN
206          YODADY=1
207          GO TO 30
208      ELSE
209          OLDVAL=NEWVAL
210      END IF
211      10  CONTINUE
212      C
213      30  IF(YODADY.EQ.0) THEN
214          FLAG=.TRUE.
215          DNF=NEWVAL
216      ELSE
217          DNF=NEWVAL
218          END IF
219      C
220      RETURN
221      END

```

Sample Input for Crack Propagation Program- THe following pages contain a printout of the input data for the sample program.

1	6	1	16	0	1.0E-10	2.0
2	1200000.0	4000.0	1.0E-10	2.0	1.0E-10	2.0
3	1200000.0	9000.0	1.0E-10	2.0	1.0E-10	2.0
4	800000.0	4000.0	1.0E-10	2.0	1.0E-10	2.0
5	800000.0	9000.0	1.0E-10	2.0	1.0E-10	2.0
6	400000.0	4000.0	1.0E-10	2.0	1.0E-10	2.0
7	400000.0	9000.0	1.0E-10	2.0	1.0E-10	2.0
8	9	12	0	0	0.0	1.0
9	808.9672	6928.043	-22642.82	17098.41	0.0	1.0
10	687.1326	5742.7	-19189.89	14661.88	0.0	1.0
11	776.454	6547.792	-22345.7	17517.9	0.0	1.0
12	611.0261	5000.017	-16980.85	13073.25	0.0	1.0
13	633.8081	5223.816	-17649.63	13556.44	0.0	1.0
14	472.8754	3650.308	-12930.04	10141.79	0.0	1.0
15	2	12	0	0	0.0	1.0
16	1297.536	7693.483	-22383.32	14619.22	0.0	1.0
17	1019.034	5847.388	-17613.8	11676.7	0.0	1.0
18	1162.857	6804.254	-20087.0	13202.72	0.0	1.0
19	875.8471	4887.16	-15129.88	10145.02	0.0	1.0
20	916.8071	5163.552	-15845.97	10587.44	0.0	1.0
21	654.5362	3373.223	-11169.04	7681.451	0.0	1.0
22	3	8	0	0	0.0	1.0
23	2047.043	6567.108	-14172.16	5067.807	0.0	0.925977
24	1490.105	4544.518	-10815.35	4237.885	0.0	0.880402
25	1753.576	5513.253	-12415.28	4625.061	0.0	0.905503
26	1260.895	3666.674	-9340.74	3857.532	0.0	0.849451
27	1351.92	3600.485	-8792.111	3060.146	0.0	0.837093
28	938.921	2345.091	-6942.935	3093.236	0.0	0.764195
29	4	8	3	0	0.0	1.0
30	-394.5381	37465.05	-117437.1	105884.9	0.010901	1.0
31	-235.5056	26687.0	-84582.0	76535.6	0.009085	1.0
32	-280.6712	30515.79	-96126.81	87240.12	0.009479	1.0
33	-137.2445	20948.11	-66598.86	60381.99	0.006694	1.0
34	-112.6183	20547.46	-64805.32	59002.9	0.005580	1.0
35	-12.82105	13339.98	-42658.1	38802.09	0.000965	1.0
36	5	8	6	0	0.0	1.0
37	-247.4966	28694.99	-89707.74	81544.99	0.008670	1.0
38	-148.9915	21328.18	-67057.85	60936.81	0.007146	1.0
39	-153.3865	23050.09	-71954.05	65549.56	0.006799	1.0
40	-72.99951	16591.39	-52166.28	47507.98	0.004463	1.0
41	-35.03687	15331.1	-48342.45	44153.58	0.002303	1.0
42	17.19202	10486.71	-32985.49	30127.45	0.0	1.0
43	0	0	0	0	0.0	1.0

Sample Output for Crack Propagation Program- The following pages contain the output for the sample problem.

MODULUS CONDITION	BASE MODULUS	SUBGRADE MODULUS	OVERLAY MODULUS	A	N
1	1200000.0	4000.0	350000.0	1000E-09	2.00
2	1200000.0	9000.0	350000.0	1000E-09	2.00
3	800000.0	4000.0	350000.0	1000E-09	2.00
4	800000.0	9000.0	350000.0	1000E-09	2.00
5	400000.0	4000.0	350000.0	1000E-09	2.00
6	400000.0	9000.0	350000.0	1000E-09	2.00

DEPTH OF BASE 16
 DEPTH OF OVERLAY 0
 MODULUS CONDITION 1

INITIAL C/B RATIO	CURRENT C/B RATIO	INCREMENTAL LOAD CYCLES	CURRENT LOAD CYCLES
0.0000	.0500	.88171E+04	.88171E+04
.0500	.1000	.55496E+04	.14367E+05
.1000	.1500	.42884E+04	.18755E+05
.1500	.2000	.398863E+04	.22741E+05
.2000	.2500	.40022E+04	.26744E+05
.2500	.3000	.43572E+04	.31101E+05
.3000	.3500	.50935E+04	.36194E+05
.3500	.4000	.63598E+04	.42554E+05
.4000	.4500	.84512E+04	.51005E+05
.4500	.5000	.11886E+05	.62891E+05
.5000	.5500	.17455E+05	.80346E+05
.5500	.6000	.25903E+05	.10625E+06
.6000	.6500	.36316E+05	.14257E+06
.6500	.7000	.43316E+05	.18588E+06
.7000	.7500	.39819E+05	.22570E+06
.7500	.8000	.27747E+05	.25345E+06
.8000	.8500	.15880E+05	.26933E+06
.8500	.9000	.83164E+04	.27764E+06
.9000	.9500	.43036E+04	.28195E+06
.9500	.0000	.22864E+04	.28423E+06

etc.
↓

END
FILMED

5-86

DTIC